GRAĐEVINSKI
MATERIJALI I KONSTRUKCIJE

Volume 67
December 2024
ISSN 2217-8139 (Print)
ISSN 2335-0229 (Online)
UDK: 06.055.2:62-03+620.1+624.001.5(497.1)=861

BUILDING
MATERIALS AND STRUCTURES

4

Society for Materials and Structures Testing of Serbia
University of Belgrade Faculty of Civil Engineering
Association of Structural Engineers of Serbia

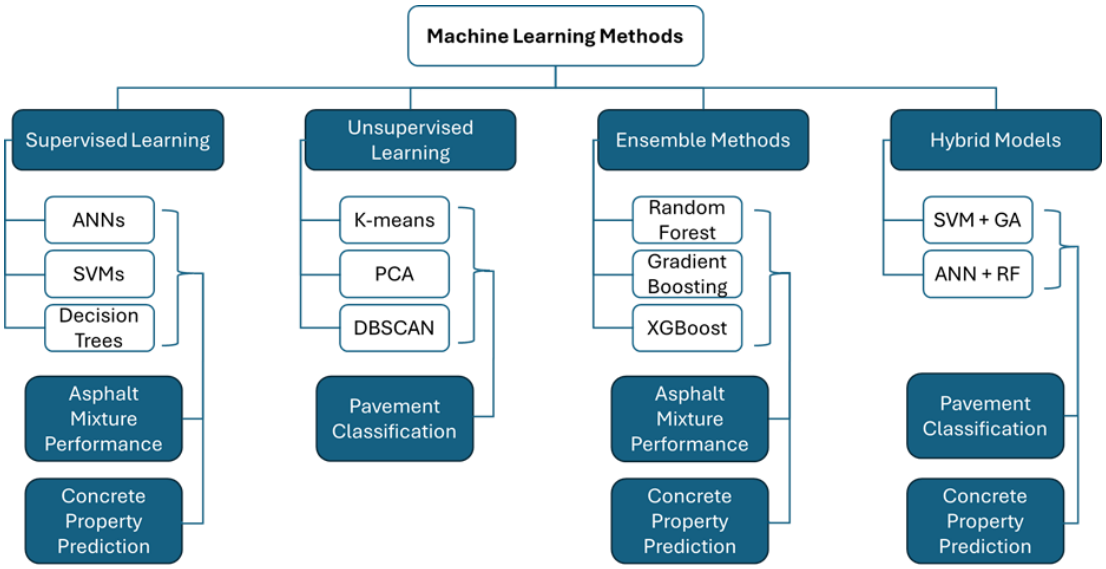

GRAĐEVINSKI MATERIJALI I KONSTRUKCIJE

BUILDING MATERIALS AND STRUCTURES

ISSN 2217-8139 (PRINT)
ISSN 2335-0229 (Online)

VOLUME 67(4)
December 2024

CONTENTS

GRAĐEVINSKI MATERIJALI I KONSTRUKCIJE

BUILDING MATERIALS AND STRUCTURES

ISSN 2217-8139 (PRINT)
ISSN 2335-0229 (Online)

VOLUME 67(4)
December 2024

EDITORIAL BOARD

Aims and scope

Building Materials and Structures aims at providing an international forum for communication and dissemination of innovative research and application in the field of building materials and structures. Journal publishes papers on the characterization of building materials properties, their technologies and modeling. In the area of structural engineering Journal publishes papers dealing with new developments in application of structural mechanics principles and digital technologies for the analysis and design of structures, as well as on the application and skillful use of novel building materials and technologies.

The scope of Building Materials and Structures encompasses, but is not restricted to, the following areas: conventional and non-conventional building materials, recycled materials, smart materials such as nanomaterials and bio-inspired materials, infrastructure engineering, earthquake engineering, wind engineering, fire engineering, blast engineering, structural reliability and integrity, life cycle assessment, structural optimization, structural health monitoring, digital design methods, data-driven analysis methods, experimental methods, performance-based design, innovative construction technologies, and value engineering.

Publishers Society for Materials and Structures Testing of Serbia, Belgrade, Serbia, veb sajt: www.dimk.rs
University of Belgrade Faculty of Civil Engineering, Belgrade, Serbia, www.grf.bg.ac.rs
Association of Structural Engineers of Serbia, Belgrade, Serbia, dgks.grf.bg.ac.rs

Print Razvojno istraživački centar grafičkog inženjerstva, Belgrade, Serbia

Edition quarterly

Peer reviewed journal

Journal homepage www.dimk.rs

Cover Machine learning methods in civil engineering material testing, from *Application of machine learning in asphalt and concrete material testing: a comprehensive review* by Meisam Khorshidi, Eshan Dave and Jo Sias

Financial support Ministry of Education, Science and Technological Development of Republic of Serbia
University of Belgrade Faculty of Civil Engineering
Institute for testing of materials-IMS Institute, Belgrade
Faculty of Technical Sciences, University of Novi Sad, Department of Civil Engineering
Serbian Chamber of Engineers

CIP - Каталогизација у публикацији
Народна библиотека Србије, Београд

620.1

GRAĐEVINSKI materijali i konstrukcije = Building materials and structures / editor-in-chief Snežana Marinković
. - God. 54, br. 3 (2011)- . - Belgrade : Society for Materials and Structures Testing of Serbia : University of Belgrade, Faculty of Civil Engineering : Association of Structural Engineers of Serbia, 2011- (Belgrade : Razvojno istraživački centar grafičkog inženjerstva). - 30 cm

Tromesečno. - Je nastavak: Materijali i konstrukcije = ISSN 0543-0798. - Drugo izdanje na drugom medijumu: Građevinski materijali i konstrukcije (Online) = ISSN 2335-0229
ISSN 2217-8139 = Građevinski materijali i konstrukcije
COBISS.SR-ID 188695820

Građevinski materijali i konstrukcije
Building Materials and Structures
journal homepage: www.dimk.rs

https://doi.org/10.5937/GRMK2400010S UDK: 666.972.1:620.1

Original scientific paper

Improving the mechanical characteristics of environmentally friendly concrete using fly ash and brick powder as partial sand replacements

Saloua Filali[*1)], Abdelkader Nasser[2)], Abdellah Azougay[3)]

[1)] *Department of Physics; Laboratory of Materials Waves, Energy, and Environment, Team of Materials, Energy, Civil Engineering and Environment; Faculty of Sciences; Mohammed Premier University; Oujda, Morocco*
[2)] *Department of Applied Engineering; Laboratory of Materials, Waves, Energy, and Environment, Team of Materials, Energy, Civil Engineering and Environment; Higher School of Technology; Mohammed Premier University; Oujda, Morocco*
[3)] *Department of Geology; Laboratory of Applied Geosciences, Mohamed Premier University, Faculty of Sciences, Oujda, Morocco*

Article history
Received: 21 September 2024
Received in revised form: 24 October 2024
Accepted: 03 November 2024
Available online: 06 December 2024

Keywords
fly ash,
brick powder,
workability,
strength,
Schmidt hammer,
ultrasonic velocity

ABSTRACT

Infrastructure and urbanization drive the demand for concrete, which puts pressure on natural resources and jeopardizes the ecosystem. Incorporating recycled materials into concrete can fulfill this demand without sacrificing quality. This study examines the mechanical properties of sustainable concrete, employing fly ash (FA) and brick powder as substitutes for sand in fine aggregates. We evaluated rebound hammer strength, ultrasonic pulse velocity (UPV), workability, compressive strength, and split tensile strength using both destructive and non-destructive assessment methods, comparing them to conventional concrete. Concrete mixtures were developed by substituting 10% of natural sand with brick powder and gradually replacing the remaining sand with fly ash at 10% to 50%. The results clearly show that the best mix of 10% brick powder and 40% fly ash increases compressive strength by 64.81%, split tensile strength by 17.78%, and workability by 48%. The identical mixture yields a notable enhancement in ultrasonic pulse velocity (UPV) of 33.15%, achieving a velocity of 4.9 km/s, and a 32.05% increase in rebound number, resulting in a rebound index of 44.92. A regression analysis indicated a significant correlation among compressive strength, UPV, and rebound index. The combination of 10% brick powder and 40% fly ash results in enhanced mechanical performance, reduced costs, and supports sustainable construction practices.

1 Introduction

Concrete, a commonly used composite material, plays a crucial role as a structural element in the development of worldwide infrastructure. It is the second most widely used substance after water, with a global production of approximately 5.3 billion cubic meters per year [1]. Mehta et al. [2] has projected an increase to 18 billion tons by 2050. The composition comprises three fundamental components: water, aggregate, and cement. Cement, the main constituent of concrete, acts as a cohesive substance when mixed with water and aggregates in its powdered form. Concrete is a versatile material that is cost-effective, adaptable, durable, and malleable in various shapes and finishes. It has a high ability to withstand compression, a low ability to withstand tension, a limited ability to deform, and a weak resistance to cracking. Consequently, guaranteeing longevity has increasingly become a significant issue in the construction industry.

The production of concrete accounts for roughly 8% of global CO_2 emissions [3]. Portland cement, a major component, plays a significant role in this negative impact on environmental pollution [4]. The extraction of raw materials used in concrete, sourced from the Earth's crust, has contributed to the global depletion of these resources. As a result, the extensive use of concrete has raised significant environmental and economic concerns [5, 6]. This necessitates the replacement of all or part of the cement with an eco-friendly material. In this scenario, we identified two objectives: the first was to reduce the CO2 emissions associated with cement manufacturing. On the other hand, the second approach aimed to reduce environmental impact by using leftover industrial materials as fine or coarse aggregates or as substitutes for cement. Over the past century, researchers have proposed various waste products from industry and agricultural materials as potential substitutes for concrete ingredients. These include rice husk ash, fly ash, sewage sludge ash, bagasse ash, polyvinyl chloride waste powder (PWP), and textile sludge ash (TSA). This approach effectively maintains natural resources, preventing their depletion, and improving the economy and sustainability of concrete production [7]. Fly ash, a by-product of burning pulverized coal in thermal power plants,

* Corresponding author:
E-mail address: saloua.filali@ump.ac.ma

has gained significant attention from researchers as a potential alternative for substitution in concrete. Researchers generally classify fly ash into two categories: Class F and Class C [8]. Class F fly ash contains at least 70% combined silica, aluminum, and iron oxides, with a calcium oxide (CaO) content below 10%. This composition reduces the water demand in concrete mixtures and exhibits pozzolanic properties, improving the material's performance.

Multiple studies have investigated the implications of substituting sand with fly ash in concrete. Siddique [9] focused his study on the effects of Class F fly ash on the mechanical and physical properties of concrete. The study involved replacing 10 to 50% of fine aggregate (sand) with fly ash. As the proportion of sand substitution increased, the concrete's compressive strength increased due to the pozzolanic effect of fly ash. The concrete exhibited enhanced tensile strength, flexural strength, and modulus of elasticity in comparison to the standard concrete. Even with the addition of a superplasticizer, the ease of handling newly mixed materials decreased, but 50% fly ash proved to be the most effective substitution. Ishimaru [10] performed a study on the use of fly ash as fine aggregates in conventional concrete and determined that it is suitable for constructing concrete structures. Their partial substitution greatly enhances the strength of conventional concrete, enabling their efficient utilization in structural concrete. Rajamane and Ambily [11] investigated the properties of concrete when less calcium fly ash replaced a portion of the sand. The levels of sand replacement were 0%, 20%, 40%, and 60%. The findings indicated that the compressive strengths at 28 days were comparable among all levels of replacement. Furthermore, fly ash concrete showed superior workability compared to control concrete. Bilir et al. [12] undertook a study to examine the impacts of using fly ash as fine aggregates on the mechanical properties of mortar. The results show that using fly ash as a replacement for 30% of the original material enhanced the mortar's ability to withstand deformation and improved its strength through its pozzolanic effect. Deo and Pofale [13] conducted a separate investigation in which he substituted fly ash at weight percentages of 12% and 27% for sand in the concrete compositions. All mixes maintained a water-to-cement ratio of 0.32, demonstrating pozzolanic properties. The findings indicated that the concretes containing fly ash demonstrated superior compressive strength, flexural strength, and workability in contrast to conventional concrete. Moreover, the inclusion of superplasticizers has the potential to enhance these properties even more. In a previous study, Islam and Rashid [14] investigated the effects of partially replacing sand with low-calcium fly ash at various amounts between 0% and 40%. According to the report, concrete with 20% and 30% fly ash showed greater compressive strength than regular concrete when they had the same water/cement ratio. Yin et al. [15] study demonstrated that utilizing both fly ash and river sand results in an optimized particle size distribution of fine aggregates. The concrete mixture containing 30% fly ash demonstrated superior compressive strength in comparison to the conventional concrete, with a notable increase of 28.8%. Mao et al. [16] conducted a study showing that the strength of concrete increases with an increase in fly ash content, as long as it does not exceed 40%.

Fly ash particles are also very small and have a large specific surface area. This lets them fill up more space between the cement and aggregate particles, which makes the concrete denser. While there have been numerous important findings on the use of fly ash in concrete, literature is scarce on its application as a component substitute for fine aggregates.

The landfill disposal of brick dust, a plentiful byproduct from brick kilns and construction sites, raises environmental concerns. Brick kilns are the main contributors to this waste, occupying valuable land and posing significant risks to both health and the environment. Researchers are increasingly interested in using brick powder (BP) as a partial alternative to sand in the composition of concrete mixtures. This is because (BP) has the potential to improve concrete's specific mechanical properties while also recycling construction waste. Researchers have conducted several studies to evaluate the viability of utilizing clay bricks as aggregates in concrete. Adamson et al. [17] showed that it is possible to substitute natural coarse aggregates with crushed bricks in concrete without causing any significant impact on its durability, as long as there are no steel reinforcements present. However, Bektas et al. [18] asserts that increasing the rate of brick substitution results in a decrease in the fluidity of the mortar. However, substituting 10% and 20% of the bricks did not hurt compressive strength and only had a minor effect on mortar shrinkage. In Nunung et al. study [19] the impact of incorporating lightweight bricks as a partial replacement for sand (at levels of 0%, 10%, 20%, and 30%) on the compressive strength of concrete was investigated. The results showed that substituting 10% and 30% of the material achieved the highest and lowest levels of compressive strength, respectively, at 24.45 MPa and 18.03 MPa after 28 days. Gaspard et al. [20] conducted a study to examine how the substitution of fine aggregates with crushed clay bricks affects the concrete's workability and compressive strength. The study examined substitution rates of 10%, 15%, 25%, 50%, and 75%. The findings revealed a negative correlation between the replacement rate and compressive strength. The strength decreased gradually as the replacement rate increased, with a minimal reduction of 9.63% observed at a replacement rate of 10%. However, a replacement rate of 75% recorded a maximum decrease of 50% compared to the control sample, which exhibited a strength of 31.81 MPa. Momoh et al. [21] conducted a study to assess the effectiveness of different amounts of recycled concrete aggregate (15%, 22.5%, and 30%) and crushed clay bricks (10%, 15%, and 20%) as substitutes for coarse and fine aggregates in concrete. The test results indicated that the compressive strength ranged from 24.22 MPa to 27.78 MPa after 7 days, from 27.95 MPa to 37.2 MPa after 18 days, and from 25.15 MPa to 32.48 MPa after 28 days. To achieve optimal performance, the authors suggest keeping the crushed brick content within the range of 15% to 20%. These findings are consistent with Srivinas et al. [22] research, which indicated that the ideal substitution of natural fine aggregates with crushed brick powder was 20%. Similarly, Aliabdo et al. [23] concluded that the amount of clay brick aggregate present in concrete. should not exceed 25% of the total aggregate content. Ibrahim et al. [24] found that lightweight concrete containing 25% used clay bricks reached a maximum strength of 25 MPa and had a density of 1647 kg/m3. This result is consistent with the findings reported by David et al. [25]. The literature review above indicates a dearth of information regarding the impact of adding clay brick powder to concrete's mechanical properties.

2 Research relevance and objectives

Reducing dependency on natural resources and mitigating environmental degradation are the primary goals of this study. The purpose of this analysis is to look closely at the properties of concrete that has had some of its natural sand replaced with fly ash and brick powder. To accomplish this, several different mixes were prepared. Brick powder replaces 10% of the sand in all the mixes, while fly ash gradually replaces the remaining sand, increasing the percentage from 10% to 50% in 10% increments. The study examines several concrete samples, including workability, compressive strength, split tensile strength, ultrasonic pulse velocity, and Schmidt rebound hammer index. We conduct an in-depth analysis to assess the feasibility and environmental benefits of this alternative method by examining the effects of these modifications on the composition and functionality of the concrete.

3 Experimental study

3.1 Characterization of materials

The binding material chosen for this project is Portland cement CPJ 45, which has a minimum clinker content of 65% and will be used to create the concrete mixture. The remaining materials consisted of additives, including fly ash, pozzolans, and fillers provided by Holcim. These additives complied with the Moroccan specifications NM10.1.004 [26]. The concrete was prepared by mixing potable water sourced from Oujda's autonomous intercommunal water and electricity distributing agency (RADEEO), which meets the physical and chemical requirements specified in NM 10.1.353 [27]. The sand used in this study was sourced from the Oujda region (Morocco) and is known for its exceptional purity. The substance's streamlined, balanced, and cuboid shape enables effortless manipulation and handling. The sand underwent a full day of air drying at room temperature to regulate the moisture content of the concrete. The sand reached a maximum size of 4.75 mm. The NF EN 12620 [28] standard guided the sand tests. This study utilized two distinct types of crushed coarse stone aggregates: G1, which had a sieve range of 5-11 mm, and G2, which had a sieve range of 11-20 mm. The NF P-18-560 [29] standard guided the selection of these aggregates. This study uses F-class fly ash from Morocco's Jerada thermal power plant. Electrostatic methods collect the fly ash from the powdery particles in the flue gas stream of boilers powered by pulverized coal. These measurements are per the NM 10.1.004 [26] standard.

The clay brick powder, derived from fragmented or demolished brick waste during manufacturing, was collected in a brick manufacturing plant (ARGILUX) located in Oujda. It was pulverized into fine particles using a ball mill until all particles were reduced to a size smaller than 4.75 mm. The particles utilized as a replacement for sand are those that can pass through a 4.75–5 mm sieve and are captured by a sieve with a size of 75–90 microns. The choice to use brick powder as a substitute material is justified by its pozzolanic properties, which require a minimum composition of SiO2, CaO, Al_2O_3, and Fe_2O_3 that exceeds 70%. Figure 1 depicts the particle size analysis of the various materials employed. Table 1 presents the physical characteristics of cement, sand, coarse aggregates, fly ash, and brick powder. Table 2 displays the chemical constituents of cement, brick powder, sand, and fly ash.

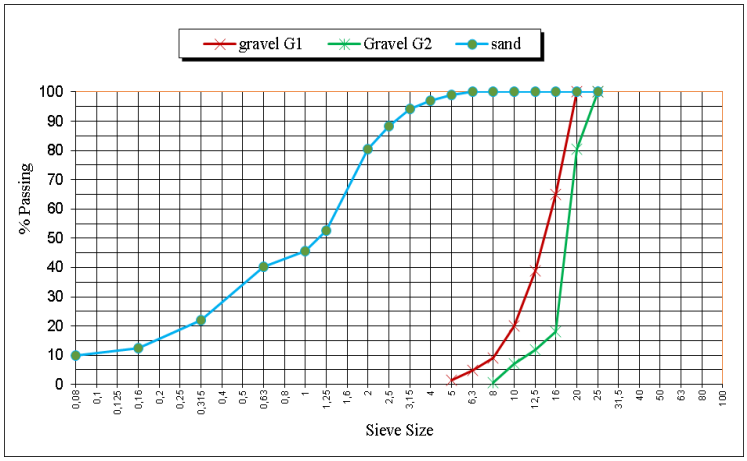

Fig. 1. Particle size distribution of aggregates

Table 1. Physical properties of constituent materials

Property	cement	fly ash	sand	G1	G2	BP
Specific Gravity	3.15	2.52	2.68	2.70	2.72	2.18
Water absorption %		3.01	2.50	1.48	1.50	5.25
Fineness modulus		0.96	2.85	6,62	6,82	2.87
Initial setting time (min)	180					
Final setting time (min)	210					
Fineness Blaine cm2/gm)	3100	3360				

Table 2. The chemical constitution of cement, sand, fly ash, and brick

Constituent (%)	cement (%) by mass	BP (%) by mass	sand (%) by mass	fly ash (%) by mass
CaO	60.06	7,12	5.58	1,12
SiO_2	20,90	43,24	77,40	55,2
Fe_2O_3	3,90	21,6	2,66	11,2
AL_2O_3	5,85	11,92	8,18	28,3
MgO	1,85	2,42	0,77	0,68
K_2O	2,14	2,15	0,25	1,45
TiO_2	0,32	1,86	0,005	1,5
SO_3	2,35	6,02	0,018	0,44
LOI	21,84	3,42	……..	1,06

In order to evaluate the effects of partially replacing natural sand with brick powder and fly ash on concrete performance, six mixtures were prepared. One of these mixtures contained only natural sand (ordinary concrete), while the others incorporated fly ash and brick powder as partial replacements for natural sand, using a water-to-cement ratio of 0.55. The concrete mixtures were prepared using the Dreux-Gorisse [30] concrete mix design method, with a constant cement dosage of 350 kg per 1 m³ of concrete in all mixtures. Table 3 specifies the proportions of fly ash, brick powder, sand, coarse aggregates, and cement. The abbreviation SFS denotes the substitution of fly ash for natural sand, while SB signifies the substitution of brick powder for natural sand. For instance, the code SB10-SFS10 signifies a blend where brick powder replaces 10% of the natural sand and fly ash replaces the remaining 10%.

3.2 Test Parameters

The Oujda Faculty of Science's building materials laboratory and the LABNORVIDA testing laboratory in Oujda were the sites of the study's experimental program. A 125-liter pan mixer was used to meticulously prepare the concrete mixes. The procedure started with adding big aggregates to the mixer, then fine aggregates. Next, a small amount of water, equal to a fraction of the total amount, was added. Following this, the remaining water was added to the cement, fly ash, and brick powder mixture. We considered the mixture complete only after running the mixer continuously.

3.2.1 Workability

The research objective was to assess the impact of substituting a portion of natural sand with a combination of brick powder and fly ash on the workability of fresh concrete. The consistency of the concrete was evaluated by conducting slump tests using the Abrams cone method, as specified in NF EN 12350-2 [31]. The slump cone had conventional measurements: 300 mm in height, with a 200 mm base diameter and a 100 mm top diameter. The workability of each mixture was evaluated by performing slump tests and measuring the slump values for the various concrete compositions. The average result was calculated using three specimens.

3.2.2 Compressive, split tensile, and flexural strength

The assessment of the structural capacity of concrete in buildings relies heavily on the measurement of compressive strength. Concrete cubes with dimensions of 150 mm on each side were created to determine the concrete's compressive strength. The NF EN 12390-3 [32] standard mandates evaluating the compressive strength at various curing ages, specifically on days 7, 14, 28, and 56. The samples were subjected to a curing process in an environment with 100% relative humidity and a constant ambient temperature of 27 ± 2°C using water. Cylinders with dimensions of 300 mm in height and 150 mm in diameter were manufactured to measure the split tensile strength of the concrete. Under the specifications outlined in NF EN 12390-6 [33], the evaluation of tensile strength was performed after curing has lasted until the day of the test.

3.2.3 Ultrasonic pulse velocity

Ultrasonic pulse velocity testing, a non-destructive method, can assess concrete quality on-site. The quality of concrete on all samples was evaluated using the NF EN 12504-4 [34] standard procedure for ultrasonic testing after 28 days of curing. The experiment was carried out using a voltage of 500 V and a frequency of 54 kHz. The device incorporates a processing unit that transmits and receives ultrasonic pulses while also measuring the time duration between these two operations. The device transmits sound energy through two probes. The time interval between the transmitting probe's transmission of sound energy into the concrete and the receiving probe's detection of this energy determines the pulse velocity. This study used a direct method to generate the pulse to carry out this process. The pulse velocity is unaffected by the substance's form and structure as it passes through, but it does depend on the

Table 3. Mixture proportions with w/c=0,55.

Mix identification	BP %	fly ash %	water (Kg/m^3)	cement (Kg/m^3)	G1 (Kg/m^3)	G2 (Kg/m^3)	sand (Kg/m^3)	fly ash (Kg/m^3)	BP (Kg/m^3)
SB0SFS0	0	0	192	350	320	815	763	0	0
SB10-SFS10	10	10	192	350	320	815	611	76	76
SB10-SFS20	10	20	192	350	320	815	534	153	76
SB10-SFS30	10	30	192	350	320	815	458	229	76
SB10-SFS40	10	40	192	350	320	815	382	305	76
SB10-SFS50	10	50	192	350	320	815	305	382	76

material's elastic properties. Longitudinal waves are detected by the receiver, which are the fastest. When the concrete's density, homogeneity, and uniformity are high, we observe greater velocity values. Compromise in quality results in reduced values.

3.2.4 Schmidt rebound hammer

For a non-destructive way to find out how strong concrete is under compression, engineers use the rebound hammer (Figure 2). This control technique, in line with NF EN 12504-2 [35], allows for the estimation of concrete strength. This technique is based on the idea that the rebound of an elastic mass is proportional to the surface hardness of the concrete it hits. The design checks the consistency and quality of the concrete, providing a quick and easy indication of its compressive strength. As the apparatus operates, a spring-loaded mass moves along a plunger within a tube. Lower rebound values are associated with lower-strength concrete due to the increased energy absorption observed in this material. After obtaining the rebound number, the manufacturer's supplied chart displayed the compressive strength for each rebound value. The rebound measurement of the sclerometer is the average of 10 measurements taken at different points on the same sample. These points must be spaced at least 20 mm apart.

4 Results and conversational analysis

4.1 The influence of brick powder and fly ash on concrete compressive strength

The compressive strength of concrete samples was measured. Throughout the process, the specimens were water-cured. On days 7, 14, 28, and 56, after allowing samples to dry for one full day, each concrete specimen was analyzed. The average result was calculated using three specimens. The results of the compressive strength were obtained using the universal testing machine. Table 4 displays the compressive strength values for each specimen.

Figure 3 shows that replacing 10% of sand with brick powder significantly improves the compressive strength by increasing the fly ash content from 10% to 40%. Compared to the conventional, the SB10SFS40 mix has better compressive strength, increasing 64.81%, 34.84%, 60.77%, and 45.80% at 7, 14, 28, and 56 days. Furthermore, the study's results indicate that the gradual improvement in compressive strength is particularly significant at the 28 and 56-day marks. This is due to the slow reaction of calcium hydroxide released during cement hydration with fly ash. The findings indicate that a blend of 10% brick powder and a maximum of 40% fly ash is optimal for improving the compressive strength of concrete mixtures. Utilizing these

Fig. 2. Schmidt rebound hammer

Table 4. Compressive strength of concrete with brick powder and fly ash

Mix designation	Concrete's compressive strength (MPa)			
	7 days	14 days	28 days	56 days
SB0SFS0	18,50	23,88	27,94	30,72
SB10-SFS10	24,62	27,04	38,74	37,37
SB10-SFS20	26,01	28,18	40,90	40,22
SB10-SFS30	28,80	31,19	43,16	42,82
SB10-SFS40	30,49	32,20	44,92	44,79
SB10-SFS50	28,68	29,94	39,87	38,95

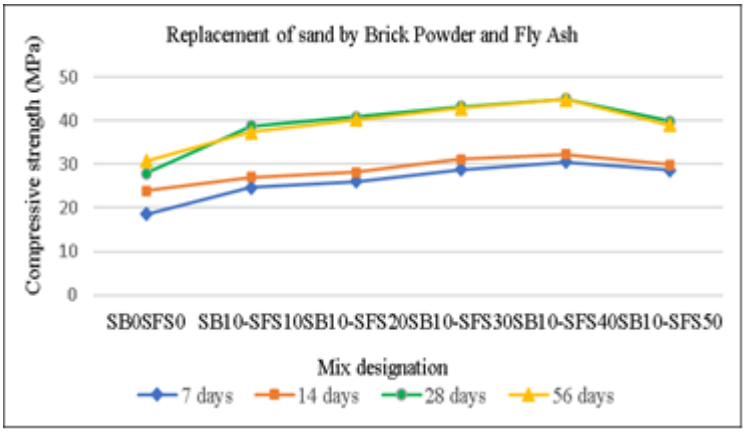

Fig. 3. Compressive strength of brick powder and fly ash concrete

materials in moderate amounts appears to enhance the density and overall strength of the concrete by promoting a more efficient pozzolanic reaction and effective pores filling. However, going over these recommended replacement rates, especially for fly ash levels above 40%, could lower the compressive strength. This could be because the mixture will have more voids in it.

4.2. The influence of brick powder and fly ash on the workability of concrete

Figure 4 shows workability values, indicating a significant decline in mixtures containing brick powder (SB) and fly ash (SFS). The lowest slump measured is 39 mm, while the highest is 75 mm. When compared to the control concrete, this combination yields a reduction of about 48%. This is because the brick powder particles are angular and irregular in shape, which has a direct impact on workability. This is because the particles are more difficult to mobilize, leading to a growth in water demand and a reduction in the mix's air content. More energy is required to overcome this internal resistance and bring about the intended collapse. Fly ash's higher water requirements for particle coating further impede mixture flow and complicate handling. Hebhoub et al. [36], Aliabdo et al. [37], Ashish [38], and Vardhan et al. [39] research recommends incorporating water or using superplasticizers to address this limitation.

4.3 The influence of brick powder and fly ash on the split tensile strength of concrete

Concrete samples were subjected to tests to determine their splitting tensile strength. The procedure involved subjecting the specimens to water curing. We allowed the concrete specimens to dry for a full day before analyzing them on days 7, 14, 28, and 56. The splitting tensile strength results were obtained using the universal testing machine. Table 5 displays the splitting tensile strength values for each test specimen under various sand substitutions. The average result was calculated using three specimens. The set of substitutions combines 10% brick powder and fly ash at rates of 10%, 20%, 30%, 40%, and 50%.

The results presented in Figure 5 indicate that replacing sand with 10% brick powder and combining it with fly ash in proportions of 10% to 40%, enhances tensile strength. The SB10-SFS40 mixture exhibits enhanced tensile strength relative to conventional concrete at 7, 14, 28, and 56 days, with improvements of 17.75%, 8.09%, 17.78%, and 17%, respectively. Adding 50% more fly ash (SB10-SFS50) lowers the tensile strength slightly at all testing ages. This could be because the concrete particles become less tightly connected or more voids are in the mix. This highlights the importance of determining an optimal substitution rate to improve concrete's mechanical efficiency.

Brick powder and fly ash synergistically enhance the strength of the concrete matrix by effectively occupying the pores and increasing density, resulting in improved strength. This approach enhances mechanical properties, minimizes expenses, and mitigates environmental impact, rendering this strategy appealing for sustainable construction applications.

4.4 The influence of brick powder and fly ash on the velocity of ultrasonic pulses

Figure 6 presents data on the ultrasonic pulse velocity (UPV) and compressive strength after 28 days for various concrete mixtures. The UPV values, ranging from 3.68 km/s to 4.9 km/s, with an average of 4.21, indicate high-quality cement paste. This suggests that adding brick powder and fly ash to the concrete has a positive impact on its UPV. Compared to conventional concrete (mix SB0-SFS0), the UPV increases by 7.88%, 14.40%, 20.92%, and 33.15%, respectively, when replacing 10% of the sand with brick powder and gradually increasing the amount of fly ash from 10% to 40%.

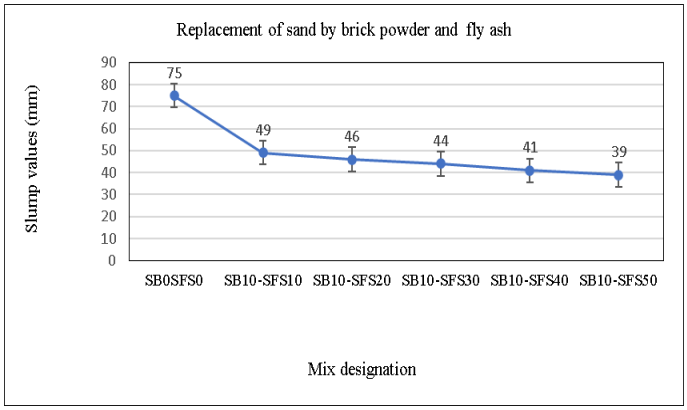

Fig. 4. Workability of brick powder and fly ash concrete

Table 5. Split tensile strength of concrete with brick powder and fly ash

Mix designation	Concrete's split tensile strength (MPa)			
	7 days	14 days	28 days	56 days
SB0-SFS0	2,76	3,09	3,43	3,60
SB10-SFS10	2,92	3,01	3,58	3,79
SB10-SFS20	3,01	3,13	3,90	3,88
SB10-SFS30	3,16	3,29	3,96	4,05
SB10-SFS40	3,25	3,34	4,06	4,14
SB10-SFS50	3,14	3,16	3,73	3,81

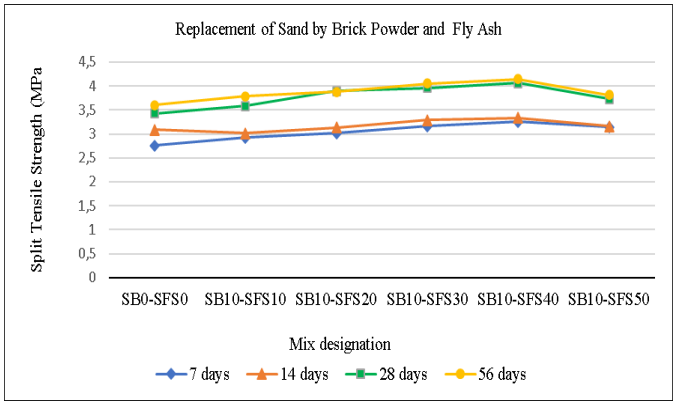

Fig. 5. Split tensile strength of brick powder and fly ash concrete

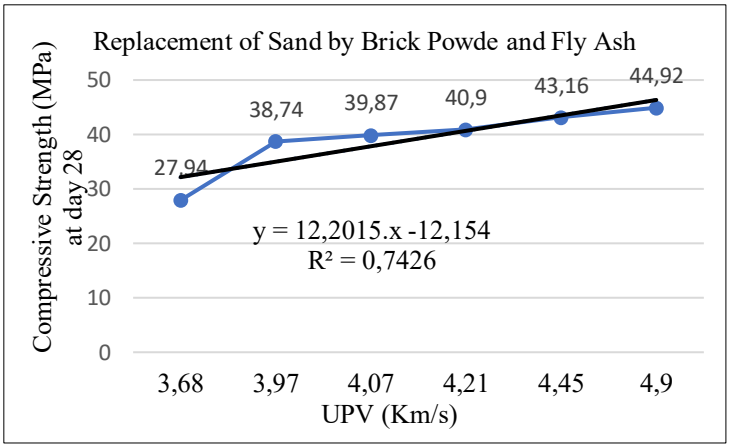

Fig. 6. UPV and compressive strength correlation in concrete with brick powder and fly ash replacement

To assess the UPV and compressive strength (f_C) of concrete containing brick powder and fly ash, a correlation between UPV and f_C was examined using a least squares regression analysis. Equation (1) presents the derived formula for calculating compressive strength, based on the acquired data.

$$f_c = 12{,}2015.(\text{uvp}) - 12{,}154 \quad \text{with} \quad R^2 = 0{,}7426 \quad (1)$$

To maximize the advantages of brick powder and fly ash while preserving the mechanical and physical properties of concrete, it is essential to ascertain the optimal substitution rate. In this context, incorporating 10% brick powder into mixtures with 10%, 20%, 30%, or 40% fly ash has been shown to improve ultrasonic pulse velocity. Factors such as the enhanced density of the concrete matrix, elevated pozzolanic reactivity, the filler effect, and a decrease in imperfections and fissures all contribute to this improvement in ultrasonic wave transmission.

4.5 The influence of brick powder and fly ash on the Schmidt rebound hammer

Tests were performed on concrete cube specimens at the 28-day mark using a Schmidt hammer. The results of the rebound number for the cement paste with various sand substitutions are shown in Figure 7. The results show that replacing 10% of the sand with brick powder and increasing the fly ash (SFS) content from 10% to 40% raises the rebound number by 20%, 25.48 %, 26.33 %, and 32.05 %, respectively. Despite a minor reduction at a fly ash percentage of 50% (SB10-SFS50), the rebound number continues to exceed that of the control mixes. The data suggests that a balanced approach, with moderate replacement levels, such as 40% fly ash and 10% brick powder, is most advantageous.

The method of least squares was utilized to perform a regression analysis of the correlation between rebound number and compressive strength, as measured by the Schmidt hammer when substituting sand with fly ash and brick powder. We used the data from Figure 7 and Equation (2) to derive the following formula for calculating compressive strength:

$$f_c = 1{,}471.(\text{Rn}) - 25{,}7143 \quad \text{with} \quad R^2 = 0{,}99 \quad (2)$$

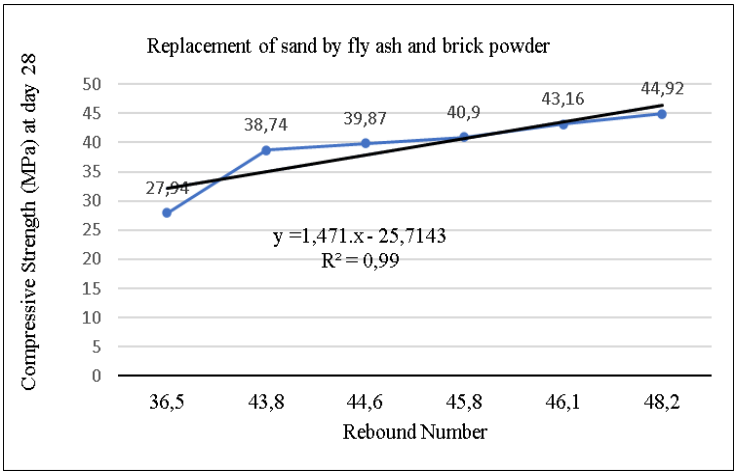

Fig.7. Rebound number and compressive strength correlation in concrete with brick powder and fly ash replacement

5 Conclusion

Investigations into sustainable substitutes for natural sand in concrete, including fly ash and brick powder, have revealed a significant deficiency in comprehending the synergistic interactions of these materials. Previous studies have examined individual substitutes, but none have thoroughly investigated the synergistic effects of fly ash and brick powder. This study sought to address that gap by assessing the effects of these alternatives on concrete's workability, rebound number, ultrasonic pulse velocity, split tensile strength, and compressive strength.

Using 40% fly ash and 10% brick powder instead of sand increased the compressive strength by 64.81% and the split tensile strength by 17.78%. However, the workability decreased by 48% compared to the control mix (SB0-SFS2). The SB10-SFS40 mix achieved an ultrasonic pulse velocity of 4.9 km/s, indicating a 33.15% improvement. Additionally, it increased the rebound number by 32.05%, reaching a maximum of 48.2 on the Schmidt hammer test. We used least squares regression to find strong links between compressive strength, rebound number, and ultrasonic pulse velocity. These links led to reliable formulas for estimating compressive strength based on these variables. Significantly, when fly ash replacement exceeded 40%, it only slightly reduced mechanical performance.

In summary, the ideal equilibrium for improving the mechanical properties of concrete, lowering expenses, and mitigating environmental effects entails the incorporation of 10% brick powder with a maximum of 40% fly ash. Better pozzolanic reactions and good pore filling enable this synergy, resulting in stronger and denser concrete. The results underscore a substantial advancement in sustainable construction, providing an environmentally friendly solution that alleviates strain on natural resources while enhancing concrete performance.

Declarations:

Funding: No financial assistance, grants, or additional support was obtained.

Declaration of competing interest: The authors declare that there is no conflict of interest regarding the publication of this paper.

Credit authorship contribution statement:

Filali. S: Investigation. Original draft. Planning, and execution of experiments Design. Data analysis and final manuscript writing.

Nasser. A: Project administration, Supervision, Validation.

Azougay. A: Supervision, Revision.

Acknowledgments

The authors express gratitude to the testing laboratory LABNORVIDA in Oujda and the laboratory of the Department of Geology at the Faculty of Sciences in Oujda for their assistance in conducting this research.

References

[1] K. Ullah, M. I. Qureshi, A. Ahmad, and Z. Ullah, Substitution potential of plastic fine aggregate in concrete for sustainable production, Structures, vol. 35, pp. 622–637, Jan. (2022).

[2] P. Kumar Mehta, P. Paulo, and J. M. Monteiro, *Concrete: Microstructure, Properties, and Materials*, 4th ed, (2014).

[3] H. Y. Aruntas, M. Gürü, M. Dayi, and I. Tekin, Utilization of waste marble dust as an additive in cement production, Materials & Design, vol. 31, pp. 4039–4042, (2010).

[4] A. Anwar, S. Mohd, A. Husain, and S. A. Ahmad, Replacement of cement by marble dust and ceramic waste in concrete for sustainable development, International Journal of Innovative Research in Science, Engineering, and Technology, vol. 2, pp. 496–503, (2015).

[5] A. M. Rashad, Metakaolin as cementitious material: History, sources, production and composition – a comprehensive overview, Construction and Building Materials, vol. 41, pp. 303–318, (2013).

[6] A. C. Sankh, P. M. Biradar, S. J. Agnathan, and M. B. Ishwargol, Recent trends in replacement of natural sand with different alternatives, Journal of Mechanical Civil Engineering, vol. 59–66, (2014).

[7] B. Arulmoly, C. Konthesingha, and A. Nanayakkara, Performance evaluation of cement mortar produced with manufactured sand and offshore sand as alternatives for river sand, Construction and Building Materials, vol. 297, (2021).

[8] A. M. Rashad, A brief on high-volume Class F fly ash as cement replacement – A guide for Civil Engineer, Building Materials Research and Quality Control Institute, International Journal of Sustainable Built Environment 4, 278–306, (2015).
[9] R. Siddique, Effect of fine aggregate replacement with Class F fly ash on the mechanical properties of concrete, Cement and Concrete Research, vol. 33, pp. 539–547, (2003).
[10] K. Ishimaru, Properties of concrete using copper slag and second-class fly ash as a part of fine aggregate, Journal of the Society of Materials Science Japan, vol. 54, pp. 828–833, (2005).
[11] N. P. Rajamane and P. S. Ambily, Fly ash as a sand replacement material in concrete – A study, Indian Concrete Journal, vol. 87, pp. 1–7, (2013).
[12] T. Bilir, O. Gencel, and I. B. Topcu, Properties of mortars with fly ash as fine aggregate, Construction and Building Materials, vol. 93, pp. 782–789, (2015).
[13] S. V. Deo and A. D. Pofale, Parametric study for replacement of sand by fly ash for better packing and internal curing, Open Journal of Civil Engineering, vol. 5, pp. 118–130, (2015).
[14] J. U. Islam and Z. B. Rashid, Partial replacement of natural fine aggregate with fly ash and its compressive strength, International Journal of Civil Engineering and Technology, vol. 9, pp. 32–36, (2018).
[15] S. Yin, Z. Yan, X. Chen, and L. Wang, Effect of fly ash as fine aggregate on the workability and mechanical properties of cemented paste backfill, Case Studies in Construction Materials, vol. 16, e01039, (2022).
[16] M. Mao, Q. Ai, D. Zhang, S. Li, and J. Li, Durability performance of concrete with fly ash as fine aggregate eroded by chloride salt, Advances in Materials Science and Engineering, vol. 6760385, (2022).
[17] M. Adamson, A. Razmjoo, and A. Poursaee, Durability of concrete incorporating crushed brick as coarse aggregate, Construction and Building Materials, vol. 94, pp. 426–432, (2015).
[18] F. Bektas, K. Wang, and H. Ceylan, Effects of crushed clay brick aggregate on mortar durability, Construction and Building Materials, vol. 23, pp. 1909–1914, (2009).
[19] M. Nunung, N. Rizka, F. R. Muhammad, A. M. A. Putera, and S. Yanuar, Compressive strength of concrete using lightweight brick waste as the substitute for fine aggregate, International Journal of GEOMATE, vol. 23, no. 98, pp. 189–196, Oct. (2022).
[20] U. Gaspard, N. Bienvenu, and U. G. B. Habimana, Effect of crushed clay brick as partial replacement of fine aggregate in concrete, Mediterranean Journal of Basic and Applied Sciences, vol. 7, no. 1, pp. 90–99, Jan.–Mar. (2023).
[21] G. O. Momoh, H. Sundaram, T. Shanmugam, and D. T. Jada, Influence of recycled concrete aggregate and crushed clay brick on mechanical properties of concrete, Civil and Environmental Research, vol. 7, no. 7, pp. 67–72, (2015).
[22] P. Srivinas, A. S. S. V. Prasad, and S. A. Kumar, Experimental study on strength of concrete with partial replacement of fine aggregate with waste clay brick powder, International Journal SART, vol. 2, no. 8, pp. 250–253, (2016).
[23] A. A. Aliabdo, A. M. Abd-Elmoaty, and H. H. Hassan, Utilization of crushed clay brick in cellular concrete production, Alexandria Engineering Journal, vol. 53, pp. 119–130, (2014).
[24] N. M. Ibrahim, S. Salahuddin, R. C. Amat, N. L. Rahim, and T. N. T. Izhar, Performance of lightweight concrete with waste clay brick as coarse aggregate, APCBEE Procedia, vol. 5, pp. 497–501, (2013).
[25] D. David, B. Sebastian, and J. M. A. Johny, Partial replacement of fine aggregate with crushed clay brick in cellular concrete, International Journal of Innovative Research in Science, Engineering, and Technology, vol. 6, no. 5, pp. 8218–8226, (2017).
[26] NM 10.1.004, Hydraulic binders; Cements, Norme Marocaine, (2003).
[27] NM 10.1.353, Concrete Mixing Water Specifications for Sampling, Testing and Evaluation of Suitability of Use, Including Process Water from the Concrete Industry, (1985).
[28] NF EN 12620, The characteristics of aggregates and fillers, (2003).
[29] NF P-18-560, AFNOR, Aggregates - Particle size analysis by sieving, (1990).
[30] H. Chbani, B. Saadouki, M. Boudlal, and M. Barakat. Formulation of Ordinary Concrete using the Dreux-Gorisse Method. Procedia Structural Integrity 28, 430–439. (2020).
[31] EN 12350-2, Testing fresh concrete - Part 2: Slump test, (2019).
[32] NF EN 12390-3, Tests for hardened concrete - Part 3: Compressive strength of specimens
[33] NF EN 12390-6, Tests for hardened concrete - Part 6: Determination of tensile splitting. strength of specimens.
[34] NF EN 12504-4, Testing concrete in structures - Part 4: Determination of ultrasonic pulse velocity, (2021).
[35] NF EN 12504-2, Tests for concrete in structures - Part 2: Non-destructive tests – Determination of rebound number, (2013).
[36] H. Hebhoub, H. Aoun, M. Belachia, H. Houari, and E. Ghorbel, Use of waste marble aggregates in concrete, Construction and Building Materials, 25, pp. 1167–1171, (2011).
[37] A. A. Aliabdo, A. M. Abd-Elmoaty, and H. H. Hassan, Utilization of crushed clay brick in the concrete industry, Alexandria Engineering Journal, 53(1), pp. 151–168, (2014).
[38] D. K. Ashish, Concrete made with waste marble powder and supplementary cementitious material for sustainable development, Journal of Cleaner Production, 211, pp. 716–729, (2018).
[39] K. Vardhan, R. Siddique, and S. Goyal, Influence of marble waste as partial replacement of fine aggregates on strength and drying shrinkage of concrete, Construction and Building Materials, 228, 116730, (2019).

Građevinski materijali i konstrukcije
Building Materials and Structures
journal homepage: www.dimk.rs

https://doi.org/10.5937/GRMK2400012K UDK: 691:620.1]:004.85

Review paper

Application of machine learning in asphalt and concrete material testing: a comprehensive review

Meisam Khorshidi*[1)] Eshan Dave[1)] Jo Sias[1)]

[1)] *Department of Civil and Environmental Engineering, University of New Hampshire, 33 Academic Way, Durham, NH 03824, USA*

Article history
Received: 21 October 2024
Received in revised form: 27 November 2024
Accepted: 30 November 2024
Available online: 20 December 2024

Keywords
predictive modeling,
material performance prediction,
pavement distress classification,
unsupervised learning,
ensemble methods,
hybrid models,
artificial neural networks (ANN),
gaussian process regression (GPR)

ABSTRACT

This literature review explores the application of machine learning (ML) techniques in civil engineering material testing, with a focus on asphalt mixtures, concrete properties, and pavement system classification. The review provides a comprehensive comparison of various ML models, including Artificial Neural Networks (ANNs), Support Vector Machines (SVMs), Random Forest (RF), Gradient Boosting (GB), and Gaussian Process Regression (GPR), assessing their strengths and limitations in predicting material performance. Key findings indicate that ensemble methods, such as Gradient Boosting and XGBoost, consistently outperformed other models in terms of prediction accuracy and handling nonlinear relationships, although they require significant computational power. In contrast, simpler models like SVM and ANN demonstrated strong predictive capabilities with smaller datasets but were prone to overfitting and computational challenges. Additionally, unsupervised learning methods, such as K-means clustering and Principal Component Analysis (PCA), proved effective in classifying pavement conditions and detecting anomalies, with K-means offering simplicity and efficiency at the cost of sensitivity to initialization and cluster definitions. The review concludes by emphasizing the potential of hybrid and ensemble models to improve prediction accuracy and reduce computational costs, highlighting the need for further research to address data availability, model interpretability, and practical implementation challenges in real-world applications.

1 Introduction

Civil engineering has long relied on empirical methods and extensive experimental testing to evaluate the performance of materials, structures, and infrastructure systems. However, the increasing complexity of modern construction projects and the growing need for more accurate predictions of material behavior under varying conditions have led to a shift towards more data-driven approaches. In this context, machine learning (ML) has emerged as a powerful tool for advancing civil engineering, particularly in the field of material testing and performance prediction [1], [2].

Machine learning enables civil engineers to analyze vast amounts of experimental data, detect patterns, and build predictive models that can forecast material behavior under different loading conditions, environmental factors, and time frames. With the ability to model nonlinear relationships and optimize multiple variables simultaneously, ML offers significant advantages over traditional statistical and empirical models [3], [4]. It can enhance decision-making processes in areas such as material design, optimization, and failure prediction, thereby reducing costs, increasing efficiency, and improving overall performance [2], [5].

1.1 Machine learning in material testing

In civil engineering, material testing is critical for determining the properties of construction materials such as asphalt, concrete, and fiber-reinforced composites. These materials exhibit complex behaviors when subjected to stress, temperature changes, and aging. Machine learning models can simulate these behaviors and offer insights that would otherwise require costly and time-consuming physical tests [6]–[8].

For example, ML algorithms are used to predict key material properties such as compressive strength, modulus of elasticity, tensile strength, rut depth, fracture energy, and more. Techniques such as Artificial Neural Networks (ANNs), Support Vector Machines (SVMs), Random Forests (RF), and Gradient Boosting (GB) have demonstrated strong predictive capabilities in areas like asphalt mixture performance and concrete strength estimation. These models not only improve the accuracy of predictions but also allow for the integration of a wide range of input parameters,

* Corresponding author:
E-mail address: meisam.khorshidi@unh.edu

such as material composition, environmental conditions, and load types [6], [9]–[11].

1.2 Advantages and challenges

The application of machine learning in material testing offers several advantages. First, it reduces the reliance on extensive experimental testing by providing accurate predictions based on historical data. This is especially beneficial in large-scale infrastructure projects with limited time and resources [12]–[14]. Second, ML models are highly flexible, and able to account for nonlinear interactions between multiple variables, thus offering deeper insights into how different factors influence material behavior [15], [16]. Finally, these models can be continually improved as more data becomes available, leading to more refined predictions over time [17]–[19].

However, the adoption of machine learning in civil engineering also presents challenges. One of the primary concerns is the availability and quality of data. ML models require large datasets to function effectively, and inconsistencies in data collection can lead to inaccurate predictions [20], [21]. Moreover, the "black box" nature of some machine learning algorithms, particularly deep learning models, may hinder the interpretability of results, making it difficult for engineers to trust the outcomes without a clear understanding of how predictions were generated [22].

1.3 Current trends in research

Recent research in civil engineering has explored the use of machine learning models to solve complex material testing problems, including asphalt mixture performance and optimization, concrete property prediction and structural performance, and classification and pattern recognition in pavement systems. Many studies have demonstrated the effectiveness of machine learning in improving accuracy, reducing experimental costs, and providing actionable insights for material design and testing. For example, Artificial Neural Networks (ANNs) have been widely used to predict the compressive strength of concrete, while Support Vector Machines (SVMs) have shown strong performance in predicting fracture energy and elastic modulus in various materials [9], [10], [15]. Figure 1 illustrates key machine learning methods in civil engineering material testing, organized by learning type (supervised, unsupervised, ensemble, hybrid) and their applications in asphalt, concrete, and pavement analysis.

1.4 Scope of this review

This literature review aims to provide a comprehensive overview of the applications of machine learning in material testing within civil engineering, focusing on the following three key areas:

- Asphalt Mixture Performance and Optimization: Includes studies predicting the properties of asphalt mixtures, such as dynamic modulus, rut depth, and binder content, as well as optimizing asphalt mix designs.
- Concrete Property Prediction and Structural Performance: Covers the prediction of concrete properties like compressive strength, elasticity, and shear strength, as well as the performance of fiber-reinforced concrete.
- Classification and Pattern Recognition in Pavement Systems: Discusses studies that use machine learning to classify pavement distress, predict cracking patterns, and identify structural issues within pavement systems.

The review will discuss the different machine learning models used in literature, the key performance metrics they predict, and the pros and cons of each approach. Special emphasis will be placed on comparing multiple models applied simultaneously in material testing, as researchers increasingly use ensemble methods and comparative analysis to identify the best-performing models for specific engineering problems.

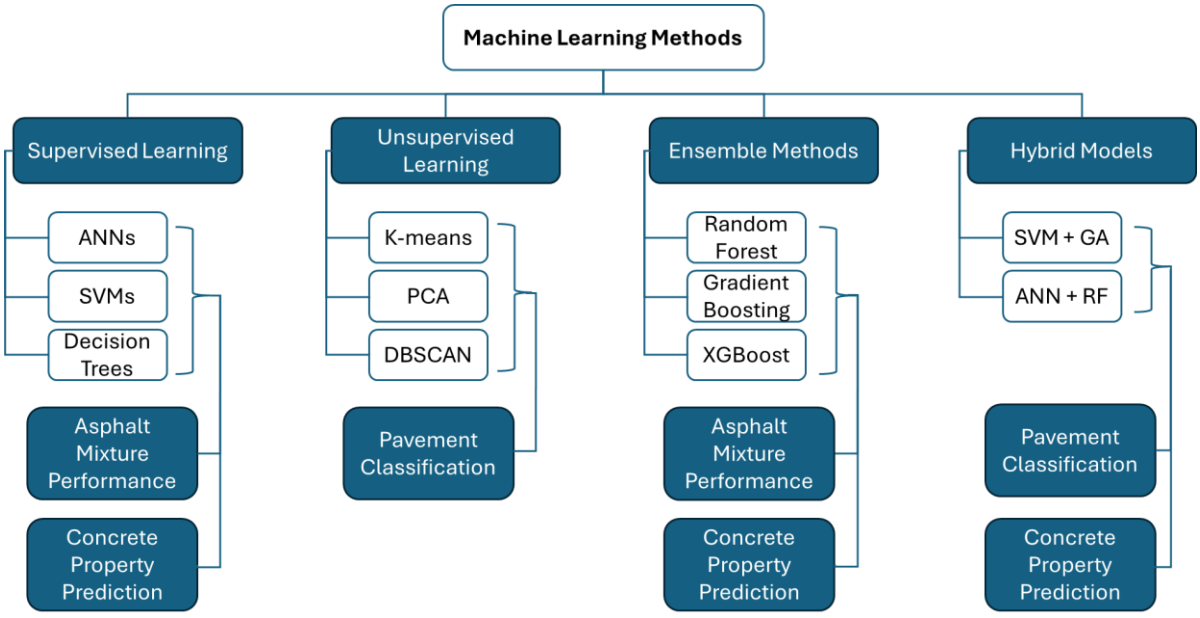

Figure 1. Machine learning methods in civil engineering material testing

2 Asphalt mixture performance and optimization

Machine learning has played a transformative role in the prediction and optimization of asphalt mixture performance, with various models being applied to forecast essential performance metrics such as dynamic modulus, rut depth, and Marshall stability.

Fan et al. (2024) utilized a Back-Propagation Neural Network (BPNN) and Support Vector Machine (SVM) to predict the strength of asphalt mixtures across diverse service conditions. They considered inputs such as stress states (direct tensile, uniaxial compression, indirect tensile, and four-point bending), temperature ranges from −25°C to 35°C, and loading rates between 0.02 MPa/s and 0.5 MPa/s. While SVM achieved slightly better accuracy (R^2 of 0.9983) than BPNN (R^2 of 0.9979), BPNN performed better in terms of minimizing small errors (Mean Absolute Percentage Deviation: 0.067 vs. 0.145). This demonstrated that although SVM excels in accuracy, BPNN could offer more consistent performance in specific scenarios by reducing smaller errors [2].

Upadhya et al. (2022) applied ANN, SVM, Gaussian Processes (GP), and Random Forest (RF) to predict the Marshall stability of glass fiber-reinforced asphalt mixes. The input variables included bitumen content, glass fiber content, fiber length, and bitumen grade, while the output variable was Marshall stability. The study showed that SVM with a Pearson Universal Kernel (PUK) achieved the best results (CC = 0.8776 and RMSE = 1.9653), making it the most accurate model for this application. ANN demonstrated reliable performance but showed higher errors during the testing phase, while GP and RF performed competitively but were outperformed by SVM. The results emphasized SVM's strength in managing nonlinear relationships, though its effectiveness depended heavily on kernel tuning, which posed a challenge in some applications [6].

In the study by Rondinella et al. (2023), SVM and Categorical Boosting (CatBoost) were applied to predict the mechanical and volumetric properties of road pavement asphalt mixtures incorporating recycled materials such as construction and demolition waste (C&DW) and reclaimed asphalt pavement (RAP). The input variables included gyratory revolutions, RAP content, water content, and bitumen properties, with the output variables being indirect tensile strength (ITS) and saturated surface dry voids (SSDV). CatBoost demonstrated superior accuracy (R^2 = 0.9916 for ITS) compared to SVM (R^2 = 0.8828), particularly excelling in handling categorical data, which made it more efficient for complex material datasets [4].

The study by Khorshidi et al. (2023) investigated the effects of different proportions of alternative materials, including Reclaimed Asphalt Pavement (RAP), crumb rubber (CR), steel slag (SS), and waste engine oil (WEO), on the performance of asphalt mixtures. Using 44 mixtures with varying RAP (0–75%), WEO (0–15%), CR (0–15%), and SS (0% or 20%) contents, the study evaluated cracking resistance, rutting resistance, and moisture damage. Machine learning models, including feed-forward neural networks (FNN), generalized linear models (GLM), support vector regression (SVR), and Gaussian process regression (GPR), were applied to predict the optimal content combinations. GPR performed the best, accurately identifying the most suitable material ratios for different high-traffic conditions. While GPR effectively modeled complex relationships, its computational demands and tuning requirements were noted as challenges. The study concluded that GPR provided reliable predictions for optimizing the balance between cracking resistance, rutting resistance, and moisture damage in asphalt mixtures with recycled materials [23].

Another study conducted by Khorshidi et al. (2023) assessed the effects of RAP, CR, SS, and WEO on the cracking resistance of asphalt mixtures. Using performance indices from the Illinois Flexibility Index Test (I-FIT), a deep neural network (DNN) model was applied to predict mixture performance and was compared with linear and polynomial regression models. The DNN outperformed the other models, achieving a coefficient of determination (R^2) of 0.84, compared to 0.60 for linear and 0.66 for polynomial regression. DNN's advantages included its ability to capture complex nonlinear relationships, providing more accurate predictions. However, it required more data and computational resources. Overall, DNN proved to be a reliable model for predicting cracking resistance in asphalt mixtures with recycled materials [5].

Liu et al. (2023) applied multiple models, including SVR, KRR, ANN, Gradient Boosting (GB), and XGBoost, to predict the dynamic modulus (|E*|) of asphalt mixtures. The input variables consisted of temperature, loading frequency, binder properties (such as viscosity and phase angle), and aggregate gradation. XGBoost delivered the highest accuracy (R^2 = 0.9867, RMSE = 2.7422) due to its ability to handle nonlinear interactions and prevent overfitting through regularization techniques. However, it required considerable computational resources, which posed a limitation for its scalability in large-scale applications. Other models like ANN, while effective, were prone to overfitting and required substantial hyperparameter tuning, which made them less practical for routine use [1].

Liu et al. (2022) further explored the prediction of rut depth using SVR, RF, ANN, and GB models. The input variables included traffic data (e.g., Equivalent Single Axle Loads, ESALs), climate conditions, pavement material properties (e.g., binder content, air voids), and structural attributes (layer thicknesses). GB was identified as the best-performing model, achieving an R^2 of 0.9236, showcasing its effectiveness in capturing nonlinear interactions within the dataset. While ANN also performed well (R^2 = 0.9021), it required more computational power and tuning. RF lagged in performance with lower accuracy, while SVR showed significant variance in predictions due to its sensitivity to parameter selection [24].

In a separate study, Liu et al. (2022) used machine learning models to predict effective asphalt content (Pbe) and absorbed asphalt content (Pba) in asphalt mixtures. Gradient Boosting was the top performer, with R^2 values of 0.9479 and 0.9459 for Pbe and Pba, respectively, excelling in managing nonlinear relationships. RF performed adequately but was less accurate compared to Gradient Boosting. SVR showed moderate accuracy but was more prone to performance drops when handling larger datasets [25].

Liu et al. (2022) also explored the prediction of the International Roughness Index (IRI) of asphalt pavements using Support Vector Regression (SVR), Random Forest (RF), Artificial Neural Networks (ANN), Gaussian Process Regression (GPR), Extra-Trees, and Gradient Boosting (GB), combined with dimensionality reduction techniques like Autoencoders (AE), Principal Component Analysis (PCA), and Recursive Feature Elimination (RFE). The input variables included temperature, Equivalent Single Axle Loads (ESALs), layer thickness, binder content, air voids, and aggregate gradation, while the output variable was IRI. The AE-GPR model demonstrated the highest accuracy

(R^2 = 0.939), outperforming other models by efficiently managing high-dimensional data. Autoencoders significantly improved model performance by reducing input noise and computational load. In contrast, models like SVR and RF showed lower performance due to overfitting and sensitivity to hyperparameter tuning, while ANN performed well but was computationally expensive [26].

Majidifard et al. (2020) employed Gene Expression Programming (GEP) to predict rut depth in asphalt mixtures subjected to the Hamburg Wheel-Tracking Test (HWTT). The model inputs included asphalt binder properties, aggregate size, and reclaimed asphalt content, while the output was rut depth. GEP outperformed ANN by providing explicit mathematical expressions, making the model more interpretable and offering engineers insights into the factors driving rutting behavior. However, GEP required careful tuning of parameters like chromosome length, limiting its practicality for complex datasets [27].

Rahman et al. (2021) explored various ensemble methods, including Extra-Trees, GB, and SVR, to predict rut depth and indirect tensile (IDT) strength in asphalt mixtures. Extra-Trees demonstrated the highest prediction accuracy (R^2 = 0.922 for rut depth), but it was sensitive to imbalanced data, which affected its generalization. GB and SVR provided more robust predictions across diverse datasets but required more extensive computational resources to minimize bias and ensure balanced predictions [9].

Tiwari et al. (2022) applied ANN with various activation functions (Exponential Linear Unit, ELU, and Hyperbolic Tangent, TanH) to predict the mechanical properties of asphalt mixes with industrial waste fillers. The input variables included air void content, filler type, and filler content, while the output variables included Marshall stability and indirect tensile strength. The TanH activation function performed better, achieving R^2 = 0.9967, though it required higher computational power due to increased complexity in capturing nonlinear relationships [28].

In another study, Tiwari et al. (2023) applied ANN with different activation functions, including TanH and ELU, to predict mechanical properties of asphalt mixtures with silica fume fillers. The TanH-SNN model achieved the highest accuracy (R^2 = 0.9988), outperforming other models in terms of capturing nonlinear relationships between inputs and outputs, though the increased complexity required more computational power [29].

Ali et al. (2021) used XGBoost to predict dynamic modulus in asphalt mixtures, outperforming traditional models such as the Witczak and Hirsch models (R^2 = 0.961). XGBoost's strength lay in its ability to handle complex nonlinear relationships and avoid overfitting, though its computational demands limited its practicality in smaller-scale applications. ANN models, while competitive, lacked interpretability and required more extensive resources to train [30].

Mirzaiyanrajeh et al. (2022) used ANN, Self-Validated Ensemble Modeling (SVEM), and Augmented Full Quadratic Model (AFQM) to predict low-temperature fracture energy of asphalt mixtures. ANN provided the highest accuracy but was computationally expensive, whereas SVEM, although slightly less accurate, was more efficient with small datasets, striking a balance between accuracy and computational efficiency [31].

Liu et al. (2023) utilized recurrent neural networks (RNN), long short-term memory (LSTM), and gated recurrent units (GRU) for time series modeling to predict rutting depth. Input variables included historical rutting depth, temperature, and pavement properties. GRU outperformed both RNN and LSTM, achieving an R^2 value of 0.90. GRU's ability to retain long-term memory with fewer parameters made it more computationally efficient, though LSTM still performed well in capturing seasonal trends in the data [32].

Finally, Al-Sabaeei et al. (2023) employed XGBoost and Random Forest Regression (RFR) to predict mixing and compaction temperatures for bio-modified asphalt using crude palm oil (CPO) and tire pyrolysis oil (TPO) as modifiers. XGBoost outperformed RFR in predicting shear viscosity, but RFR demonstrated better accuracy for temperature predictions, with R^2 values of 0.96583 for mixing temperature and 0.96281 for compaction temperature. Both models excelled in accuracy but were limited by their high computational requirements [33].

2.1 Summary of methods

Table 1 provides a detailed summary of studies focusing on machine learning approaches and their applications in asphalt mixture performance prediction. Across the studies reviewed, several machine learning methods were employed to predict key asphalt mixture performance metrics, including dynamic modulus, rut depth, Marshall stability, International Roughness Index (IRI), and crack resistance. Each method presented unique strengths and weaknesses, as highlighted below:

- Artificial Neural Networks (ANNs): Frequently used for predicting complex performance metrics, ANNs demonstrated strong accuracy in predicting properties such as Marshall stability, dynamic modulus, and fracture energy. ANNs excel in capturing intricate nonlinear relationships between variables, especially when paired with activation functions like TanH and ReLU. However, their major drawbacks include computational expense, the need for large datasets, and a propensity for overfitting without careful tuning of hyperparameters. In studies by Upadhya et al. (2022) Tiwari et al. (2022), and Khorshidi et al. (2023), ANNs and DNNs performed well but required significant computational resources and hyperparameter optimization [5], [6], [28].
- Support Vector Machines (SVMs): SVM models, particularly when paired with kernel methods like the Pearson Universal Kernel (PUK), were highly accurate in predicting metrics such as strength and Marshall stability. SVMs excel in handling nonlinear relationships and are particularly effective with small- to medium-sized datasets. However, as seen in studies like Fan et al. (2024) and Upadhya et al. (2022), SVMs require careful kernel tuning and can struggle with large datasets due to high computational costs and sensitivity to hyperparameters [2], [6].
- Gradient Boosting (GB) and XGBoost: These ensemble learning methods consistently outperformed other models in predicting dynamic modulus, rut depth, and other asphalt mixture properties. XGBoost, in particular, has proven to be highly effective at managing nonlinear interactions, regularizing models to avoid overfitting, and delivering superior prediction accuracy. This method was widely used in studies such as Liu et al. (2023) and Ali et al. (2021), where XGBoost delivered top results in predicting dynamic modulus and shear viscosity [1], [30]. However, XGBoost requires significant computational power and tuning, which can limit its practicality in certain applications.
- Gaussian Process Regression (GPR): GPR excels at modeling complex nonlinear relationships and provides both predictions and uncertainty estimates. It is particularly effective for small to medium datasets but can be

computationally demanding and requires careful tuning of hyperparameters. In studies by Khorshidi et al. (2023), GPR outperformed other models in predicting the optimal combinations of alternative materials in asphalt mixtures, accurately balancing cracking resistance, rutting resistance, and moisture damage, though its high computational requirements were noted [23].

- Random Forest (RF): While RF models provided solid predictions, particularly in larger datasets, they generally lagged behind ensemble methods like Gradient Boosting in terms of accuracy. Studies such as Liu et al. (2022) and Rahman et al. (2021) showed that RF models, though effective in certain scenarios, were prone to higher error rates when handling complex datasets and large feature spaces [9], [26]. RF's strength lies in its ability to handle overfitting better than simpler models, but it can underperform when compared to more advanced techniques like XGBoost.
- Gene Expression Programming (GEP): GEP, as applied by Majidifard et al. (2020), provided interpretable models that elucidate the relationships between input variables and performance metrics, such as rut depth. This transparency made GEP attractive for engineers who require interpretable results [27]. However, GEP required precise parameter tuning, making it less effective for highly complex datasets or situations where rapid model development was needed.
- Autoencoders (AE) and Dimensionality Reduction Techniques: In Liu et al. (2022), the combination of Autoencoders (AE) with Gaussian Process Regression (GPR) showed how dimensionality reduction can improve machine learning models by reducing input noise and computational complexity. AE-GPR outperformed models like SVR and RF by effectively managing high-dimensional data in predicting IRI, proving that reducing input space can lead to improved accuracy and efficiency [26].
- Self-Validated Ensemble Modeling (SVEM): While less commonly used, SVEM provided a balanced approach between accuracy and computational efficiency, especially for smaller datasets. In Mirzaiyanrajeh et al. (2023), SVEM was found to be more practical than ANN in predicting fracture energy for smaller datasets, offering reliable results with fewer computational resources [31]. However, its predictive capacity could be slightly lower than ANN in more complex scenarios.

Table 1. Summary of machine learning applications in predicting asphalt mixture performance: overview of data collection methods, model types, and justifications for model selection across studies

Reference	Method of Data Collection	Database Size	Input Variables	Output Variables	Type of Model	Justification for Model Selection	Availability of Code/Database
Fan et al., 2024[2]	Experimental tests under various conditions	Not specified	Stress state, temperature, loading rate	Asphalt mixture strength	BPNN, SVM	Chosen for multi-field interaction prediction in asphalt strength; SVM showed better accuracy	Data available upon request
Upadhya et al., 2022[6]	Experimental data from lab tests and literature	110 observations	Bitumen content, glass fiber, bitumen grade, fiber length, fiber diameter	Marshall stability	ANN, SVM, GP, RF	SVM_PUK was optimal for accuracy in predicting Marshall stability	Not disclosed
Rondinella et al., 2023[4]	Experimental data with hot and cold asphalt mixtures, using C&DW and RAP	70 observations	RAP, construction and demolition waste content, water, cement, emulsion bitumen, total bitumen, gyratory revolutions	SSDV, ITS	SVM, CatBoost	CatBoost was chosen for high predictive accuracy, with R^2 = 0.99 in ITS predictions	Data available upon request
Khorshidi et al., 2023[23]	Experimental data with varying RAP, CR, WEO, and SS contents	44 mixtures	RAP content, crumb rubber, waste engine oil, steel slag	Rutting, cracking, moisture resistance	FNN, GLM, SVM, GPR	GPR chosen for accuracy in identifying optimal material ratios for performance	Data unavailable due to privacy restrictions
Khorshidi et al., 2023[5]	Experimental data from I-FIT tests with recycled materials in RAP mixtures	Not specified	RAP, crumb rubber, waste engine oil, steel slag aggregates	Cracking performance indices (RDCI, FI, CT-index, FN, TSR)	DNN, Linear, Polynomial regression	DNN selected for best prediction accuracy; MAE, RMSE, and R^2 validation metrics support model choice	Not disclosed

Ali et al., 2021[30]	Tiwari et al., 2023[29]	Tiwari et al., 2022[9]	Rahman et al., 2021[9]	Majidifard et al., 2021[27]	Jian Liu et al., 2022[26]	Jian Liu et al., 2022[25]	Liu et al., 2022[24]	Liu et al., 2023[1]
Experimental data from dynamic modulus tests on asphalt mixtures	Experimental data comparing OPC with silica fume as a filler	Experimental data from lab tests using industrial waste fillers	Data from Texas Department of Transportation (TxDOT) SMGR database	Comprehensive collection of Hamburg test results for asphalt mixtures	LTPP database for IRI prediction with ML models	Data from LTPP program focusing on rut depth for surface AC layer design	Literature and lab data from Superpave mix design	Combined experimental data and NCHRP 9–19 database
1152 observations	24 mixtures	32 samples (expanded to 56 through data	3,139 samples (HWT), 2,805 samples (IDT)	96 tests (288 samples)	194 sections	356 pavement sections	512 entries (cleaned to 441)	7400 samples
Testing conditions, volumetric properties, gradation	Filler content, bitumen content, material type	Filler type, filler content, air voids	Aggregate gradation, absorption, binder content, PG, warm mix additive, RAP/RAS, density, wheel-passes	Mix type, temperature, high-temperature PG grade, AC, NMAS, ABR, RAP, RAS, gradation type, aggregate type, CRC, wheel passes	Climate, subgrade, base, binder, asphalt layer properties	Traffic, climate, pavement material properties, pavement structure	Gradation, binder properties, bulk specific gravity, blend absorption, air void, PG grade, gyrations (Ndes)	Test conditions, binder properties, gradation, volumetric properties
Dynamic modulus	Marshall stability, ITS, water sensitivity	Marshall stability, Marshall quotient, ITS, ITSR	HWT rut depth, IDT strength	Rut depth	International roughness index (IRI)	Rut depth	Effective asphalt content (Pbe), absorbed asphalt content (Pba)	Dynamic modulus ($\|E^*\|$)
XGBoost	ANN (Shallow Neural Network)	SNN (ANN-based model)	SVR, Bagging, RF, Extra-trees, GB	GEP, ANN	SVR, RF, ANN, GPR, Extra-trees, GB	SVR, RF, ANN, Gradient Boosting	SVR, Ridge, RF, AdaBoost, GB	SVR, KRR, ANN, GPR, GB, XGBoost
XGBoost chosen for high accuracy in nonlinear relationships; robust performance across varying temperatures and frequencies	ANN was chosen for small data modeling with high accuracy, enhanced by leave-one-out cross-validation	SNN chosen for reliability in small datasets, enhanced through k-fold cross-validation and MAKIMA data augmentation	Extra-trees achieved highest accuracy (R^2 = 0.922 for HWT and R^2 = 0.904 for IDT)	GEP was chosen for transparency and interpretability, with superior accuracy over ANN on validation	AE-GPR model chosen for optimal prediction accuracy (R^2 = 0.94) when combined with autoencoders	Gradient Boosting selected for highest performance (R^2 = 0.92) compared to other models	Gradient Boosting chosen for best prediction accuracy (R^2 = 0.948)	XGBoost chosen for highest predictive accuracy (R^2 = 0.987); feature importance shows binder and test conditions as key factors
Not disclosed	Data available upon request	Not disclosed	Data available upon request	Data available upon request	Not disclosed	Not disclosed	Data unavailable due to permission restrictions	Not disclosed

Mirzaiyanrajeh et al., 2023 [31]	Experimental data from DCT tests for fracture energy	852 samples	Binder grade, aggregate type, RAP content, ESALs, VMA, gradation	Fracture energy	ANN, SVEM, AFQM	SVEM chosen for high reliability and efficiency; ANN for non-linear accuracy	Web-based model provided
Liu et al., 2023[32]	Time-series data from RIOHTrack on rutting depth of 19 pavement sections	19 sections (44 months)	Climate, traffic, pavement structure, material properties	Rutting depth	RNN, LSTM, GRU, ARIMAX, GP, K-means	GRU with time series architecture chosen for high accuracy in capturing seasonal patterns	Code available on Google Colab
Al-Sabaei et al., 2023[33]	Experimental lab data from dynamic shear viscosity tests on bio-modified asphalt	16 samples (various CPO and TPO levels)	CPO%, TPO%, test temperature	Shear viscosity, mixing and compaction temperatures	XGBoost, RFR, RSM	XGBoost chosen for high accuracy in shear viscosity; RFR for optimal mixing and compaction prediction accuracy	Not disclosed

2.2 Overall trends

The studies reviewed consistently demonstrated that ensemble methods such as Gradient Boosting and XGBoost were the most effective in terms of both accuracy and robustness. These models were particularly useful in handling large datasets and complex, nonlinear relationships within asphalt mixture data. However, their high computational costs and complexity in hyperparameter tuning limited their practicality in some real-world scenarios. On the other hand, simpler models like SVM and ANN, while still effective in certain cases, struggled with overfitting and computational demands when faced with large, high-dimensional datasets. GPR also proved highly effective, particularly for small to medium datasets, though it required substantial computational resources and careful tuning. Dimensionality reduction techniques such as Autoencoders (AE) and Principal Component Analysis (PCA) helped mitigate these issues by streamlining input features, improving the efficiency and accuracy of models like GPR and SVR.

Finally, interpretability remains a key consideration, with methods like Gene Expression Programming (GEP) offering more transparent models than black-box approaches like ANN and XGBoost. This interpretability can be critical for engineers looking to understand the underlying relationships between variables and performance outcomes.

3 Concrete property prediction and structural performance

Machine learning (ML) models have become an essential tool in predicting concrete properties and optimizing structural performance, addressing the limitations of traditional empirical methods. This section explores various machine learning techniques applied to predict key concrete properties such as compressive strength, tensile strength, modulus of elasticity, and fracture energy. These studies demonstrate the advantages and disadvantages of different ML approaches in terms of prediction accuracy, computational complexity, and model interpretability.

Song et al. (2022) applied machine learning models such as Artificial Neural Networks (ANN), Support Vector Machines (SVM), Decision Trees (DT), Random Forest (RF), and Gradient Boosted Regression Trees (GBRT) to optimize cementitious material mixtures. Input variables included water content, cement content, supplementary cementitious materials (SCMs), and aggregate content, while the outputs were uniaxial compressive strength (UCS) and durability. ANN excelled in capturing nonlinear relationships but required significant computational resources and careful tuning to avoid local minima. SVM performed well in generalization but was highly sensitive to hyperparameter tuning, and RF improved accuracy by reducing variance, though it came with higher computational costs. GBRT offered the highest accuracy in UCS prediction but increased computational complexity. Metaheuristic algorithms such as Particle Swarm Optimization (PSO) and Genetic Algorithms (GA) were used to optimize the model parameters and enhance the performance of the ML models [34].

Hafez et al. (2022) developed a machine learning regression model, Pre-bcc, to predict slump, compressive strength, carbonation, and chloride ingress resistance for blended cement concrete (BCC) using supplementary cementitious materials (SCMs) such as fly ash, ground granulated blast-furnace slag, silica fume, lime powder, and calcined clay. Input variables included SCM types and proportions. ANN, RF, and SVM models were tested, with RF showing better accuracy and interpretability, though computationally intense. SVM required careful tuning but handled generalization well. Pre-bcc offers high prediction accuracy for slump and strength but is computationally complex when handling multiple SCMs, improving the understanding of SCM effects in BCC [16].

Hafez et al. (2023) then introduced Opt-bcc, an optimization tool using Genetic Algorithms (GA) with Pre-bcc to optimize sustainability scores of blended cement concrete mixes. Input variables included various SCM types and proportions, while output variables were strength, slump, and durability indices. GA effectively minimized environmental and cost impacts but required complex tuning. Opt-bcc achieved significant cost and environmental reductions compared to existing models, though functional parameter prediction models were nonlinear, demanding higher computational resources. This study highlighted GA's potential in eco-friendly concrete optimization while balancing functional and economic criteria [35].

Pfeiffer et al. (2024) utilized an amortized Gaussian Process (GP) model integrated with an inverse optimization framework to design concrete mixes minimizing climate impact and cost. Input variables were SCM proportions, water/cementitious material ratio, and aggregate composition, while the output variable was compressive

strength at 28 days. The GP model provided mean predictions and uncertainty estimates, making it more robust than traditional models like ANN and RF, which lack uncertainty measures. The GP's flexibility for industrial-scale datasets added accuracy, but computational demands were significant. This study demonstrated GP's effectiveness for mix design, balancing environmental and economic objectives with structural performance requirements [36].

Moein et al. (2023) reviewed several machine learning and deep learning models for predicting concrete properties, including SVM, ANN, Random Forest, and Extreme Learning Machines (ELM). The input variables included cement content, aggregate composition, water-cement ratio, and curing age. ANN showed high accuracy but was prone to overfitting without proper tuning, while SVM was more effective for smaller datasets but struggled with high-dimensional data. ELM provided faster training times compared to ANN but at the cost of prediction accuracy. Genetic Algorithms (GA) were used to enhance model optimization when combined with other ML models. Random Forest and ANN were identified as the most reliable models for concrete property prediction, with RF offering better interpretability and ANN excelling in predictive performance [11].

Yu et al. (2018) compared an Enhanced Cat Swarm Optimization (ECSO)-optimized SVM model with traditional models like ANN and Extreme Learning Machines (ELM) for predicting the compressive strength of high-performance concrete (HPC). Input variables included water content, cement content, and supplementary materials. The ECSO-optimized SVM model achieved superior accuracy (R^2 = 0.9526), outperforming ANN (R^2 = 0.8716). While SVM required significant parameter tuning, ECSO improved the convergence rate and avoided local minima, making it more efficient. ANN, though effective, suffered from overfitting and was computationally expensive [37].

Pham et al. (2016) used a Least Squares Support Vector Regression (LS-SVR) model optimized by the Firefly Algorithm (FA) to predict the compressive strength of high-performance concrete (HPC). Input variables included cement, aggregates, and curing conditions. FA-LS-SVR achieved the highest accuracy (R^2 = 0.89) compared to ANN and traditional SVM models. The optimized SVM model outperformed ANN by providing better generalization and reducing prediction errors. However, the model required careful tuning of parameters like penalty factors, making it computationally demanding [38].

Yaseen et al. (2018) used Extreme Learning Machines (ELM) to predict the compressive strength of lightweight foamed concrete, outperforming other models like Multivariate Adaptive Regression Splines (MARS) and M5 Tree. Input variables included cement content, oven dry density, and foam volume. ELM achieved an R^2 of 0.875, making it the fastest model in terms of training speed, though it was less accurate for highly complex data. MARS and M5 Tree provided reasonable accuracy but failed to capture complex relationships, while ELM's fast training and simplicity made it an efficient option for lightweight concrete strength prediction [39].

Omran et al. (2016) compared Gaussian Process Regression (GPR), Multilayer Perceptron (MLP), and Support Vector Machines (SVM) for predicting the compressive strength of environmentally friendly concrete. GPR outperformed the other models, achieving the highest accuracy (R^2 = 0.9842) and offering better generalization through its probabilistic approach. However, GPR was computationally intensive. Ensemble methods like Additive Regression and Bagging with GPR also provided high accuracy, while SVM and MLP required extensive parameter tuning to avoid overfitting. GPR was highlighted for its balance between accuracy and computational efficiency, making it a strong choice for concrete strength prediction [40].

Bonifácio et al. (2019) applied Support Vector Regression (SVR) and the Finite Element Method (FEM) to predict the compressive strength and Young's modulus of lightweight aggregate concrete (LWAC). SVR outperformed FEM slightly, achieving a lower deviation from experimental results (5.46% for compressive strength), with the key advantage being SVR's reusability with new data and speed. FEM, although slightly less accurate, required fewer inputs and was advantageous in cases where experimental results were scarce. SVR required a larger training dataset, making it more computationally intensive [10].

Tanyildizi (2018) applied ANN and SVM to predict the strength properties of carbon fiber-reinforced lightweight concrete exposed to high temperatures. Input variables included silica fume, carbon fiber content, and temperature. ANN achieved the highest accuracy (R^2 = 0.9902 for compressive strength), outperforming SVM (R^2 = 0.9701). While ANN offered superior predictive accuracy, it required more computational resources and careful optimization of hidden neurons and learning algorithms. SVM was simpler to use but less accurate, making it a better choice for smaller datasets [15].

Mozumder et al. (2017) used Support Vector Regression (SVR) to predict the uniaxial compressive strength of fiber-reinforced polymer (FRP) confined concrete, achieving higher accuracy (R^2 = 0.9832 for CFRP) than ANN models and empirical methods. SVR's ability to avoid local minima and provide better generalization made it a more reliable method, though it required substantial computational effort and parameter tuning compared to ANN, which suffered from slower convergence and higher prediction errors [8].

Keshtegar et al. (2019) applied a hybrid RSM-SVR model to predict the shear strength of steel fiber-reinforced concrete beams (SFRCBs). The hybrid model outperformed ANN and other traditional methods, achieving an R^2 of 0.9508, thanks to its ability to capture nonlinear relationships and cross-correlations between input variables. Although the hybrid model required significant computational power, it proved to be the most accurate for predicting SFRCBs shear strength, demonstrating the advantage of combining multiple modeling approaches [7].

Aiyer et al. (2014) compared Least Square Support Vector Machines (LSSVM) and Relevance Vector Machines (RVM) for predicting the compressive strength of self-compacting concrete. RVM outperformed LSSVM and ANN, offering additional benefits such as handling variance and uncertainty. While LSSVM was accurate, RVM's ability to calculate variance made it a better tool for assessing uncertainty in predictions, especially in civil engineering applications [41].

Yuvaraj et al. (2013) applied SVR to predict fracture characteristics, such as fracture energy and failure load, of high-strength and ultra-high-strength concrete beams. The SVR model achieved high prediction accuracy (R^2 close to 1 for all parameters), outperforming traditional empirical models. The SVR model's strength lay in its ability to handle nonlinear relationships even with limited datasets, though it required careful parameter tuning to optimize its predictive performance [42].

Yan & Shi (2010) used SVM to predict the elastic modulus of normal and high-strength concrete,

outperforming traditional empirical models. SVM achieved better accuracy with fewer parameters compared to empirical models, though it required careful tuning of kernel parameters. ANN, while effective, was more complex to tune and prone to local minima, making SVM the preferred model for this application [43].

Nazari & Sanjayan (2015) optimized SVM using Genetic Algorithm (GA), Particle Swarm Optimization (PSO), and other metaheuristic algorithms to predict the compressive strength of geopolymer concrete. The hybrid models, particularly the ICOA-SVM model, achieved superior prediction accuracy (R^2 = 0.8993), though they were computationally intensive due to the optimization process [44].

Deng et al. (2018) used Convolutional Neural Networks (CNN) to predict the compressive strength of recycled aggregate concrete (RAC), outperforming both Backpropagation Neural Networks (BPNN) and SVM in terms of accuracy and efficiency. CNN's advantage was its ability to automatically extract deep features from input data without requiring manual preprocessing, though it was more computationally intensive [45].

Kaloop et al. (2019) compared LSSVM, ANN, and regression models to predict the resilient modulus (Mr) of recycled concrete aggregate blends. LSSVM achieved the highest accuracy (R^2 = 0.982), outperforming both ANN and regression models, particularly with smaller datasets, though it required careful tuning of regularization parameters [46].

Cheng et al. (2014) applied the Genetic Weighted Pyramid Operation Tree (GWPOT) to predict the compressive strength of high-performance concrete, outperforming ANN and SVM models. GWPOT provided interpretable mathematical formulas, offering better transparency, though it required higher computational resources for optimization [47].

Zhang et al. (2019) used Random Forest (RF) optimized with Beetle Antennae Search (BAS) to predict the uniaxial compressive strength of lightweight self-compacting concrete. BAS improved the hyperparameter tuning process, resulting in an R^2 value of 0.97, significantly outperforming traditional regression models. However, the computational complexity was higher due to the optimization process [48].

3.1 Summary of methods

Table 2 provides a detailed summary of studies focusing on machine learning approaches and their applications in predicting concrete properties. In the reviewed studies, machine learning techniques were applied to predict concrete properties such as compressive strength, tensile strength, modulus of elasticity, and fracture energy, offering improvements in accuracy and efficiency over traditional empirical methods. The following methods were highlighted for their strengths and weaknesses:

- Artificial Neural Networks (ANNs): ANNs were frequently applied in predicting nonlinear relationships in concrete properties, such as compressive strength and fracture energy. Studies like Tanyildizi (2018) and Song et al. (2022) demonstrated that ANNs performed well in capturing complex data patterns [15], [34]. However, ANNs often faced challenges such as overfitting and the need for large datasets, which made them computationally expensive. Yu et al. (2018) and Mozumder et al. (2017) further emphasized that proper tuning of hyperparameters, such as the number of hidden neurons and learning rates, is crucial to achieving high accuracy without overfitting [8], [37].
- Support Vector Machines (SVMs): SVMs were consistently highlighted as strong performers, especially when dealing with smaller datasets, as shown in Yu et al. (2018), Mozumder et al. (2017), and Yan & Shi (2010) [8], [37], [43]. SVM models excelled at predicting compressive strength, fracture characteristics, and elastic modulus, particularly when optimized using techniques such as Enhanced Cat Swarm Optimization (ECSO) and the Firefly Algorithm (FA) [37], [38]. These optimizations significantly improved convergence and accuracy. However, SVMs can be computationally intensive and sensitive to hyperparameter tuning, requiring careful selection of kernel functions.
- Random Forest (RF): Random Forest models, applied in studies such as Song et al. (2022) and Zhang et al. (2019), were particularly effective in handling complex, high-dimensional datasets [34], [48]. RF's ability to reduce overfitting by averaging multiple decision trees made it a popular choice for predicting properties like compressive strength. Despite its robustness, RF models are computationally demanding and require tuning of hyperparameters such as the number of trees and depth to achieve optimal results.
- Gradient Boosting and Boosted Regression Trees (GBRT): Gradient Boosting models were often the most accurate in predicting concrete properties, particularly in Song et al. (2022) where they excelled at predicting uniaxial compressive strength (UCS) [34]. These models effectively captured nonlinear relationships between variables but came at a high computational cost due to their iterative learning process. Gradient Boosting methods like XGBoost are powerful but require significant tuning to prevent overfitting, especially when dealing with large datasets.
- Extreme Learning Machines (ELM): Yaseen et al. (2018) demonstrated that ELM models provided a fast and computationally efficient method for predicting concrete properties, particularly lightweight foamed concrete [39]. ELM's ability to train quickly made it useful for simpler datasets, but it lacked the accuracy of more complex models like RF and Gradient Boosting when dealing with high-dimensional or intricate data.
- Gaussian Process Regression (GPR): Omran et al. (2016) highlighted that GPR was highly accurate in predicting concrete compressive strength [40]. GPR's probabilistic approach offered the added benefit of estimating uncertainty, which made it suitable for cases where confidence in the predictions was critical. However, GPR's computational demands increase significantly with larger datasets, limiting its practicality for large-scale applications.
- Least Squares Support Vector Machines (LSSVM): Enhanced versions of SVM, such as LSSVM, were applied in Pham et al. (2016) and Kaloop et al. (2019) to improve predictive performance and computational efficiency [38], [46]. LSSVM, optimized by metaheuristic algorithms like the Firefly Algorithm (FA), outperformed standard SVM and ANN models, especially in smaller datasets. However, LSSVM still required careful tuning of parameters like the regularization factor to achieve high accuracy.
- Convolutional Neural Networks (CNNs): In Deng et al. (2018), CNNs were shown to outperform traditional models like SVM and Backpropagation Neural Networks (BPNN) when predicting compressive strength in recycled aggregate concrete [45]. CNNs excelled at automatically extracting deep features from raw data, which improved accuracy and reduced the need for manual feature engineering. However,

CNNs are computationally intensive and require large datasets to fully leverage their potential.

- Hybrid Models (e.g., RSM-SVR, ANN-MOGWO): Hybrid models combining machine learning algorithms with optimization techniques, such as Keshtegar et al. (2019)'s RSM-SVR model, showed superior performance in predicting complex properties like shear strength [7]. These models combine the strengths of multiple techniques, improving accuracy by capturing nonlinearities and complex relationships between variables. However, hybrid models are computationally expensive due to the complexity of integrating multiple approaches.

Table 2. Summary of Machine Learning Applications in Predicting Concrete Properties: Overview of Data Collection Methods, Model Types, and Justifications for Model Selection Across Studies

Reference	Method of Data Collection	Database Size	Input Variables	Output Variables	Type of Model	Justification for Model Selection	Availability of Code/Database
Hafez et al., 2022[16]	Experimental data from >150 sources	1650+ data points	SCM types, replacement percentages, mix design parameters (e.g., slump, strength, carbonation resistance)	Slump, strength, carbonation resistance, chloride ingress	Multi-layer regression	Captures wide variety of SCMs and functional properties with high statistical accuracy (R = 0.94-0.97)	Available online via Pre-bcc tool
Pfeiffer et al., 2024[36]	Industrial dataset (job site data from 2017-2020)	9296 mixes	Water/cement ratio, SCM quantities, 12 constituent features	Compressive strength	Amortized Gaussian Process	Captures strength evolution with uncertainty estimates and supports optimization for cost and climate impact	Not disclosed
Hafez et al., 2023[35]	Regression model predictions via Pre-bcc	Derived from Pre-bcc model	SCM types, mix proportions, sustainability indicators	Strength, slump, chloride resistivity, carbonation	Genetic Algorithm (Opt-bcc tool)	Optimizes sustainability score (economic, environmental, and functional properties) with superior results	Available online via Opt-bcc tool
Yu et al., 2018[37]	Data collected from 183 studies (1998–2015)	1761 groups of data	Water, cement, blast furnace slag, fly ash, superplasticizer, coarse and fine aggregates, curing age	Compressive strength	Enhanced Cat Swarm Optimization-SVM	Superior optimization of SVM parameters for high accuracy and efficiency	Not disclosed
Pham et al., 2015[38]	Experimental data from the Nga Ba Hue infrastructure project	239 tests	Cement, sand, small and medium coarse aggregate, water, superplasticizer, curing time	Compressive strength	Firefly Algorithm-Optimized LS-SVR	High accuracy and generalization for HPC strength prediction; RMSE validation	Not disclosed
Yaseen et al., 2018[39]	Experimental database retrieved from literature	91 data points	Cement content, oven dry density, water/binder ratio, foam volume	Compressive strength	Extreme Learning Machine (ELM), MARS, M5 Tree, SVR	ELM chosen for superior accuracy and reliability over other methods in predicting compressive strength of foamed concrete	Not disclosed
Omran et al., 2016[40]	Experimental data for compressive strength prediction	144 data points	Cement type, curing age, water, cementitious material, fly ash, sand, pea gravel, Haydite lightweight aggregate, Micro Air	Compressive strength	Gaussian Processes Regression, Additive Regression, Bagging, M5P, REPTree, Multilayer Perceptron	GPR achieved the highest prediction accuracy (R^2 = 0.9842); additive regression and bagging enhanced predictive performance	Not disclosed
Bonifácio et al., 2019[10]	Experimental data from Lightweight Aggregate Concrete (LWAC)	180 mixtures	Water/cement ratio, quantity of cement, aggregate volume, aggregate density	Compressive strength, Young's modulus	Support Vector Regression (SVR), Finite Element Method (FEM)	SVR achieved lower average error compared to FEM; both methods validated against experimental results	Not disclosed

Zhang et al., 2019[48]	Cheng et al., 2014[47]	Kaloop et al., 2019[46]	Deng et al., 2018[45]	Nazari and Sanjayan, 2015[44]	Yan and Shi, 2010[43]	Yuvaraj et al., 2013[42]	Aiyer et al., 2014[41]	Keshtegar et al., 2019[7]	Mozumder et al., 2017[8]	Tanyildizi, 2018[15]
Laboratory-based dataset for lightweight self-compacting concrete	Experimental data from UCI repository	Experimental data from recycled aggregate/ concrete blends	Experimental data on recycled concrete	Experimental data from literature	Experimental data for NSC and HSC	Experimental data from fracture tests on HSC and UHSC	Experimental data from SCC with database by Siddique et al. (2011)	Experimental data for steel fiber-reinforced concrete beams	Experimental data from various FRP-wrapped concrete tests	Experimental data for lightweight concrete
131 samples	1030 samples	128 datasets	74 datasets	1347 datasets	89 cases (HSC), 70 cases (NSC)	87 datasets	80 samples	139 samples	238 samples	144 data points
w/b ratio, PP and steel fiber content, scoria and CR content, NFA and NCA content, temperature	Cement, fly ash, slag, water, superplasticizer, coarse and fine aggregates, age	RCM ratio, stress states, bulk stress, shear stress	Water-cement ratio, recycled coarse/fine aggregate replacement ratio, fly ash replacement ratio	Fly ash, slag, coarse and fine aggregate, water, superplasticizer, NaOH, KOH, curing conditions	Compressive strength (fc)	Beam geometry, water/cement ratio, compressive strength, tensile strength, modulus of elasticity	Cement, fly ash, water/powder ratio, superplasticizer, sand, coarse aggregate	Compressive strength, longitudinal steel strength, shear span-to-depth ratio, steel fiber properties	Cylinder diameter, height/diameter ratio, compressive strength, FRP thickness, tensile strength	Cement, silica fume, carbon fiber, aggregate content, temperature
Uniaxial compressive strength	Compressive strength	Resilient modulus	Compressive strength	Compressive strength	Elastic modulus (Ec)	Fracture energy, critical stress intensity factor, critical crack tip opening isplacement, failure load	Compressive strength	Shear capacity of SFRC beams	Compressive strength of FRP-confined concrete	Compressive strength, flexural strength
Beetle Antennae Search-Random Forest (BAS-RF)	Genetic Weighted Pyramid Operation Tree (GWPOT)	LSSVM, ANN	CNN-based deep learning model	SVM optimized by GA, PSOA, ACOA, ABCOA, ICOA	Support Vector Machine (SVM)	SVR	LSSVM, RVM, ANN	Hybrid RSM-SVR	SVR (RBF, Polynomial, Exponential RBF), ANN	ANN, SVM
High accuracy (R^2 = 0.97); BAS tuned RF hyperparameters; identified temperature and w/b ratio as key variables	Outperformed ANN, SVM, and ESIM; generated explicit formulas for practical applications	LSSVM outperformed ANN and regression models in accuracy and computational efficiency	Achieved higher precision, efficiency, and generalization ability compared to traditional models	Hybrid models achieved superior accuracy in predicting compressive strength of geopolymer concrete	SVM outperformed ANN, fuzzy logic, and regression methods in RMSE and MAPE for HSC and NSC prediction	SVR achieved excellent predictive performance (R^2 > 0.99) for all fracture parameters and failure load	RVM achieved the best accuracy with variance prediction, outperforming LSSVM and ANN on RMSE and MAE criteria	RSM-SVR demonstrated superior accuracy over standalone RSM, SVR, ANN, and empirical formulations in predicting shear capacity	SVR (RBF) demonstrated the highest prediction accuracy (R = 0.9908, RMSE = 6.03, MAPE = 2.61) compared to ANN and empirical models	ANN showed the best predictive accuracy (R^2 = 0.99 for compressive, 0.968 for flexural), followed by SVM (R^2 = 0.9701)
Not disclosed	Not disclosed	Not disclosed	Not disclosed	Not disclosed	Not disclosed	Not disclosed	Not disclosed	Not disclosed	Not disclosed	Not disclosed

3.2 Overall trends

The studies consistently demonstrated that ensemble methods like Random Forest and Gradient Boosting delivered the best performance in predicting concrete properties, excelling in handling high-dimensional datasets and capturing complex nonlinear relationships. However, these methods were computationally demanding and required careful tuning.

Support Vector Machines (SVMs), particularly when enhanced with optimization algorithms, were effective for smaller datasets but required significant computational resources and careful parameter tuning. Artificial Neural Networks (ANNs) were highly accurate in capturing complex relationships but often suffered from overfitting and required large datasets and computational resources.

Hybrid models, such as RSM-SVR and ANN-MOGWO, offered the highest accuracy by combining the strengths of multiple approaches, but their complexity and computational requirements made them more suitable for research applications.

Convolutional Neural Networks (CNNs) and Gaussian Process Regression (GPR) were also strong performers, with CNNs excelling at feature extraction and GPR providing uncertainty estimates. However, both models required substantial computational power.

In summary, ensemble methods and hybrid models proved to be the most accurate, while SVMs and ANNs were useful but required extensive tuning. The model choice ultimately depended on the dataset size, complexity, and available computational resources.

4 Classification and pattern recognition in pavement systems

Machine learning models, particularly unsupervised learning methods, have been instrumental in classifying pavement conditions, detecting cracks, and identifying patterns that are crucial for effective pavement management. Below is a detailed analysis of several studies using unsupervised models to address pavement-related problems.

Shao et al. (2022) applied K-means clustering to classify pavement performance patterns based on long-term Pavement Condition Index (PCI) and Riding Quality Index (RQI) data. Their model classified pavement performance into five distinct patterns, facilitating the evaluation of road maintenance strategies. The key strengths of K-means were its simplicity and ability to process large datasets effectively. However, its requirement to predefine the number of clusters and its sensitivity to data with varying densities or missing values were major limitations, suggesting the need for more adaptive models to achieve greater accuracy [49].

Mathavan et al. (2014) used a Self-Organizing Map (SOM), an unsupervised neural network, to classify doweled concrete pavement joints based on Falling Weight Deflectometer (FWD) data. Input parameters included load transfer efficiency (LTE), void intercepts (VI), and absolute deflection (D). SOM classified the joints into three categories: good, marginal, and poor. The model achieved an accuracy of 65-70%, improving to 87.5% when only LTE and D were used, demonstrating the potential to reduce human inconsistencies in manual assessments. The pros of SOM include its ability to capture complex patterns and automate classification, though its slow training process and sensitivity to unbalanced data were notable drawbacks [50].

Mubashshira et al. (2020) employed K-means clustering to detect road surface cracks by segmenting 2D road surface images. After preprocessing to reduce noise, K-means was used for image segmentation, followed by Otsu thresholding and morphological operations to refine the detected cracks. The model achieved an average detection accuracy of 97.75%, outperforming traditional edge detection methods by reducing false negatives. While K-means clustering was effective in handling noise and irregularities, its efficiency was limited by the reliance on post-processing steps, particularly for large-scale real-time applications [51].

Li et al. (2021) proposed a novel model that fused Convolutional Neural Networks (CNN) with K-means clustering for road crack classification. The input data consisted of crack images collected via automated vehicles and smartphones, and the model classified crack types—transverse, longitudinal, and alligator cracks—with accuracies of 80.6%, 79.2%, and 91.3%, respectively. The fusion of CNN and K-means allowed for iterative refinement of clustering assignments, reducing the need for manually labeled data. However, the model faced challenges due to its high computational cost during training and the need for extensive optimization [52].

Golmohammadi et al. (2024) combined PCA and DBSCAN for anomaly detection in pavement health monitoring using Fiber Bragg Grating (FBG) sensors. The system processed strain and temperature data to detect structural anomalies in pavement layers. DBSCAN effectively distinguished between normal and abnormal patterns without labeled data, demonstrating high accuracy in anomaly detection. The system, however, was sensitive to sensor placement and required considerable computational resources for continuous monitoring [53].

Abdelmawla et al. (2021) utilized PCA and K-means clustering to classify pavement cracks from 1,125 road surface images. The input images were preprocessed with edge detection and morphological operations, followed by dimensionality reduction using PCA and clustering using K-means. The study identified three clusters: multi-directional cracks, longitudinal cracks, and images without cracks. PCA reduced dimensionality, improving computational efficiency, but struggled with nonlinear relationships in the data. K-means effectively classified the cracks, although it was sensitive to initial cluster assignments [54].

Dong et al. (2021) classified climatic regions for pavement systems using PCA and K-means clustering. Input data from the Long-Term Pavement Performance (LTPP) database included 16 climate variables. Four primary clusters—wet no freeze, dry no freeze, dry freeze, and snow freeze—were identified, and results from Artificial Neural Networks (ANN) and Fisher's linear discriminant analysis were compared. ANN achieved higher prediction accuracy than discriminant analysis, though ANN required more tuning and computational power. K-means clustering proved efficient for handling large datasets, though the need to predefine clusters remained a limitation [55].

Shi et al. (2024) applied K-means clustering to analyze Acoustic Emission (AE) data from epoxy asphalt mixtures with varying crumb rubber (CR) content. Four damage modes were identified: cohesive cracking, aggregate-asphalt interface cracking, aggregate fracture, and aggregate friction. The model effectively classified AE signals and demonstrated that 4% CR content was optimal for balancing toughness and strength. However, the model's sensitivity to initial cluster selection and overlapping clusters presented challenges, especially when dealing with highly correlated data [56].

Akhtar et al. (2020) implemented a parallel K-means clustering model to assess adhesion failure in Warm Mix Asphalt (WMA) through high-resolution image processing. The model reduced execution time by 30-46% compared to sequential K-means clustering, improving the detection of adhesion failure. Although the parallel model handled large image datasets more efficiently, its complexity and sensitivity to initial cluster centers posed challenges during the implementation [57].

Sahari Moghadam et al. used K-means clustering in conjunction with k-nearest neighbors (KNN) and support vector machines (SVM) to classify asphalt coating conditions in loose mixtures. The input images from static immersion tests were segmented using K-means, followed by classification using KNN and SVM. The model improved classification accuracy by reducing human bias, though it was sensitive to image quality and relied on robust preprocessing steps to ensure accuracy [58].

4.1 Summary of methods

Table 3 provides a detailed summary of studies focusing on machine learning approaches and their applications in classification and pattern recognition for pavement systems. Unsupervised learning techniques, particularly clustering and pattern recognition methods, have been extensively applied in pavement system classification and anomaly detection. Here's an overview of the key methods:

- K-means Clustering: Widely used for classifying pavement performance patterns, crack detection, and assessing asphalt coating conditions (Shao et al., 2022; Akhtar et al., 2020). Its simplicity and efficiency in handling large datasets are advantageous, but it often struggles with predefined cluster requirements and sensitivity to initial conditions [49], [57].
- Principal Component Analysis (PCA): Commonly paired with K-means for dimensionality reduction, PCA improved computational efficiency in multi-dimensional data applications like crack classification and climate region analysis (Abdelmawla et al., 2021; Dong et al., 2021) [54], [55]. However, PCA's linearity limits its ability to capture complex relationships.
- Self-Organizing Maps (SOM): Used for classifying pavement joint conditions (Mathavan et al., 2014). SOM excels at handling high-dimensional data but has a slow training process and reduced accuracy with unbalanced datasets [50].
- Convolutional Neural Networks (CNN): When combined with K-means, CNN was effective for road crack classification, automating feature extraction and improving classification performance (Li et al., 2021). The downside is its high computational cost and complexity in optimization [52].
- DBSCAN: Applied for anomaly detection in pavement monitoring systems (Golmohammadi et al., 2024), DBSCAN is effective in handling unlabelled data, though sensitive to sensor placement and computationally intensive in continuous monitoring [53].
- Parallel K-means Clustering: Enhanced efficiency in large-scale image processing tasks by reducing execution time (Akhtar et al., 2020). However, its implementation is complex, particularly when managing communication between computing nodes [57].
- K-means with Supervised Classifiers (KNN, SVM): Combining K-means with KNN or SVM improved accuracy in tasks like asphalt coating assessment but required high-quality image data for optimal performance (Sahari Moghadam et al.) [58].

Table 3. Summary of machine learning applications in classification and pattern recognition in pavement systems: overview of data collection methods, model types, and justifications for model selection across studies

Reference	Method of Data Collection	Database Size	Input Variables	Output Variables	Type of Model	Justification for Model Selection	Availability of Code/Database
Shao et al., 2022[49]	Long-term historical data from expressways	762 road sections (439 valid)	PCI and RQI time series	Pavement performance evolution patterns	K-means clustering (unsupervised learning)	Chosen for its ability to effectively categorize long-term evolution patterns; identified five distinct performance patterns	Not disclosed
Mathavan et al., 2014[50]	Falling Weight Deflectometer (FWD) data	1,409 deflection bowls	Absolute deflection, Load transfer efficiency (LTE), Void intercepts	Concrete pavement joint condition (Good, Marginal, Poor)	Self-Organizing Map (SOM)	SOM achieved 87.5% classification accuracy for joint conditions; captures engineering expertise for non-subjective decisions	Not disclosed
Mubashshira et al., 2020[51]	Road surface images from multiple sources	200 images (120 for road detection)	RGB values, cracks morphology	Crack detection accuracy (Precision, Recall, IoU)	K-means clustering with Otsu binarization	Efficiently segmented crack regions with high accuracy; achieved 97.75% overall accuracy; outperformed edge detection methods	Not disclosed

Sahari Moghaddam et al., 2019[58]	Akhtar et al., 2020[57]	Shi et al., 2024[56]	Dong et al., 2021[55]	Abdelmawla et al., 2021[54]	Golmohammadi et al., 2024[53]	Li et al., 2021[52]
Image processing of loose asphalt mixtures	Image processing of WMA and HMA samples	Acoustic Emission (AE) data from UC and IDT tests	Historical climatic data from LTPP program	Pavement surface images	FBG sensor data collected from a test track	Automated vehicle and smartphone crack images
159 samples	High-resolution images (RGB, HSV)	4 rubberized epoxy asphalt mixtures with varying CR contents	21,666 annual datasets from 800 weather stations	Not specified	4 months of data from 12 FBG sensors	2,995 images (various types)
Image pixel intensities, specular highlights, RGB histograms of coated/uncoated areas	Pixel intensity values, adhesion failure, moisture sensitivity test results	Nine AE parameters, including rise time, ringing count, energy count, peak frequency, and amplitude	16 climatic variables: temperature, precipitation, humidity, snowfall, freezing conditions	Processed crack patterns via image processing and PCA	Strain and temperature readings processed using PCA	Crack image features extracted by AlexNet CNN
Retained asphalt coating (%)	Adhesion failure quantification	Damage evolution patterns, damage modes, toughness	Climatic region classification	Clusters of crack patterns	Anomaly detection in strain data	Crack classification (Transverse, Longitudinal, Alligator)
K-means clustering with SVM and KNN classifiers	Parallel K-means clustering (PKIP algorithm)	K-means clustering (unsupervised learning)	PCA, Factor Analysis, K-means Clustering, Fisher's Discriminant Analysis, ANN	K-means clustering (unsupervised learning)	DBSCAN clustering (unsupervised learning)	AlexNet CNN with K-means clustering
Automated stripping assessment system; demonstrated a mean difference of 4.91% compared to manual technician assessment	PKIP algorithm optimized for execution time (30–46% faster than sequential K-means); effectively quantified adhesion failure in different conditions	Efficiently classified AE signals into damage patterns, highlighting CR's effects on toughness and cracking mechanisms; identified four distinct damage modes	PCA and Factor Analysis identified key components (temperature and humidity) for dimensionality reduction; ANN achieved high accuracy in climatic region classification	Applied classic image processing and PCA to delineate and cluster crack patterns; revealed meaningful correlations between crack patterns and derived clusters	Efficiently detected anomalies using PCA feature fusion and clustering, aiding in proactive maintenance strategies	Fused CNN and K-means achieved unsupervised classification; superior accuracy (AP = 0.806, 0.792, and 0.913) for crack types
Not disclosed	Not disclosed	Not disclosed	TPP dataset available: InfoPave	Not disclosed	Not disclosed	Dataset available on GitHub: CrackDataset_DL_HY

4.2 Overall trends

K-means clustering emerged as a dominant method for its simplicity and effectiveness in pavement performance analysis, but it often required careful parameter tuning and was limited by predefined clusters. PCA was valuable for dimensionality reduction but struggled with nonlinearity. SOM and DBSCAN offered robust classification and anomaly detection in high-dimensional and sensor data, respectively, though at the cost of computational efficiency.

The combination of CNN with K-means showed promise in handling complex, image-based data, albeit with high computational demands. Parallel implementations, like Parallel K-means, improved processing times but introduced complexity in deployment. Hybrid models combining unsupervised and supervised techniques, such as K-means with KNN and SVM, offered higher accuracy but depended on data quality and preprocessing efforts.

Table 4 below provides a concise summary of the machine learning methods applied across various studies in asphalt mixture performance, concrete property prediction, and pavement classification. It outlines the key advantages and disadvantages of each method, complementing the trends discussed in the preceding sections.

Table 4. Summary of machine learning methods, advantages, and disadvantages across pavement and concrete applications

Method	Category			Advantages	Disadvantages
	A	C	P		
Artificial Neural Networks (ANNs)	×	×		Captures complex nonlinear relationships High accuracy in predicting performance metrics	Computationally intensive Prone to overfitting Requires large datasets
Support Vector Machines (SVMs)	×	×		Handles nonlinear relationships well Effective with smaller datasets	Sensitive to parameter tuning Computationally expensive for large datasets
Gradient Boosting/XGBoost	×	×		High accuracy and handles complex nonlinear relationships Regularization avoids overfitting	Requires significant computational power Complex tuning required
Random Forest (RF)	×	×		Good interpretability and robust handling of overfitting	Less accurate compared to ensemble methods Computationally expensive
Gaussian Process Regression (GPR)	×	×		Provides accurate predictions and uncertainty estimates. Handles complex nonlinear relationships well	Computationally demanding. Requires careful tuning of hyperparameters
Gene Expression Programming (GEP)	×			Offers transparent, interpretable models	Requires precise tuning Limited for large and complex datasets
Hybrid Models (e.g., SVM with optimization)	×	×		Optimizes parameter selection Improves prediction accuracy and model convergence	Computationally intensive Requires additional resources for optimization algorithms
Self-Organizing Maps (SOM)			×	Captures complex patterns in high-dimensional data Reduces inconsistencies in manual classification	Slow training process Struggles with unbalanced datasets
DBSCAN			×	Effective in anomaly detection with unlabelled data Handles noisy data	Sensitive to sensor placement Computationally intensive for continuous monitoring
Convolutional Neural Networks (CNN)			×	Automatically extracts deep features from images Highly effective for image-based crack detection and classification	High computational cost Requires extensive optimization and tuning of hyperparameters
Parallel K-means			×	Reduces execution time by 30-46% Efficient for large-scale image processing	Complex implementation Communication overhead between nodes
K-means Clustering			×	Simple and efficient for large datasets Effective in crack detection and pavement classification	Requires predefined cluster number Sensitive to initial conditions and varying densities
Principal Component Analysis (PCA)			×	Reduces dimensionality, improving computational efficiency	Limited by linearity, struggles with complex relationships

Note: A is Asphalt Mixture Performance and Optimization, C is Concrete Property Prediction and Structural Performance, P is Classification and Pattern Recognition in Pavement Systems

5 Conclusion

This literature review examines the application of machine learning techniques in material testing across three key areas: asphalt mixture performance, concrete property prediction, and classification and pattern recognition in pavement systems. The studies demonstrate the significant potential of machine learning to improve prediction accuracy, optimize material design, and reduce reliance on costly experimental testing.

Across all categories, models such as Artificial Neural Networks (ANNs), Support Vector Machines (SVMs), Random Forests (RF), Gradient Boosting (GB), Gaussian Process Regression (GPR), and Convolutional Neural Networks (CNN) show strong predictive capabilities for complex material behaviors. While ANN and SVM models are effective for smaller datasets, ensemble methods like GB and RF excel in handling larger, nonlinear data sets but are computationally expensive. GPR stands out for its ability to model complex relationships and provide uncertainty estimates, particularly in small to medium datasets, though it requires extensive tuning and computational power. Deep learning methods, such as CNN, extract deep features without manual preprocessing but require significant computational resources.

In classification and pattern recognition, unsupervised models, especially K-means clustering, are frequently applied for pavement condition classification and crack detection. Principal Component Analysis (PCA) is often used for dimensionality reduction, improving model efficiency but facing challenges with nonlinearity. Advanced techniques such as DBSCAN and CNNs are gaining traction for anomaly

detection and feature extraction but require extensive computational power and proper parameter tuning.

In general, machine learning models are effective tools in material testing and performance prediction, offering flexibility and accuracy, though computational complexity and data quality remain key challenges.

Credit Authorship Contribution Statement

Meisam Khorshidi: Conceptualization, Methodology, Literature review, Investigation, Writing - original draft, Visualization.

Eshan Dave: Conceptualization, Supervision, Writing - review & editing, Project administration.

Jo Sias: Conceptualization, Supervision, Writing - review & editing, Project administration.

The authors declare that they have no known competing financial interests or personal relationships that could have appeared to influence the work reported in this paper.

Acknowledgments:

No external funding or assistance was received for this research.

References

[1] J. Liu, F. Liu, Z. Wang, E. O. Fanijo, and L. Wang, "Involving prediction of dynamic modulus in asphalt mix design with machine learning and mechanical-empirical analysis," *Constr. Build. Mater.*, vol. 407, no. October, p. 133610, 2023, doi: 10.1016/j.conbuildmat.2023.133610.

[2] X. Fan, S. Lv, C. Xia, D. Ge, C. Liu, and W. Lu, "Strength prediction of asphalt mixture under interactive conditions based on BPNN and SVM," *Case Stud. Constr. Mater.*, vol. 21, no. July, p. e03489, 2024, doi: 10.1016/j.cscm.2024.e03489.

[3] J. Zhang, Y. Huang, Y. Wang, and G. Ma, "Multi-objective optimization of concrete mixture proportions using machine learning and metaheuristic algorithms," *Constr. Build. Mater.*, vol. 253, p. 119208, 2020, doi: 10.1016/j.conbuildmat.2020.119208.

[4] F. Rondinella, C. Oreto, F. Abbondati, and N. Baldo, "Laboratory Investigation and Machine Learning Modeling of Road Pavement Asphalt Mixtures Prepared with Construction and Demolition Waste and RAP," *Sustain.*, vol. 15, no. 23, 2023, doi: 10.3390/su152316337.

[5] M. Khorshidi, M. Ameri, and A. Goli, "Cracking performance evaluation and modelling of RAP mixtures containing different recycled materials using deep neural network model," *Road Mater. Pavement Des.*, 2023, doi: 10.1080/14680629.2023.2222835.

[6] A. Upadhya, M. S. Thakur, A. Mashat, G. Gupta, and M. S. Abdo, "Prediction of Binder Content in Glass Fiber Reinforced Asphalt Mix Using Machine Learning Techniques," *IEEE Access*, vol. 10, pp. 33866–33881, 2022, doi: 10.1109/ACCESS.2022.3157639.

[7] B. Keshtegar, M. Bagheri, and Z. M. Yaseen, "Shear strength of steel fiber-unconfined reinforced concrete beam simulation: Application of novel intelligent model," *Compos. Struct.*, vol. 212, no. January, pp. 230–242, 2019, doi: 10.1016/j.compstruct.2019.01.004.

[8] R. A. Mozumder, B. Roy, and A. I. Laskar, "Support Vector Regression Approach to Predict the Strength of FRP Confined Concrete," *Arab. J. Sci. Eng.*, vol. 42, no. 3, pp. 1129–1146, 2017, doi: 10.1007/s13369-016-2340-y.

[9] S. Rahman, A. Bhasin, and A. Smit, "Exploring the use of machine learning to predict metrics related to asphalt mixture performance," *Constr. Build. Mater.*, vol. 295, p. 123585, 2021, doi: 10.1016/j.conbuildmat.2021.123585.

[10] A. L. Bonifácio, J. C. Mendes, M. C. R. Farage, F. S. Barbosa, C. B. Barbosa, and A. L. Beaucour, "Application of support vector machine and finite element method to predict the mechanical properties of concrete," *Lat. Am. J. Solids Struct.*, vol. 16, no. 7 CILAMCE 2018, pp. 1–11, 2019, doi: 10.1590/1679-78255297.

[11] M. Mohtasham Moein *et al.*, "Predictive models for concrete properties using machine learning and deep learning approaches: A review," *J. Build. Eng.*, vol. 63, no. August 2022, 2023, doi: 10.1016/j.jobe.2022.105444.

[12] Ba-Nhan Phung, Thanh-Hai Le, Minh-Khoa Nguyen, Thuy-Anh Nguyen, and Hai-Bang Ly, "Practical Numerical Tool for Marshall Stability Prediction Based On Machine Learning: An Application for Asphalt Concrete Containing Basalt Fiber," *J. Sci. Transp. Technol.*, vol. 3, no. 3, pp. 27–45, 2023, doi: 10.58845/jstt.utt.2023.en.3.3.27-45.

[13] D. C. Feng *et al.*, "Machine learning-based compressive strength prediction for concrete: An adaptive boosting approach," *Constr. Build. Mater.*, vol. 230, p. 117000, 2020, doi: 10.1016/j.conbuildmat.2019.117000.

[14] N. Baldo, M. Miani, F. Rondinella, J. Valentin, P. Vackcová, and E. Manthos, "Stiffness Data of High-Modulus Asphalt Concretes for Road Pavements: Predictive Modeling by Machine-Learning," *Coatings*, vol. 12, no. 1, pp. 1–20, 2022, doi: 10.3390/coatings12010054.

[15] H. Tanyildizi, "Prediction of the strength properties of carbon fiber-reinforced lightweight concrete exposed to the high temperature using artificial neural network and support vector machine," *Adv. Civ. Eng.*, vol. 2018, 2018, doi: 10.1155/2018/5140610.

[16] H. Hafez, A. Teirelbar, R. Kurda, N. To, and A. De, "Pre-bcc : A novel integrated machine learning framework for predicting mechanical and durability properties of blended cement concrete," vol. 352, no. August, 2022, doi: 10.1016/j.conbuildmat.2022.129019.

[17] P. Marcelino, M. de Lurdes Antunes, E. Fortunato, and M. C. Gomes, "Machine learning approach for pavement performance prediction," *Int. J. Pavement Eng.*, vol. 22, no. 3, pp. 341–354, 2021.

[18] H. Nguyen, T. Vu, T. P. Vo, and H. T. Thai, "Efficient machine learning models for prediction of concrete strengths," *Constr. Build. Mater.*, vol. 266, p. 120950, 2021, doi: 10.1016/j.conbuildmat.2020.120950.

[19] A. Behnood and E. M. Golafshani, "Predicting the compressive strength of silica fume concrete using hybrid artificial neural network with multi-objective grey wolves," *J. Clean. Prod.*, vol. 202, pp. 54–64, 2018, doi: 10.1016/j.jclepro.2018.08.065.

[20] S. E. Whang and J. G. Lee, "Data Collection and Quality Challenges for Deep Learning," *Proc. VLDB Endow.*, vol. 13, no. 12, pp. 3429–3432, 2020, doi: 10.14778/3415478.3415562.

[21] H. G. Melhem and S. Nagaraja, "Machine learning and its application to civil engineering systems," *Civ. Eng. Syst.*, vol. 13, no. 4, pp. 259–279, 1996, doi: 10.1080/02630259608970203.

[22] C. Rudin, “Stop explaining black box machine learning models for high stakes decisions and use interpretable models instead,” *Nat. Mach. Intell.*, vol. 1, no. 5, pp. 206–215, 2019, doi: 10.1038/s42256-019-0048-x.

[23] M. Khorshidi, A. Goli, M. Orešković, K. Khayambashi, and M. Ameri, “Performance Evaluation of Asphalt Mixtures Containing Different Proportions of Alternative Materials,” *Sustainability*, vol. 15, no. 18, p. 13314, 2023, doi: 10.3390/su151813314.

[24] J. Liu, F. Liu, C. Zheng, D. Zhou, and L. Wang, “Optimizing asphalt mix design through predicting the rut depth of asphalt pavement using machine learning,” *Constr. Build. Mater.*, vol. 356, no. September, p. 129211, 2022, doi: 10.1016/j.conbuildmat.2022.129211.

[25] J. Liu, F. Liu, C. Zheng, D. Zhou, and L. Wang, “Optimizing asphalt mix design through predicting effective asphalt content and absorbed asphalt content using machine learning,” *Constr. Build. Mater.*, vol. 325, no. November 2021, p. 126607, 2022, doi: 10.1016/j.conbuildmat.2022.126607.

[26] J. Liu, F. Liu, C. Zheng, E. O. Fanijo, and L. Wang, “Improving asphalt mix design considering international roughness index of asphalt pavement predicted using autoencoders and machine learning,” *Constr. Build. Mater.*, vol. 360, no. April, p. 129439, 2022, doi: 10.1016/j.conbuildmat.2022.129439.

[27] H. Majidifard, B. Jahangiri, P. Rath, L. Urra Contreras, W. G. Buttlar, and A. H. Alavi, “Developing a prediction model for rutting depth of asphalt mixtures using gene expression programming,” *Constr. Build. Mater.*, vol. 267, p. 120543, 2021, doi: 10.1016/j.conbuildmat.2020.120543.

[28] N. Tiwari, N. Baldo, N. Satyam, and M. Miani, “Mechanical Characterization of Industrial Waste Materials as Mineral Fillers in Asphalt Mixes: Integrated Experimental and Machine Learning Analysis,” *Sustain.*, vol. 14, no. 10, pp. 1–25, 2022, doi: 10.3390/su14105946.

[29] N. Tiwari, F. Rondinella, N. Satyam, and N. Baldo, “Experimental and Machine Learning Approach to Investigate the Mechanical Performance of Asphalt Mixtures with Silica Fume Filler,” *Appl. Sci.*, vol. 13, no. 11, 2023, doi: 10.3390/app13116664.

[30] Y. Ali, F. Hussain, M. Irfan, and A. S. Buller, “An eXtreme Gradient Boosting model for predicting dynamic modulus of asphalt concrete mixtures,” *Constr. Build. Mater.*, vol. 295, p. 123642, 2021, doi: 10.1016/j.conbuildmat.2021.123642.

[31] D. Mirzaiyanrajeh, E. V. Dave, J. E. Sias, and P. Ramsey, “Developing a prediction model for low-temperature fracture energy of asphalt mixtures using machine learning approach,” *Int. J. Pavement Eng.*, vol. 24, no. 2, 2022, doi: 10.1080/10298436.2021.2024185.

[32] J. Liu, C. Cheng, C. Zheng, X. Wang, and L. Wang, “Rutting prediction using deep learning for time series modeling and K-means clustering based on RIOHTrack data,” *Constr. Build. Mater.*, vol. 385, no. April, p. 131515, 2023, doi: 10.1016/j.conbuildmat.2023.131515.

[33] A. M. Al-Sabaeei *et al.*, “Utilization of response surface methodology and machine learning for predicting and optimizing mixing and compaction temperatures of bio-modified asphalt,” *Case Stud. Constr. Mater.*, vol. 18, no. April, p. e02073, 2023, doi: 10.1016/j.cscm.2023.e02073.

[34] Y. Song, X. Wang, H. Li, Y. He, Z. Zhang, and J. Huang, “Mixture Optimization of Cementitious Materials Using Machine Learning and Metaheuristic Algorithms: State of the Art and Future Prospects,” *Materials (Basel).*, vol. 15, no. 21, 2022, doi: 10.3390/ma15217830.

[35] H. Hafez, A. Teirelbar, N. To, and A. De Fuente, “Data-driven optimization tool for the functional , economic , and environmental properties of blended cement concrete using supplementary cementitious materials,” vol. 67, no. February, 2023, doi: 10.1016/j.jobe.2023.106022.

[36] O. P. Pfeiffer *et al.*, “Cement and Concrete Research Bayesian design of concrete with amortized Gaussian processes and multi-objective optimization,” *Cem. Concr. Res.*, vol. 177, no. October 2022, p. 107406, 2024, doi: 10.1016/j.cemconres.2023.107406.

[37] Y. Yu, W. Li, J. Li, and T. N. Nguyen, “A novel optimised self-learning method for compressive strength prediction of high performance concrete,” *Constr. Build. Mater.*, vol. 184, pp. 229–247, 2018, doi: 10.1016/j.conbuildmat.2018.06.219.

[38] A.-D. Pham, N.-D. Hoang, and Q.-T. Nguyen, “Predicting Compressive Strength of High-Performance Concrete Using Metaheuristic-Optimized Least Squares Support Vector Regression,” *J. Comput. Civ. Eng.*, vol. 30, no. 3, pp. 28–31, 2016, doi: 10.1061/(asce)cp.1943-5487.0000506.

[39] Z. M. Yaseen *et al.*, “Predicting compressive strength of lightweight foamed concrete using extreme learning machine model,” *Adv. Eng. Softw.*, vol. 115, no. September 2017, pp. 112–125, 2018, doi: 10.1016/j.advengsoft.2017.09.004.

[40] B. A. Omran, Q. Chen, and R. Jin, “Comparison of Data Mining Techniques for Predicting Compressive Strength of Environmentally Friendly Concrete,” *J. Comput. Civ. Eng.*, vol. 30, no. 6, pp. 1–13, 2016, doi: 10.1061/(asce)cp.1943-5487.0000596.

[41] B. G. Aiyer, D. Kim, N. Karingattikkal, P. Samui, and P. R. Rao, “Prediction of compressive strength of self-compacting concrete using least square support vector machine and relevance vector machine,” *KSCE J. Civ. Eng.*, vol. 18, no. 6, pp. 1753–1758, 2014, doi: 10.1007/s12205-014-0524-0.

[42] P. Yuvaraj, A. Ramachandra Murthy, N. R. Iyer, S. K. Sekar, and P. Samui, “Support vector regression based models to predict fracture characteristics of high strength and ultra high strength concrete beams,” *Eng. Fract. Mech.*, vol. 98, no. 1, pp. 29–43, 2013, doi: 10.1016/j.engfracmech.2012.11.014.

[43] K. Yan and C. Shi, “Prediction of elastic modulus of normal and high strength concrete by support vector machine,” *Constr. Build. Mater.*, vol. 24, no. 8, pp. 1479–1485, 2010, doi: 10.1016/j.conbuildmat.2010.01.006.

[44] A. Nazari and J. G. Sanjayan, “Modelling of compressive strength of geopolymer paste, mortar and concrete by optimized support vector machine,” *Ceram. Int.*, vol. 41, no. 9PartB, pp. 12164–12177, 2015, doi: 10.1016/j.ceramint.2015.06.037.

[45] F. Deng, Y. He, S. Zhou, Y. Yu, H. Cheng, and X. Wu, “Compressive strength prediction of recycled concrete based on deep learning,” *Constr. Build. Mater.*, vol. 175, pp. 562–569, 2018, doi: 10.1016/j.conbuildmat.2018.04.169.

[46] M. R. Kaloop, A. R. Gabr, S. M. El-Badawy, A. Arisha, S. Shwally, and J. W. Hu, “Predicting resilient modulus of recycled concrete and clay masonry blends for

pavement applications using soft computing techniques," *Front. Struct. Civ. Eng.*, vol. 13, no. 6, pp. 1379–1392, 2019, doi: 10.1007/s11709-019-0562-2.

[47] M. Y. Cheng, P. M. Firdausi, and D. Prayogo, "High-performance concrete compressive strength prediction using Genetic Weighted Pyramid Operation Tree (GWPOT)," *Eng. Appl. Artif. Intell.*, vol. 29, pp. 104–113, 2014, doi: 10.1016/j.engappai.2013.11.014.

[48] J. Zhang, G. Ma, Y. Huang, J. sun, F. Aslani, and B. Nener, "Modelling uniaxial compressive strength of lightweight self-compacting concrete using random forest regression," *Constr. Build. Mater.*, vol. 210, pp. 713–719, 2019, doi: 10.1016/j.conbuildmat.2019.03.189.

[49] M. Shao, Y. Sun, and X. Yun, "Long-term Evolution Recognition and Management Level Evaluation of Pavement Performance Based on Clustering Analysis," *Int. Conf. Geoinformatics*, vol. 2022-Augus, pp. 1–6, 2022, doi: 10.1109/Geoinformatics57846.2022.9963880.

[50] S. Mathavan, M. M. Rahman, and M. Stonecliffe-Jones, "Unsupervised artificial neural network for efficient mapping of doweled concrete pavement joints condition," *Int. J. Pavement Res. Technol.*, vol. 7, no. 4, pp. 287–296, 2014, doi: 10.6135/ijprt.org.tw/2014.7(4).287.

[51] S. Mubashshira, M. M. Azam, and S. M. Masudul Ahsan, "An Unsupervised Approach for Road Surface Crack Detection," *2020 IEEE Reg. 10 Symp. TENSYMP 2020*, no. June, pp. 1596–1599, 2020, doi: 10.1109/TENSYMP50017.2020.9231023.

[52] W. Li, J. Huyan, R. Gao, X. Hao, Y. Hu, and Y. Zhang, "Unsupervised Deep Learning for Road Crack Classification by Fusing Convolutional Neural Network and K_Means Clustering," *J. Transp. Eng. Part B Pavements*, vol. 147, no. 4, 2021, doi: 10.1061/jpeodx.0000322.

[53] A. Golmohammadi, D. Hernando, and W. Van Den Bergh, *Advanced data-driven FBG sensor-based pavement monitoring system using multi-sensor data fusion and an unsupervised learning approach*. Elsevier Ltd, 2024. doi: 10.1016/j.measurement.2024.115821.

[54] A. Abdelmawla, J. J. Yang, and S. S. Kim, "Unsupervised Learning of Pavement Distresses from Surface Images," in *Advances in Innovative Geotechnical Engineering*, Y. Liu, S. Cuomo, and J. Yang, Eds., Cham: Springer International Publishing, 2021, pp. 1–8.

[55] Q. Dong, X. Chen, S. Dong, and J. Zhang, "Classification of pavement climatic regions through unsupervised and supervised machine learnings," *J. Infrastruct. Preserv. Resil.*, vol. 2, no. 1, 2021, doi: 10.1186/s43065-021-00020-7.

[56] C. Shi *et al.*, "Analysis of crumb rubber content influence on damage evolution and pattern recognition of rubberised epoxy asphalt mixture using acoustic emission techniques," *Int. J. Pavement Eng.*, vol. 25, no. 1, pp. 1–15, 2024, doi: 10.1080/10298436.2024.2356762.

[57] M. N. Akhtar, W. Ahmed, M. R. Kakar, E. A. Bakar, A. R. Othman, and M. Bueno, "Implementation of Parallel K-Means Algorithm to Estimate Adhesion Failure in Warm Mix Asphalt," *Adv. Civ. Eng.*, vol. 2020, 2020, doi: 10.1155/2020/8848945.

[58] A. Sahari Moghaddam, E. Rezazadeh Azar, Y. Mejias, and H. Bell, "Estimating Stripping of Asphalt Coating Using k-Means Clustering and Machine Learning–Based Classification," *J. Comput. Civ. Eng.*, vol. 34, no. 1, pp. 1–11, 2020, doi: 10.1061/(asce)cp.1943-5487.0000864.

Građevinski materijali i konstrukcije
Building Materials and Structures
journal homepage: www.dimk.rs

https://doi.org/10.5937/GRMK2400011R UDK: 624.014.27:620.1

Preliminary report

Failure modes of steel beams with web openings

Maja Ranisavljević[*1)], Jelena Dobrić[1)]

[1)] *University of Belgrade, Faculty of Civil Engineering, Bulevar kralja Aleksandra 73, 11000 Belgrade, Serbia*

Article history
Received: 31 October 2024
Received in revised form:
28 November 2024
Accepted: 30 November 2024
Available online: 16 December 2024

Keywords
web openings,
failure modes,
local buckling,
global lateral-torsional buckling,
web-post buckling,
Vierendeel mechanism

ABSTRACT

As an alternative to trusses and open-web joist systems, beams with web openings are lightweight, long-spanning structural elements that bind structural role (efficient load distribution) and functionality in a visually acceptable way by allowing service routes to be installed within their cross-section height. Owing to its specific production process, this beam type has a beneficial impact on rational use of material for low-carbon structures. In recent years, extensive scientific research has been conducted to assess the structural behavior and ultimate capacity of beams with web openings. Due to the presence of web openings, load transfer is accompanied by complex stress distributions in the section web, causing failure modes that are distinguishable from those of solid I-section beams. This paper summarizes the different failure modes of the beams with web openings that have been discovered and confirmed in numerous experiments of reference scientific researches. Based on the state-of-the art in this structural area, the predictions of different failure modes that are affected by influencing geometric parameters are provided.

1 Introduction

Steel floor structures consisting of solid beams often require the formation of large web openings for the transit of service ducts. Economical solutions, which integrate installation routes within beam cross-section height (see Figure 1a), should include simple design, automated fabrication methods and minimum costs. The costs can be further minimized if it is shown that no stiffeners (reinforcements) are required; if this is not possible, simple stiffener configurations are required that allow straightforward manufacturing. Compared to conventional steel structures, the beams with web openings possess a better strength-to-weight ratio, classifying them as lightweight and long-span structural components. To maximize efficiency, they are most commonly used in composite structures [1,2]. Additionally, they can be applied in non-composite structures as beams, slender columns, or cantilever elements [3–6]. Beyond structural advantages, these elements are also appreciated for their attractive appearance. The most common opening shapes are hexagonal and circular. Beams with hexagonal openings are called castellated beams, while those with circular openings are referred to as cellular beams. Cellular beams exhibit the highest load-bearing capacity but also result in the greatest material waste among other shapes configurations [7]. However, the introduction of the Angelina beam, featuring sinusoidal shaped openings, achieves a balance, providing sufficient capacity while optimizing material usage. Other shapes such as rectangular, oval, and octagonal can also be utilize.

The manufacturing process of steel structural elements with web openings consists from three stages (see Figure 1b): (1) flame cutting of a solid hot-rolled I-section beam along a specified path determined by the opening shape; this results in two Tee sections that are (2) subsequently separated, (3) re-assembled, and welded together [8]. Castellated beams are fabricated by using a computer-controlled cutting torch to cut a zigzag pattern along the section web, whereas cellular beams are fabricated in a similar manner using a nested semicircular cutting pattern. The waste at the ends of the beam (castellated and circular) and along semicircular pattern (circular) is removed. Through this process, the parent I-section can achieve a significant increase in flexural stiffness without any increase in weight. Moreover, welded I-section beams with web openings can enable efficient hybrid structural compositions by rationally using different geometries and/or steel grades for the cross-section elements (parts). Additional material savings, up to 40%, can be achieved using corrugated webs instead of flat webs [9].

As part of second generation of the Eurocodes, new code EN 1993-1-13 [10] will provide supplementary provisions and design rules that extend the application of EN 1993-1-1 [11] and EN 1993-1-5 [12] to the design of rolled and welded steel sections with various shapes of web openings. The design of beams with web openings is also addressed in American national standard, AISC Steel design guide 31 [13].

* Corresponding author:
E-mail address: maja@imk.grf.bg.ac.rs

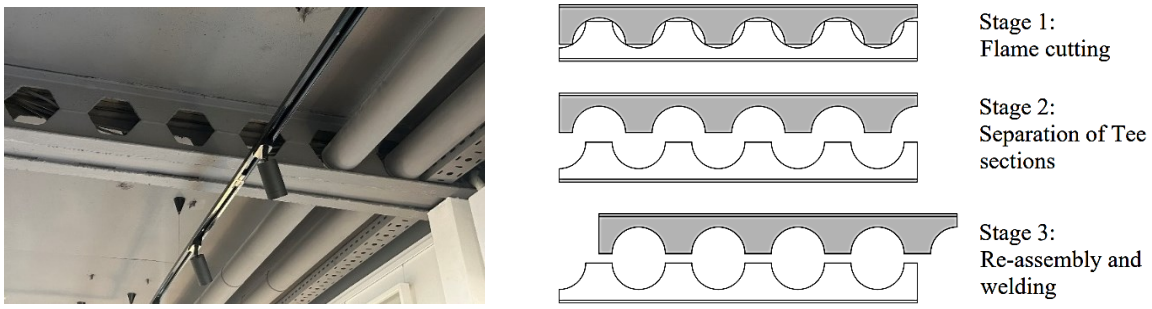

(a) application in floor structures (b) fabrication process

Figure 1: Steel beams with web openings

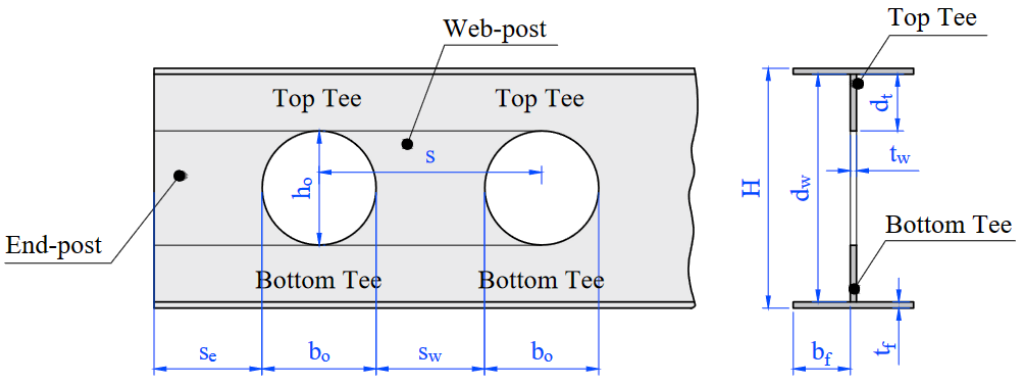

Figure 2: Definition of terms commonly used for beams with web openings

The failure modes of beams with web openings are diverse and influenced by load distribution, structural solution of floor structure (composite or non-composite), boundary conditions, steel grade, beam span (length), opening parameters (opening shape, dimensions and spacing), cross-section parameters (beam depth, flange width-to-thickness ratio and web thickness) and stiffener geometry and position. The collapse mechanism is not uniform and can include the multi-failure mode interactions.

The interaction between the failure modes and the mechanical properties of beams with web openings has been extensively investigated. The history of experimental tests reaches back to the 1940s, particularly emphasizing studies on castellated beams with hexagonal openings. Today, research databases have expanded to include various opening shapes, parent I-sections, and steel grades.

This paper briefly summarizes the key finding of experiments conducted on beams with web openings, with a focus on failure mode identification. The aim is to define the limit ranges for cross-section and opening parameters that affect a particular (specific) failure mode.

2 Failure modes

In the case of beams with web openings, localized internal forces are developed both around the openings and at the web posts (part of the web between adjacent openings); therefore, additional failure modes can occurre beyond those which are common for conventional solid web beams. In general, failure modes are categorized into those related to loss of cross-section strength and stability (local failure mode), and those related to loss of overall beam stability (global failure mode). Common local failure modes include shear and flexural failure, Vierendeel mechanism, buckling of the compressed Tee section, and failure of the web-post due to bending, shear, and compression. The global failure mode that can occur is lateral-torsional buckling.

2.1 Local failure modes

Characteristic local failure modes that occur (localized) around openings and web posts are shear failure, flexural failure, Vierendeel mechanism failure, yielding or local buckling of Tee sections (flange and web), web post buckling, local web buckling. The failure modes related to shear and moment resistance, already familiar in case of solid I-sections, are altered due to the presence of the openings.

When openings are positioned near beam supports or loading points, or when widely spaced openings (between transverse stiffeners) are present, web vertical shear failure (in opening area) can occur. In the post-peak regime, when the shear capacity of the web post is exceeded, the failure pattern is featured by a diagonally formed buckle around the opening, as illustrated in Figure 3a. The vertical shear, caused by the global shear force, should be resisted by the net cross-section at each web openings, or the gross section at web posts.

The flexure mechanism is characterized by noticeable vertical deflection [14–17] and the yielding of the top and bottom Tee sections (primarily flanges) in the critical cross-section under the action of extreme bending moments, see Figure 3b. The failure mode can also be accompanied by local buckling of the wide flange of the beam (compressed Tee section). Hence, the yielding pattern is similar to that of a beam with solid I-section.

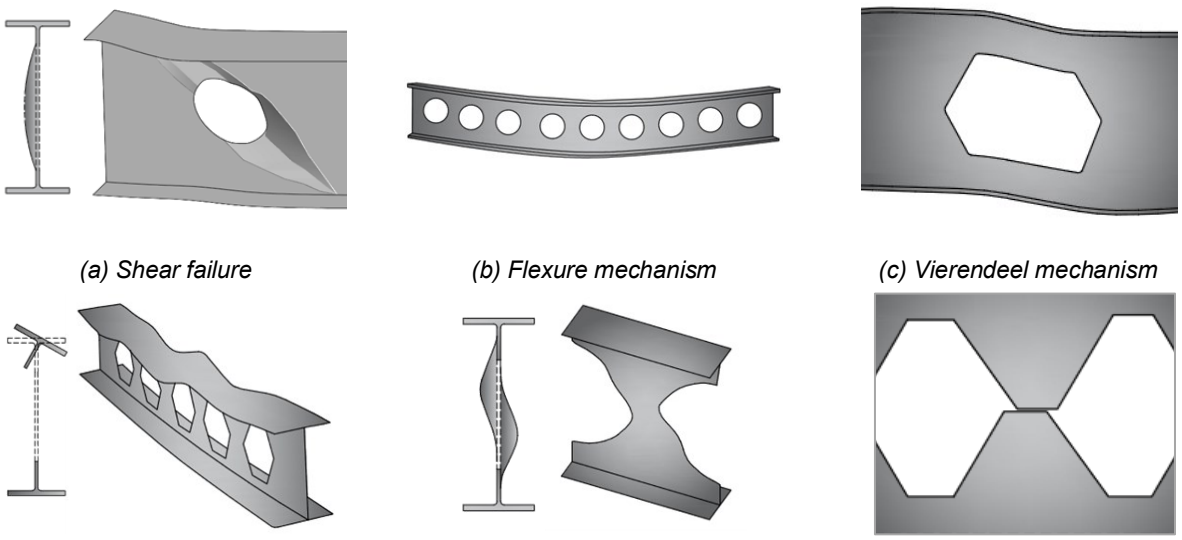

(a) Shear failure (b) Flexure mechanism (c) Vierendeel mechanism

(d) Tee buckling (e) Web-post buckling (f) Rupture of the welded joint

Figure 3: Local failure modes of beams with web openings under bending (adapted from [36])

The structural behaviour of beams with web openings under bending is usually explained through the Vierendeel analogy: the design approach involves an integral model consisting of individual horizontal components (Tees around the openings) and individual vertical components (web posts between the openings). The presence of web openings alters stress distributions around them, making the critical sections approximately at the opening corners [18]. Under a global moment and a global shear force, three local actions are induced in the Tees above and below the web opening: (i) axial force in the Tee section, due to the global moment, (ii) shear force in Tee section, due to the global shear force, (iii) local Vierendeel moment in the Tee section, due to the transfer of shear force across the opening length. The high stress interaction leads to the yielding of Tee sections and the formation of four plastic hinges, above and below the web opening, see Figure 3c. This failure mechanism is known as the Vierendeel mechanism [19]. Vierendeel mechanism is critical in beams with single large web openings or widely spaced web openings [20]. In composite beams, Vierendeel bending distribution is similar to that in non-composite beams. Composite action results in smaller forces in the Tees, resulting in a more favourable structural response [21–24]. However, at web openings near the ends (supports) of the beams, the composite action provides lower strength due to the limited number of studs between the end of the beam and the end opening. As a result, the concrete transmits less internal forces, and the Tee sections transmits the greater internal forces which should be taken into account during design.

In the case of thin-webbed beams with openings of a smaller height, the yielding of deeper Tee section under compression in Vierendeel action can be limited by its instability leading to different failure mode known as buckling of Tee section web. The local buckling of the Tee section web may cause torsional deformations of the Tee section flange, see Figure 3d. The mode of failure is dependent on the geometrical dimensions (slenderness) of Tee sections. Additionally, this type of failure may affect the load-carrying capacity of castellated beams made of high-strength steel [25]. To avoid plastic deformations and local yielding around the openings, the webs of the Tee sections can be reinforced with additional stiffening [26–28]. The research shown that long horizontal stiffeners provide the better section strengthening compared to framed and vertical ones [29].

Web post buckling is caused by the horizontal shear force passing through the web post. The failure of the web post is governed by one of three modes: (i) flexural failure caused by the development of a plastic hinge in the web post, (ii) buckling failure of the web post (see Figure 3e) and (iii) rupture of the welded joint (see Figure 3f). The mode of failure is dependent on the geometry and the thickness (slenderness) of the web post [30–35].

2.2 Global failure modes

The lateral-torsional buckling failure of beams with web openings under pure bending is similar to that of the equivalent beams with solid web [37,38]; in this case, the openings have less effect on the ultimate structural response, see Figure 4a. The failure mode is characteristic of narrow flanged beams with insufficient lateral stiffness [39], or when lateral stability within the length of the beam is not provided by sufficient lateral restraints to the compression flange. Along with lateral-torsional buckling, web distortion can occur, leading to a combined failure mode known as lateral-distortional buckling [40], see Figure 4b.

2.3 Review of research on failure modes

Structural behaviour and ultimate response (failure modes) of beams with web openings have been extensively investigated over the past years. Initially, research focused on castellated beams, and later it expanded to include different shaped openings. Table 1 provides a summary of the gathered database for failure modes occurred in steel beams with web openings under pure bending moment. The collected database covers a wide range of cross-section and opening parameters, structural steels and numbers of tests.

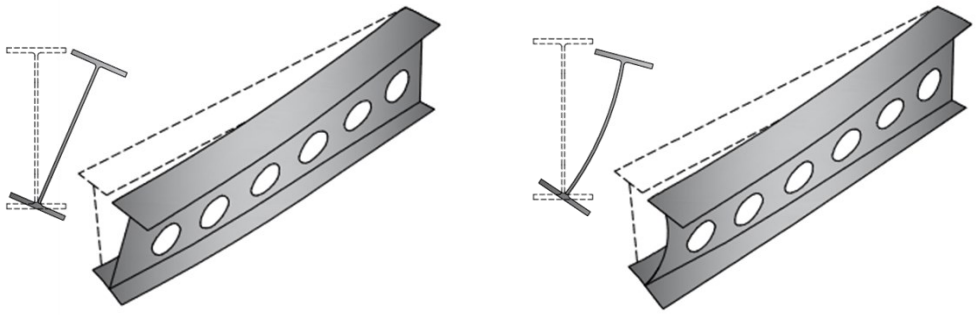

(a) Lateral-torsional buckling (b) Lateral-distortional buckling

Figure 4: Global failure modes of beams with web openings under bending (adapted from [36])

Table 1: Summary of research on failure modes of beams with web openings

Reference	E / FE	Load type	Number of tests	Failure modes
Castellated beams with hexagonal openings				
Altfillisch, Cooke and Toprac, 1957. [41]	E	2P	2	TB
Toprac and Cooke, 1959. [42]	E	2P	8	VM, TB, LTB
Sherbourne, 1966. [43]	E	1P 2P	1 5	FM, WPB, FM + LTB
Bazile and Texier, 1968. [44]	E	U	6	WB, LTB, WPB
Hussain and Speirs, 1971. [45]	E	1P 2P	4 2	WR
Hussain and Speirs, 1973. [46]	E	1P 2P	6 3	FM, WB, VM
Zaarour, 1995. [47]	E	1P	4	WPB, TB, LTB
Redwood and Demirdjian, 1998. [35]	E	1P	4	WPB
Zirakian and Showkati, 2006. [48]	E	1P	6	LDB
Ellobody, 2011. [49]	FE	1P	96	LTB, LDB, WD
Sonck and Belis, 2016. [50]	E	2P	3	LTB
Weidlich, Sotelino and Gardoso, 2021. [51]	FE	1P	17	LTB, TB, FM
Morkhade and Gupta, 2022. [52]	FE	1P	6	VM, WPB + VM
Tas, Erdal, Tunca and Ozcelik, 2024. [53]	E	1P 2P U	1 1 1	VM, WPB
Cellular beams with circular openings				
Redwood and McCutcheon, 1968. [54]	E	1P 2P	7 2	FM, VM
Surtees, 1995. [55]	E	1P	1	WD + WPB
Warren, 2001. [56]	E	1P 2P	4 3	VM, FM
Tsavdaridis, D'Mello and Hawes, 2009 [57]	E	1P	2	WPB +FM
Tsavdaridis and D'Mello, 2011. [58]	E	1P	2	WPB
Ellobody, 2012. [59]	FE	1P	120	LTB, LDB, WPB + WD, LDB + WPB, LTB + FM
Erdal and Saka, 2013. [60]	E	1P	4	LTB, WPB, VM + WPB
Lawson, Basta and Uzzaman, 2015. [61]	E	1P	7	WPB, WPB + TB
Sonck and Belis, 2015. [62]	E	2P	3	LTB
Morkhade and Gupta, 2017. [63]	E	1P	6	WPB, WPY, VM + WPB, TB + LTB
Ferreira, Rossi and Martins, 2019. [64]	FE	1P U	180 180	LTB, LDB, WPB, VM
Morkhade and Gupta, 2022. [52]	FE	1P	7	VM, WPB + VM

Abbas, 2023. [65]	E	1P	5	FM
Tas, Erdal, Tunca and Ozcelik, 2024. [53]	E	1P 2P U	1 1 1	VM, WPB

E – experiments; **FE** – finite element analysis; **1P** – one point load; **2P** – two points load; **U** – uniform distributed load; **FM** – flexure mechanism; **VM** – Vierendeel mechanism; **WB** – web buckling (shear failure); **WPB** – web-post buckling; **WPY** – web-post yielding; **WR** – weld rupture; **WD** – web distortion; **TB** – local Tee buckling; **LTB** – lateral-torsional buckling; **LDB** – lateral-distortional buckling

In addition to the experimental tests and numerical analysis performed on simple beams with circular and hexagonal openings (as listed in Table 1), a comparatively smaller number of study have been carried out on beams with sinusoidal [18,53,66–71], rectangular openings [4,52,54,63,72,73] and other shapes such as oval and octagonal [74–81].

3 Influence of different parameters on failure modes

Different parameters can result in different failure modes. Based on the knowledge and experience gained through numerous experimental tests, it is possible to predict the most common failure mode that will occur in a particular case. For example, short-length beams with web openings can experience high shear forces, leading to web buckling or vertical shear failure, particularly near supports. Mid-length beams can exhibit Vierendeel bending and web post buckling. Long-length beams are more susceptible to global lateral-torsional buckling.

The collected database is made according to Table 1 and is limited to the domain of simple I-section beams with unstiffened openings, due to the number of available experiments in this field. It includes information on various parameters such as steel grade, beam length, cross-section dimensions and slenderness, opening parameters, and additional details on lateral bracings and web stiffeners.

Morkhade and Gupta [63] highlighted that adopting spacing-to-diameter ratio of circular openings (s/b_o according to Figure 2) in the range of 1.5 to 2.0 can provide enough web post width to achieve vertical shear resistance. However, there are tested specimens with hexagonal and circular openings where web post buckling occurs for spacing-to-diameter ratios such as 1.47, 1.6, 2, and 2.5 [46,52,60]. It is worth noting that to prevent web post buckling, beside adequate s/b_o ratio, the transverse stiffeners should be provided at the supports and load point. Morkhade and Gupta [63] also noted that web post buckling failure modes are predominant when (s/b_o) was between 1.07 and 1.4; in these cases, beams can fail by web post buckling before the Vierendeel mechanism occurred (featured by formation of four plastic hinges around the openings) [52]. Another group of authors [82] likewise observed and noted that buckling generally occurred when the spacing ratio s/b_o was equal to 1.2. Based on numerous studies [41-53], predictions can be made using edge-to-edge spacing-to-opening height ratio (s_w/h_o). For circular and hexagonal openings, web post buckling occurred when s_w/h_o is less than 0.3. For higher values of this ratio, Vierendeel failure take place. When close to limit value, determining factor is not clear. The long-length beams can be more susceptible to Vierendeel mechanism before web-post buckling. In some cases, where web between openings is not slender and h_o/d_w ratio does not exceed 0.8, mid-length beams failed due to flexure mechanism before web post buckling.

For long-length beams, where L_{cr}/H ratio (where L_{cr} is length between lateral bracings) is higher than approximately 7, a global failure mode is more likely to occur, regardless of the openings' size. Sweedan [83] revealed that widely spaced web opening configurations provide higher shear stiffness, resulting in minute or no web distortion. In this case, the beam failure is governed by lateral buckling (LTB or LDB) modes [83]. However, web distortion is found to be dominant even for widely spaced openings in cases where Tee section web is very slender [49]. Whether global lateral instability or web distortion occurs depends on the web slenderness at the opening. When d_t/t_w is 25 or higher, web distortion occurred without any lateral movement [49]. For less slender Tee section web, with a d_t/t_w of about 13, the failure mode is governed by lateral displacement. The smaller the difference between the slenderness of the web and the flange, the greater the chance for lateral-torsional buckling without any web distortion.

In case of very slender beams (L/H > 18, where L is beam length), if sufficient lateral bracings are provided, rupture of welded joint will take place before flexure mechanism or web post buckling. Otherwise, in case of short-span beams with a shallow tee depth, such as h_0/d_w equal to 0.8 or higher, Vierendeel failure is generally observed [82]. In such cases, yielding in the tees around opening may occur prior to buckling in the web-post. Nevertheless, plastic deformations may begin in the web-posts and spread to the tee sections, potentially leading to a combination of Vierendeel and web-post buckling failure modes. Notably, only a few experimental studies have investigated this specific opening geometry, particularly with h_0/d_w ratios of 0.8 and higher. Four studies were conducted by Morkhade and Gupta [63] which focused on a single point load where web-post buckling occurred. In contrast, Toprac and Cooke [42] carried out one study under two points load, resulting in Vierendeel failure.

As shown in Table 1, shear failure is less common in these structural elements. This may be because there is sufficient space between the supports and the first opening, allowing for full web engagement in shear transfer at the location of maximum shear force, and the bigger issue is the interaction between other inner forces leading to Vierendeel or web-post buckling failures. Notably, some literature does not even mention this failure type [36]. However, the shear failure with the buckle around the opening, as illustrated in Figure 3a, was captured in experimental tests that had been conducted by Lian and Shanmugam [84].

The presence of irregular openings that are offset from the beam axis can significantly enhance the buckling capacity of tees; however, it may also reduce the buckling capacity of the adjacent web post [85,86].

Table 2 summarizes expected failure modes considering different cross-section and opening parameters, as explained above, where:

Table 2: Predicted failure modes for $s/b_o \leq 1.5$

$L_{cr}/H < 7$				$L_{cr}/H > 7$		
$s_w/h_o < 0.3$			$s_w/h_o > 0.3$	$d_t/t_w < 25$		$d_t/t_w > 25$
$h_o/d_w > 0.8$	$h_o/d_w < 0.8$ **			$\lambda_w/\lambda_f < 7$	$\lambda_w/\lambda_f > 7$	
	W K1-3*	W K4*				
WPB/VM	FM	WPB	VM	LTB	LDB	WD

FM – flexure mechanism; **VM** – Vierendeel mechanism; **WPB** – web-post buckling; **WD** – web distortion; **LTB** – lateral-torsional buckling; **LDB** – lateral-distortional buckling

* Web classification according to prEN 1993-1-13 [10]; For example, W K1-3 stands for web class one to three

** For large-span beams (L/H > 18, where L is the total beam length), failure is characterized by weld rupture. Otherwise, the failure type depends on the web slenderness according to Table 2.

λ_w is web slenderness d_w/t_w,

λ_f is flange slenderness b_f/t_f.

Table 2 refers to beams with circular and hexagonal openings as well as to beams with transverse stiffeners at the supports and load points. If there are no adequate stiffeners, web post buckling can occur at higher values of s_w/h_o than specified in Table 2. All parameters are in accordance with Figure 2.

Although the use of beams with web openings is becoming more commonplace and there is a growing body of scientific literature on the topic, there are very few technical publications that include comprehensive design recommendations (there is small amount of data available for different steel grades and load types, such as pure axial compression [87–91] or axial force–bending moment interaction [92]). Meanwhile, research results are being incorporated into code documents as conclusive design methods become available. As part of second generation of the Eurocodes, new code EN 1993-1-13 [10] which provides design rules for the design of I-section beams with web openings, is due to be published within the next three years in Europe.

4 Conclusions

Numerous research projects that aim at accounting for the post-ultimate strength degradation of steel beams with web openings have been undertaken to achieve the objectives: (i) to determine and quantify the influencing parameters (for e.g. opening shape and rates, beam depth, flange width-to-thickness ratio and web thickness) on the particular failure mode, (ii) to develop new or improving the available design rules predicting the ultimate strength based on failure mode with high accuracy and reliability, and thus achieve the full efficiency of these structural elements.

The prediction and analysis of failure modes in I-section beams with unstiffened web openings, as discussed in this paper, highlight the intricate interactions among various geometric parameters. Key factors such as beam length, opening spacing, slenderness ratios, and web-flange interactions play a critical role in determining the manifestation of failure, whether it is local buckling, Vierendeel mechanisms, or global instability. While short beams are more susceptible to shear-related failures, long beams typically exhibit lateral-torsional or distortional buckling, particularly when the compressed flange lacks adequate stabilization. Furthermore, opening configurations — including spacing-to-diameter ratios and edge-to-edge spacing ratios — significantly impact the buckling behavior of web posts and the limits for Vierendeel failure. These findings underscore the importance of carefully balancing design parameters to mitigate failure risks and enhance beam performance. The specific threshold values and critical relationships, as outlined in this research, are presented in tabular form, providing practical insights and a concise reference for engineers and researchers. Future experimental investigations on less-studied parameters, such as irregular opening geometries and h_0/d_w ratios above 0.8, are essential to further refine predictive models and broaden design applications.

CRediT authorship contribution statement

Maja Ranisavljević: Conceptualization, Data curation, Formal Analysis, Investigation, Methodology, Visualization, Writing – original draft, Writing – review & editing. **Jelena Dobrić**: Conceptualization, Methodology, Supervision, Writing – original draft, Writing – review & editing.

Declaration of competing interest

The authors declare that they have no known competing financial interests or personal relationships that could have appeared to influence the work reported in this paper.

Acknowledgments

This study was conducted without any external funding or institutional support.

References

[1] R.M. Lawson, S.J. Hicks, Design of Composite Beams with Large Web Openings, (2011).

[2] W.K. Lucas, D. Darwin, Steel and Composite Beams With Web Openings, The University of Kansas, Lawrence, Kansas, 1990. https://hdl.handle.net/1808/20406.

[3] S.G. Morkhade, L.M. Gupta, Parametric Study of Steel Beams with Web Openings, in: 2014: pp. 3289–3296.

[4] V. Thevendran, N.E. Shanmugam, Lateral buckling of doubly symmetric beams containing openings, J. Eng. Mech. 117 (1991) 1427–1441. https://doi.org/10.1061/(ASCE)0733-9399(1991)117:7(1427).

[5] S. Durif, A. Bouchaïr, O. Vassart, Validation of an analytical model for curved and tapered cellular beams at normal and fire conditions, Period. Polytech. Civ. Eng. 57 (2013) 83–95. https://doi.org/10.3311/PPci.2144.

[6] N.D. Lagaros, L.D. Psarras, M. Papadrakakis, G. Panagiotou, Optimum design of steel structures with web openings, Eng. Struct. 30 (2008) 2528–2537. https://doi.org/10.1016/j.engstruct.2008.02.002.

[7] P. Wang, Q. Ma, X. Wang, Investigation on Vierendeel mechanism failure of castellated steel beams with fillet corner web openings, Eng. Struct. 74 (2014) 44–51. https://doi.org/10.1016/j.engstruct.2014.05.008.
[8] D. Sonck, R. Van Impe, J. Belis, Experimental investigation of residual stresses in steel cellular and castellated members, Constr. Build. Mater. 54 (2014) 512–519. https://doi.org/10.1016/j.conbuildmat.2013.12.045.
[9] A.M. Sayed, Numerical study of the effects of web openings on the load capacity of steel beams with corrugated webs, J. Constr. Steel Res. 196 (2022) 107418. https://doi.org/10.1016/j.jcsr.2022.107418.
[10] prEN 1993-1-13, Eurocode 3 — Design of steel structures — Part 1-13: Rules for beams with large web openings, CEN, Brussels
[11] EN 1993-1-1, Eurocode 3 — Design of steel structures — Part 1-1: General rules and rules for buildings, CEN, Brussels, (2005).
[12] EN 1993-1-5, Eurocode 3 — Design of steel structures — Part 1-5: Plated structural elements, CEN, Brussels, (2006).
[13] American Institute of Steel Construction AISC. Steel design guide 31: Castellated and cellular beams design, (2016).
[14] S.L. Srimani, An Investigation of Deflections in Castellated Beams, J. Inst. Engi- Neers 58 (1977).
[15] D. Zhou, L. Li, J. Schnell, W. Kurz, P. Wang, Elastic Deflections of Simply Supported Steel I-Beams with a Web Opening, Procedia Eng. 31 (2012) 315–323. https://doi.org/10.1016/j.proeng.2012.01.1030.
[16] W. Yuan, N. Yu, Z. Bao, L. Wu, Deflection of castellated beams subjected to uniformly distributed transverse loading, Int. J. Steel Struct. 16 (2016) 813–821. https://doi.org/10.1007/s13296-015-0120-2.
[17] P. Panedpojaman, T. Thepchatri, Finite element investigation on deflection of cellular beams with various configurations, Int. J. Steel Struct. 13 (2013) 487–494. https://doi.org/10.1007/s13296-013-3008-z.
[18] S. Durif, A. Bouchair, Analytical model to predict the resistance of cellular beams with sinusoidal openings, J. Constr. Steel Res. 121 (2016) 80–96. https://doi.org/10.1016/j.jcsr.2016.01.015.
[19] K.F. Chung, T.C.H. Liu, A.C.H. Ko, Investigation on Vierendeel mechanism in steel beams with circular web openings, J. Constr. Steel Res. 57 (2001) 467–490. https://doi.org/10.1016/S0143-974X(00)00035-3.
[20] D. Kerdal, D.A. Nethercot, Failure modes for castellated beams, J. Constr. Steel Res. 4 (1984) 295–315. https://doi.org/10.1016/0143-974X(84)90004-X.
[21] R. Redwood, S.H. Cho, Design of steel and composite beams with web openings, J. Constr. Steel Res. 25 (1993) 23–41. https://doi.org/10.1016/0143-974X(93)90050-3.
[22] R.M. Lawson, K.P. Chung, A.M. Price, Tests on Composite Beams with Large Web Openings to Justify Existing Design Methods, Struct. Eng. 70 (1992).
[23] S. Hicks, C. Müller, O. Hechler, A. Bureau, D. Bitar, D. Joyeux, L.-G. Cajot, T. Demarco, M. Lawson, P. Devine, O. Lagerqvist, E. Hedman-Petursson, E. Unosson, M. Feldmann, Large web opening for service integration in composite floors, 2006.
[24] K.F. Chung, R.M. Lawson, Simplified design of composite beams with large web openings to Eurocode 4, J. Constr. Steel Res. 57 (2001) 135–164. https://doi.org/10.1016/S0143-974X(00)00011-0.
[25] J.P. de Oliveira, D.C.T. Cardoso, E.D. Sotelino, Elastic flexural local buckling of Litzka castellated beams: Explicit equations and FE parametric study, Eng. Struct. 186 (2019) 436–445. https://doi.org/10.1016/j.engstruct.2019.02.034.
[26] B. Anupriya, K. Jagadeesan, Shear strength of castellated beam with and without stiffeners using FEA (ANSYS 14), Int. J. Eng. Technol. 6 (2014) 1970–1981.
[27] K.D. Tsavdaridis, G. Galiatsatos, Assessment of cellular beams with transverse stiffeners and closely spaced web openings, Thin-Walled Struct. 94 (2015) 636–650. https://doi.org/10.1016/j.tws.2015.05.005.
[28] R. Lupien, R.G. Redwood, Steel beams with web openings reinforced on one side, Can. J. Civ. Eng. 5 (1978) 451–461. https://doi.org/10.1139/l78-051.
[29] T. Al-Dafafea, S. Durif, A. Bouchaïr, E. Fournely, Experimental study of beams with stiffened large web openings, J. Constr. Steel Res. 154 (2019) 149–160. https://doi.org/10.1016/j.jcsr.2018.11.026.
[30] A.A. Aglan, R.G. Redwood, Web Buckling in Castellated Beams, in: 1974: pp. 7687–7701. https://www.scribd.com/document/531475565/1974-Aglan-AA.
[31] K. Tsavdaridis, D. C, Finite Element Investigation on Web-Post Buckling of Perforated Steel Beams with Various Web Opening Shapes Subjected Under Different Shear-Moment Interaction, 2011.
[32] P. Panedpojaman, T. Thepchatri, S. Limkatanyu, Novel design equations for shear strength of local web-post buckling in cellular beams, Thin-Walled Struct. 76 (2014) 92–104. https://doi.org/10.1016/j.tws.2013.11.007.
[33] F.P.V. Ferreira, C.H. Martins, S. De Nardin, Assessment of web post buckling resistance in steel-concrete composite cellular beams, Thin-Walled Struct. 158 (2021) 106969. https://doi.org/10.1016/j.tws.2020.106969.
[34] P. Wang, K. Guo, M. Liu, L. Zhang, Shear buckling strengths of web-posts in a castellated steel beam with hexagonal web openings, J. Constr. Steel Res. 121 (2016) 173–184. https://doi.org/10.1016/j.jcsr.2016.02.012.
[35] R. Redwood, S. Demirdjian, Castellated Beam Web Buckling in Shear, J. Struct. Eng. 124 (1998) 1202–1207. https://doi.org/10.1061/(ASCE)0733-9445(1998)124:10(1202).
[36] A.S. De Carvalho, C.H. Martins, A. Rossi, V.M. De Oliveira, S.G. Morkhade, Moment gradient factor for steel I-beams with sinusoidal web openings, J. Constr. Steel Res. 202 (2023) 107775. https://doi.org/10.1016/j.jcsr.2023.107775.
[37] D.E.-D. Kerdal, Lateral-torsional buckling strength of castellated beams, phd, University of Sheffield, 1982. https://etheses.whiterose.ac.uk/2981/.
[38] J. Nseir, M. Lo, D. Sonck, H. Somja, O. Vassart, N. Boissonnade, Lateral Torsional Buckling of Cellular Steel Beams, in: Proc. Annu. Stab. Conf. Struct. Stab. Res. Counc., Grapevine, Texas, 2012.
[39] H. Showkati, T. Ghanbari Ghazijahani, A. Noori, T. Zirakian, Experiments on elastically braced castellated beams, J. Constr. Steel Res. 77 (2012) 163–172. https://doi.org/10.1016/j.jcsr.2012.05.008.
[40] T. Zirakian, H. Showkati, Experiments on Distortional Buckling of I-Beams, J. Struct. Eng. 133 (2007) 1009–1017. https://doi.org/10.1061/(ASCE)0733-9445(2007)133:7(1009).

[41] M.D. Altifillisch, Cooke B.R., Toprac A.A., An investigation of open web expanded beams, Weld. Res. 47 (1957) 77–88.
[42] A. Toprac, B. Cooke, An experimental investigation of open-web beams, in: 1959.
[43] Sherboume A.N., The plastic behaviour of castellated beams, in: London, 1966: pp. 1–5.
[44] A. Bazile, J. Texier, Tests on castellated beams, Constr. Met. 3 (1968) 12–25.
[45] M.U. Hosain, W.G. Speirs, Failure of castellated beams due to rupture of welded joints, Acier-Stahl-Steel (1971).
[46] M. Hosain, W.G. Speirs, EXPERIMENTS ON CASTELLATED STEEL BEAMS, in: 1973.
[47] W.J. Zaarour, Web buckling in thin webbed castellated beams, McGill University, 1995. https://escholarship.mcgill.ca/concern/theses/7m01bn785.
[48] T. Zirakian, H. Showkati, Distortional buckling of castellated beams, J. Constr. Steel Res. - J CONSTR STEEL RES 62 (2006) 863–871. https://doi.org/10.1016/j.jcsr.2006.01.004.
[49] E. Ellobody, Interaction of buckling modes in castellated steel beams, J. Constr. Steel Res. - J CONSTR STEEL RES 67 (2011) 814–825. https://doi.org/10.1016/j.jcsr.2010.12.012.
[50] D. Sonck, J. Belis, Lateral-Torsional Buckling Resistance of Castellated Beams, J. Struct. Eng. 143 (2016) 04016197. https://doi.org/10.1061/(ASCE)ST.1943-541X.0001690.
[51] C.M. Weidlich, E.D. Sotelino, D.C.T. Cardoso, An application of the direct strength method to the design of castellated beams subject to flexure, Eng. Struct. 243 (2021) 112646. https://doi.org/10.1016/j.engstruct.2021.112646.
[52] S. Morkhade, L. Gupta, Critical study of steel beams with web openings, Aust. J. Struct. Eng. 24 (2022) 1–12. https://doi.org/10.1080/13287982.2022.2117319.
[53] S. taş, F. Erdal, O. Tunca, R. Ozcelik, Effect of geometry on flexural behavior of optimal designed web-expanded beams, J. Constr. Steel Res. 2015 (2024) 108500. https://doi.org/10.1016/j.jcsr.2024.108500.
[54] R.G. Redwood, J.O. Mccutcheon, Beam Tests with Unreinforced Web Openings, J. Struct. Div. 94 (1968) 1–17.
[55] J.O. Surtees, Z. Lui, Report of loading tests on cellform beams., University of Leeds, Leeds, 1995.
[56] J. Warren, Ultimate load and deflection behaviour of cellular beams., (2001). http://hdl.handle.net/10413/5272 (accessed October 7, 2024).
[57] K. Tsavdaridis, D. C, H. M, Experimental Study of Ultra Shallow Floor Beams (USFB) with Perforated Steel Sections, 2009.
[58] K. Tsavdaridis, C. D'Mello, Web buckling study of the behaviour and strength of perforated steel beams with different novel web opening shapes, J. Constr. Steel Res. - J CONSTR STEEL RES 67 (2011) 1605–1620. https://doi.org/10.1016/j.jcsr.2011.04.004.
[59] E. Ellobody, Nonlinear analysis of cellular steel beams under combined buckling modes, Thin-Walled Struct. 52 (2012) 66–79. https://doi.org/10.1016/j.tws.2011.12.009.
[60] F. Erdal, M. Saka, Ultimate load carrying capacity of optimally designed steel cellular beams, J. Constr. Steel Res. 80 (2013) 355–368. https://doi.org/10.1016/j.jcsr.2012.10.007.
[61] R.M. Lawson, A. Basta, A. Uzzaman, Design of stainless steel sections with circular openings in shear, J. Constr. Steel Res. 112 (2015) 228–241. https://doi.org/10.1016/j.jcsr.2015.04.017.
[62] D. Sonck, J. Belis, Lateral–torsional buckling resistance of cellular beams, J. Constr. Steel Res. 105 (2015) 119–128. https://doi.org/10.1016/j.jcsr.2014.11.003.
[63] S. Morkhade, Experimental investigation for failure analysis of steel beams with web openings, Steel Compos. Struct. 23 (2017) 647–656. https://doi.org/10.12989/scs.2017.23.6.647.
[64] F. Ferreira, A. Rossi, C. Martins, Lateral-torsional buckling of cellular beams according to the possible updating of EC3, J. Constr. Steel Res. 153 (2019) 222–242. https://doi.org/10.1016/j.jcsr.2018.10.011.
[65] J. Abbas, Behaviour of Steel I Beams with Web Openings, Civ. Eng. J. 9 (2023) 596–617. https://doi.org/10.28991/CEJ-2023-09-03-08.
[66] S. Durif, A. Bouchaïr, Behavior of Cellular Beams with Sinusoidal Openings, Procedia Eng. 40 (2012) 108–113. https://doi.org/10.1016/j.proeng.2012.07.064.
[67] S. Durif, A. Bouchaïr, O. Vassart, Experimental tests and numerical modeling of cellular beams with sinusoidal openings, J. Constr. Steel Res. 82 (2013) 72–87. https://doi.org/10.1016/j.jcsr.2012.12.010.
[68] S. Durif, Comportement mécanique des poutres cellulaires à ouvertures sinusoïdales : développement d'un modèle anlytique adapté, phdthesis, Université Blaise Pascal - Clermont-Ferrand II, 2012. https://theses.hal.science/tel-00872126.
[69] N. Boissonnade, J. Nseir, M. Lo, H. Somja, Design of cellular beams against lateral torsional buckling, Proc. Inst. Civ. Eng. - Struct. Build. 167 (2014) 436–444. https://doi.org/10.1680/stbu.12.00049.
[70] P. Wang, X. Wang, N. Ma, Vertical shear buckling capacity of web-posts in castellated steel beams with fillet corner hexagonal web openings, Eng. Struct. 75 (2014) 315–326. https://doi.org/10.1016/j.engstruct.2014.06.019.
[71] P.-O. Martin, M. Couchaux, O. Vassart, A. Bureau, An analytical method for the resistance of cellular beams with sinusoidal openings, Eng. Struct. 143 (2017) 113–126. https://doi.org/10.1016/j.engstruct.2017.03.048.
[72] S. Morkhade, L. Gupta, Analysis of steel I-beams with rectangular web openings: experimental and finite element investigation, Eng. Struct. Technol. 7 (2015) 13–23. https://doi.org/10.3846/2029882X.2015.1085332.
[73] J.E. Bower, Ultimate strength of beams with rectangular holes, J. Struct. Div. (1968). https://trid.trb.org/View/105397.
[74] T.C.H. Liu, K.F. Chung, Steel beams with large web openings of various shapes and sizes: finite element investigation, J. Constr. Steel Res. 59 (2003) 1159–1176. https://doi.org/10.1016/S0143-974X(03)00030-0.
[75] S. Tudjono, Sunarto, A.L. Han, Analysis of castellated steel beam with oval openings, IOP Conf. Ser. Mater. Sci. Eng. 271 (2017) 012104. https://doi.org/10.1088/1757-899X/271/1/012104.
[76] P. Panedpojaman, T. Thepchatri, S. Limkatanyu, Novel simplified equations for Vierendeel design of beams with (elongated) circular openings, J. Constr. Steel Res. 112 (2015) 10–21. https://doi.org/10.1016/j.jcsr.2015.04.007.

[77] K.D. Tsavdaridis, C. D'Mello, Optimisation of novel elliptically-based web opening shapes of perforated steel beams, J. Constr. Steel Res. 76 (2012) 39–53. https://doi.org/10.1016/j.jcsr.2012.03.026.
[78] K.D. Tsavdaridis, C. D'Mello, Vierendeel bending study of perforated steel beams with various novel web opening shapes through nonlinear finite-element analyses, J. Struct. Eng. U. S. 138 (2012) 1214–1230. https://doi.org/10.1061/(ASCE)ST.1943-541X.0000562.
[79] K.F. Chung, C.H. Liu, A.C.H. Ko, Steel beams with large web openings of various shapes and sizes: an empirical design method using a generalised moment-shear interaction curve, J. Constr. Steel Res. 59 (2003) 1177–1200. https://doi.org/10.1016/S0143-974X(03)00029-4.
[80] S.L. Srimani, Investigation on Deflection of Castellated Beams with Octagonal Shaped Holes, J. Inst. Eng. 62 (1981).
[81] M.R. Soltani, A. Bouchaïr, M. Mimoune, Nonlinear FE analysis of the ultimate behavior of steel castellated beams, J. Constr. Steel Res. 70 (2012) 101–114. https://doi.org/10.1016/j.jcsr.2011.10.016.
[82] P. Panedpojaman, W. Sae-Long, T. Chub-uppakarn, Cellular beam design for resistance to inelastic lateral–torsional buckling, Thin-Walled Struct. 99 (2015). https://doi.org/10.1016/j.tws.2015.08.026.
[83] A.M.I. Sweedan, Elastic lateral stability of I-shaped cellular steel beams, J. Constr. Steel Res. (2011).
[84] V.T. Lian, N.E. Shanmugam, Openings in horizontally curved plate girder webs, Thin-Walled Struct. 41 (2003) 245–269. https://doi.org/10.1016/S0263-8231(02)00090-3.
[85] A.R. Zainal Abidin, B.A. Izzuddin, Meshless local buckling analysis of steel beams with irregular web openings, Eng. Struct. 50 (2013) 197–206. https://doi.org/10.1016/j.engstruct.2012.10.006.
[86] P.B. Cooper, R.R. Snell, H. Knostman, Failure Tests on Beams with Eccentric Web Holes, J. Structuml Div. 103 (1972) 1731–1737.
[87] W. Yuan, B. Kim, L. Li, Buckling of axially loaded castellated steel columns, J. Constr. Steel Res. 92 (2014) 40–45. https://doi.org/10.1016/j.jcsr.2013.10.013.
[88] M. Ranisavljević, J. Dobrić, Experimental responses of compressed I-section short columns with web openings, in: 16th Int. Sci. Conf. INDiS Novi Sad, Personal communication: pp. 70–79.
[89] M. Ranisavljević, J. Dobrić, A. Filipović, M. Spremić, Design cross-section resistances of perforated columns under compression, in: 9th Int. Conf. Civ. Eng. – Sci. Pract. GNP Kolašin, Personal communication: pp. 347–354.
[90] J.G. Verweij, Cellular beam-columns in portal frame structures, Delft University of Technology, 2010.
[91] D. Sonck, N. Boissonnade, R.V. Impe, Instabilities of Cellular Members Loaded in Bending or Compression, in: Proc. Annu. Stab. Conf. Struct. Stab. Res. Counc., Grapevine, Texas, 2012.
[92] M. Najafi, Y.C. Wang, Behaviour and design of steel members with web openings under combined bending, shear and compression, J. Constr. Steel Res. 128 (2017) 579–600. https://doi.org/10.1016/j.jcsr.2016.09.011.

Građevinski materijali i konstrukcije
Building Materials and Structures
journal homepage: www.dimk.rs

https://doi.org/10.5937/GRMK2400009A UDK: 624.042.7(497.7)

Technical paper

Building exposure model for seismic risk assessment of the city of Strumica

Nadica Angova Kolevska[*1)], Marija Vitanova[1)]

[1)] *Institute of Earthquake Engineering and Engineering Seismology (IZIIS), Ss, Cyril and Methodius" University, Skopje, St. ,,Todor Aleksandrov" nb.165, 1000 Skopje, North Macedonia*

Article history
Received: 10 October 2024
Received in revised form:
11 November 2024
Accepted: 13 November 2024
Available online: 05 December 2024

Keywords
seismic risk assessment,
hazard,
exposure,
vulnerability models,
disasters

ABSTRACT

Seismic risk assessment at the city scale has always been useful for pre-earthquake planning, managing future investments, and prioritizing the seismic repair and retrofit of existing buildings immediately after the earthquake. It is carried out by combining hazard, exposure, and vulnerability models. Exposure in this context, refers to the elements at risk: population, buildings, lifeline systems, or socio-economic activities. Risk assessment analysis for different regions and cities worldwide shows that exposure and vulnerability are key elements for effective risk assessment.

This paper provides an inside into the development of an exposure model of Strumica, North Macedonia, that describes the distribution of Strumica's main residential, industrial, and commercial building classes. The exposure database consisting of the existing building inventory is created using the international standard taxonomy for earthquake risk assessment, proposed by the Global Earthquake Model.

This exposure model points out problems and concerns brought about by the implementation process and details the practical solutions and strategies used to achieve the set goals.

The long-term expectation is that this exposure model will allow updating existing plans for emergencies, crises, and disasters, allowing city planners to include seismic risk assessment analyses that contain real data to encourage future risk reduction strategies.

1 Introduction

Over half of the world's population lives in high-risk areas exposed to at least one type of natural hazard: floods, cyclones, droughts, or earthquakes. Earthquakes are one of the most devastating and terrifying natural disasters that a human being can experience, and they can cause almost two-thirds of total annual world economic losses [1].

Seismic risk assessment can be defined as a process that determines the probability of losses by analyzing potential hazards and evaluating existing vulnerability conditions that could threaten or harm people, properties, and the environment on which they depend [2], [3].

The assessment of seismic vulnerability as one of the primary components of risk depends on the characteristics of the buildings or group of buildings being analyzed and the available information about them, the appropriate assessment method (qualitative or quantitative), and the field data collected.

Identifying relevant parameters of the exposed building stock is the first step in establishing a rational basis for creating risk reduction strategies and providing a realistic estimation of seismic vulnerability [4].

Data on social and economic losses from past earthquakes show that the most frequent and greatest losses are those caused by damage and collapse of buildings [1]. Precisely because of this, the data on the existing building stock must be adequately evaluated and updated promptly. An assessment of damage and losses to existing building stock cannot be done without first creating an exposure model that contains all the necessary information about the buildings that are the subject of assessment.

The exposure model is a key component of a seismic risk model, which captures the spatial distribution of population and built assets along with their structural characteristics and valuation that are required for seismic risk assessment [5].

This study describes the development of a building exposure model for the City of Strumica [6] containing information on geographical distributions, structural characteristics, age, number of stories above ground, ductility of building structures, structural cost for each building, and building occupancy. Existing available data

* Corresponding author:
E-mail address: nadica_angova@hotmail.com

which includes 4367 buildings, have been updated to create the most relevant building exposure database possible.

2. Study area

2.1 Seismicity

The territory of the Republic of North Macedonia and the bordering countries (Albania, Bulgaria, Greece, Serbia-South) are among the most seismically active regions of the Balkan Penisula. Historically, these territories have been affected by several moderate, strong, and major earthquakes associated with damaging intensities reaching IX to X degrees of MSK-64 seismic intensity scale [7]. According to the existing historical records, many destructive earthquakes struck the territory of Macedonia and its adjacent regions, before 1900.

Strumica is a city in the Southeastern region of the Republic of North Macedonia [6], where tectonic activity is less pronounced [8]. It belongs to the Valandovo-Gevgelija Seismotectonic Zone out of 10 Active Seismotectonic Zones determined from consideration of the present-day SBER tectonic regime of the region and the subset of the Macedonian earthquake catalog [9]. Along the Strumica fault which is very traceable in the relief and limits the graben from the Belasica horst, occur rare and weak earthquakes [7]. The strongest earthquakes that affected the Strumica region took place in 1904 (Pehchevo-Kresna Mw.7.2) [10] and 1931 (Valandovo-Dojran Mw.6.7) [11].

Relatively weak earthquake activity in the Strumica city area should not be a reason to underestimate seismic risks. Even if future studies for the city prove that seismic risk due to local seismicity can be neglected compared to some other risks for the existing building stock, recent studies have shown that the closeness of the Valandovo area as the seismically most active area in that region [7] can influence the behavior of the buildings in case of stronger earthquakes.

2.2 Seismic exposure

The uneven distribution of the population and rural-urban migration are important demographic characteristics not only in North Macedonia but in all European countries nowadays. According to the data available, following the Detailed urban plan of the city of Strumica, for which a general urban plan was also adopted, the city itself covers a total area of around 529,41 ha.

According to the Housing and Population Census of the Macedonian Statistical Office in 2021, the population of the city of Strumica is 49,995 thousand inhabitants, of which 33,825 thousand are urban and 16,170 thousand rural, with a total number of 17,400 households located in the city [12]. The size of the city and its population make it one of the largest cities in the southeast of the country.

The available census data are only partially useful because, apart from the housing and population data, they contain no data about the structural characteristics of the existing building stock in the city (material, load-resisting system, number of floors above ground).

The assessment of exposure and damage to the building stock in the city of Strumica, in this paper is based on original data (geographical coordinates, gross and net floor area, and height of the buildings) taken from the Agency for Real Estate Cadastre of North Macedonia [13] and field observations made by the authors and local experts with relevant experience and knowledge in the field of research, to determine the structural system, year/period of construction of the buildings, and/or ductility of building structures.

To obtain a more reliable exposure model of the city of Strumica, it must contain the main structural characteristics of the existing building stock, as the most important data. Only relevant data in the exposure model applied can create relevant risk assessment analysis contributing to reducing negative effects on buildings and people's health and life during and after an earthquake happened.

3. Exposure model for the city of Strumica

3.1 Development of an exposure model

The exposure model intends to collect building-level data only for certain, valuable attributes that are related to specific typologies of buildings and allow risk calculations for each examined building [1]. For the exposure model for the city of Strumica, a working methodology is elaborated, which started the whole process of building exposure modeling by first providing an orthogonal photo of the city of Strumica taken by authorized Geodetic work companies located in Strumica. After obtaining the orthogonal photo of the city it was processed with the help of photogrammetric recording carried out by licensed and authorized geodetic engineers, during which a model of the terrain was obtained, where with the help of special parameters for our country, this model was brought to the exact position according to x and y coordinates and georeferenced rasters were obtained for the city of Strumica. The obtained georeferenced rasters for the city are adopted and applicable by the Real Estate Cadastre Agency of Macedonia [13] Fig.1 (right). These georeferenced rasters for the city of Strumica represent a base on which the existing buildings at the city level proceeded.

All the information about the analyzed building stock, which consists of a total of 4367 objects (Fig. 1 right), was obtained through the process of vectorization and attribution of the real estate (buildings) performed in two software platforms (CAD and GIS): the graphic display of the objects is carried out in the AutoCAD software, while the attribute data for the objects (gross and net floor area, number of buildings, its dimensions and height) were processed in the QGIS software tool [14], based on data previously taken from The official web portal of the Real Estate Cadastre Agency of Macedonia [13] and from the authorized offices of the Real Estate Cadastre Agency of Macedonia located in Strumica.

The structural characteristics of the existing building stock, including 4367 buildings, were collected in situ. The structural system of the buildings was determined through the evaluation of field inspectors based on their experience/knowledge while for determining the year/period of construction, interviews were conducted and questionnaires were distributed which were duly filled by the local citizens living/working in the buildings which were subject to analysis. After collecting the data, it was initially recorded on paper forms, and then transferred to Excel spreadsheets. To continue the procedure, the existing Excel file was converted into a so-called CSV (comma-separated values file) which contains attribute data and coordinates that are closely related to the geometry of the objects in question. It was this file that was imported into the QGIS software tool [14], a tool through which we graphically displayed the obtained results.

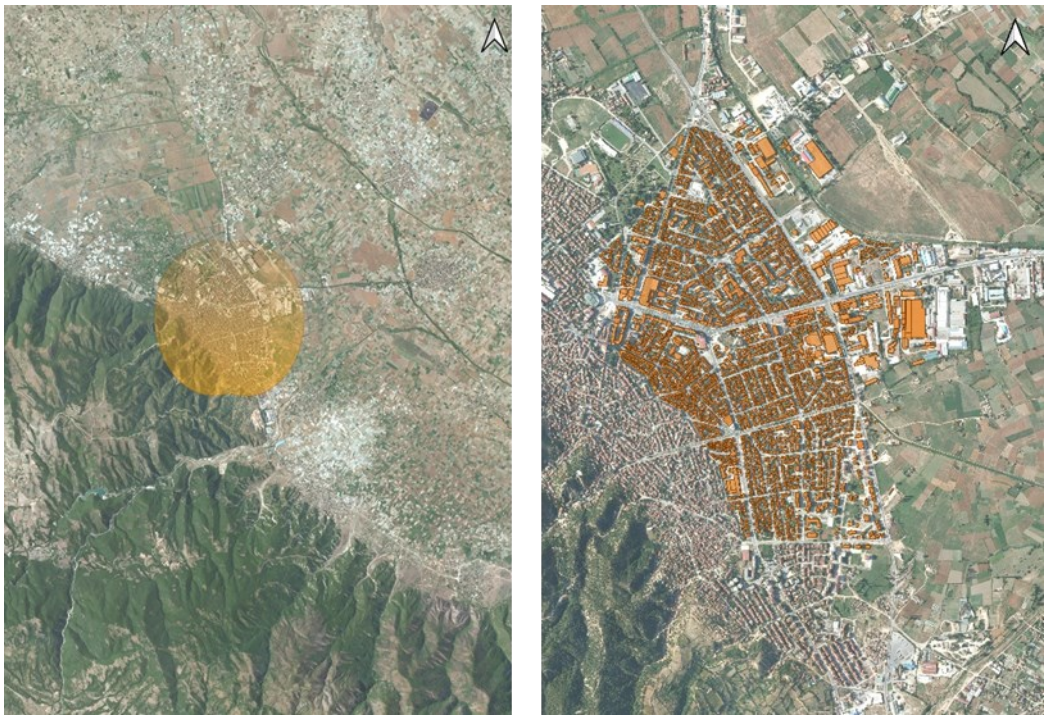

Figure 1. Location layout (left) and existing building stock in the city of Strumica (right) graphically processed in OGIS software tool

After the basic database for the city's exposure model was formed, building classification using the GEM building taxonomy was done. The attribute data such as the building taxonomy was entered and completed by automation in the selected software.

3.2 Classification of the existing building stock using gem building taxonomy

Records of past earthquakes and numerous scientific studies show that some building features have a greater impact on a building's earthquake resistance than others. The building material (brick, reinforced concrete, steel, etc.) and the lateral load-resisting system of the building are very important features that largely define the behavior of buildings during and after an earthquake.

Each material has a different behavior during and after an earthquake. For example, reinforced concrete buildings and steel frame buildings have shown very good behavior during past earthquakes, compared to unreinforced masonry constructions that have shown the worst behavior causing a huge number of losses (human and economic) during earthquakes that occurred in the past [15]. To assess the behavior of buildings in post-earthquake conditions, it is necessary to systematize the existing building stock and provide information on the number of residential, commercial, and industrial buildings and the number of its residents even in the smallest administrative unit of a state-level, data contained in the city's exposure model.

In 2012, the Global Earthquake Model (GEM Building Taxonomy v2.0) adopted 13 attributes that create an exposure model that, alone or in synergy, can significantly affect the seismic behavior of the buildings [16]. In this paper, an exposure model of the city of Strumica, which contains a total of 4367 buildings located in the city, corresponding to the existing situation on the field, graphically presented in Fig. 1 (right) is created. The existing building stock in the city is classified into different building classes according to the building taxonomy scheme developed by GEM (GEM building taxonomy scheme) [16] according to four (4) attributes: main constructional material, number of floors above the ground, year of construction (seismic code), or ductility of the building structure (Table 1). Two more attributes such as the structural cost of each building and building occupancy are taken into consideration while developing the exposure model.

Taking into account the recommendations of the GEM Building typology [16], the available data sources, and the construction specificities in the urban area, the attributes that have been adopted to describe the analyzed buildings classified according to GEM are elaborated (Fig. 2,3,4,5) by:

a) information on the main constructional material used,
b) number of floors above ground level
c) year or period of construction of the building or
d) ductility of building structures

Information about the main construction material used was provided through a visual inspection on site involving field inspectors with previous experience/knowledge.

Data on the number of floors above ground are provided online through the official web portal of the Real Estate Cadastre Agency of Macedonia [13].

The year/period of construction was determined through conducted interviews with local citizens and questionnaires that were properly filled out by them and referred to the buildings in which they live or work and are defined as the main subject of our analysis.

The seismic code of the existing building stock in Strumica is determined considering the evolution of seismic design codes and construction practices in the Republic of North Macedonia (RNM), based on [17], where it is confirmed that three out of four categories of seismic design codes are present in our country: Absence of Seismic Design (CDN) for structures designed before 1948, Low Code Level (CDL) for structures designed between 1948 and 1964, and

Moderate Code Level (CDM) for structures designed from 1964 up to today.

Regarding the ductility of the building structure, for this paper, the European and Global Exposure Model experiences from [18], are applied, where it is confirmed that the ductility of each building structure directly depends on the year of construction and the development of the valid seismic codes and standards of aseismic design in the country/region/town that we are investigating.

In addition to the defined building taxonomy for the existing building stock in the city of (Tab. 1) and their number at a city level (Fig. 4) to more accurately assess the expected vulnerability of buildings from an earthquake, two other important attributes that should be included when completing the exposure data are the: structural cost of each building individually, which in this paper is obtained value using an Official template for determining the value of the building per m^2 prescribed in the Methodology for determining the value of the apartment (Official Gazette of the Republic of Macedonia 13/10) [19] and the building occupancy, an attribute that contains the exact number of users/occupants in each building at different periods of the day, day/night/transit, obtained using available information officially published by the State Statistical Office based on the 2021 North Macedonia, census region 14 - Strumica [20]. Building occupancy is a parameter that is usually used to estimate seismic risk in terms of the number of deaths or injuries after an earthquake happens.

Table 1. Structural typologies for the building's stock in the city of Strumica using the GEM Building Taxonomy scheme [16]

Material	Lateral load-resisting system	Ductility	Seismic Code	Height
MCF (Masonry)	LWAL (Wall)	DUL (Ductility Low)		H:1-H:3
MUR-STDRE (Unreinforced masonry, dressed stone)	LWAL (Wall)	DNO (Non Ductile)		H:2-H:3
MUR-ADO (Adobe Structures)	LWAL (Wall)	DNO (Non Ductile)		H:1
CR (Concrete)	LFINF (Infilled frame)		CDM (Moderate code)	H:1-H:5
CR (Concrete)	LDUAL (Dual frame)	DUM (Ductile, medium)		H:4-H:8
CR (Concrete)	LWAL (Wall)	DUM (Ductile, medium)		H:5
CR (Concrete)	LFM (Moment frame)	DUM (Ductile, medium)		H:1-H:5
S (Steel)	LFM (Moment frame)	DUM (Ductile, medium)		H:1-H:2
S (Steel)	LFBR (Braced frame)	DUM (Ductile, medium)		H:1

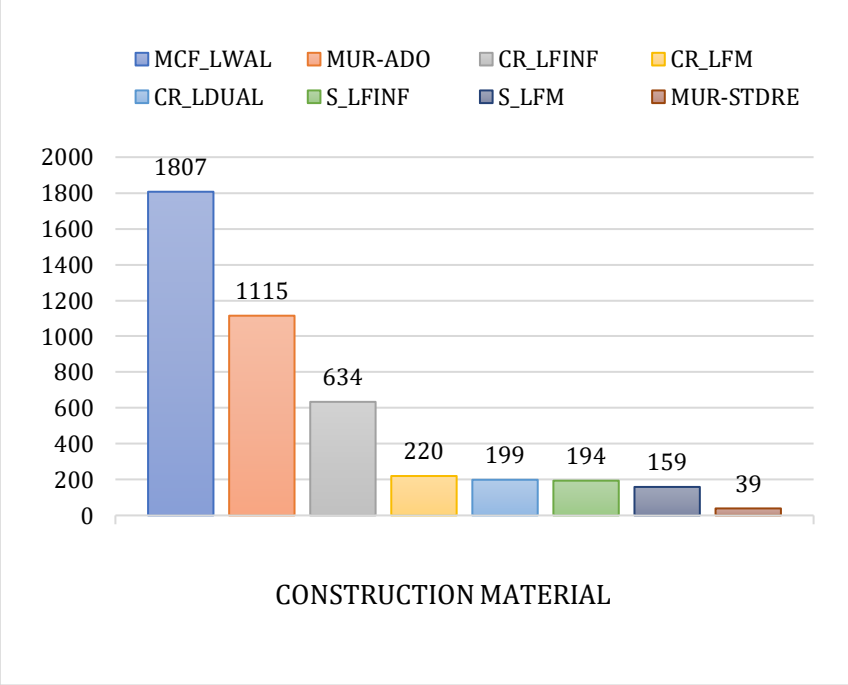

Figure 2. Number of buildings at Strumica city according to: construction material

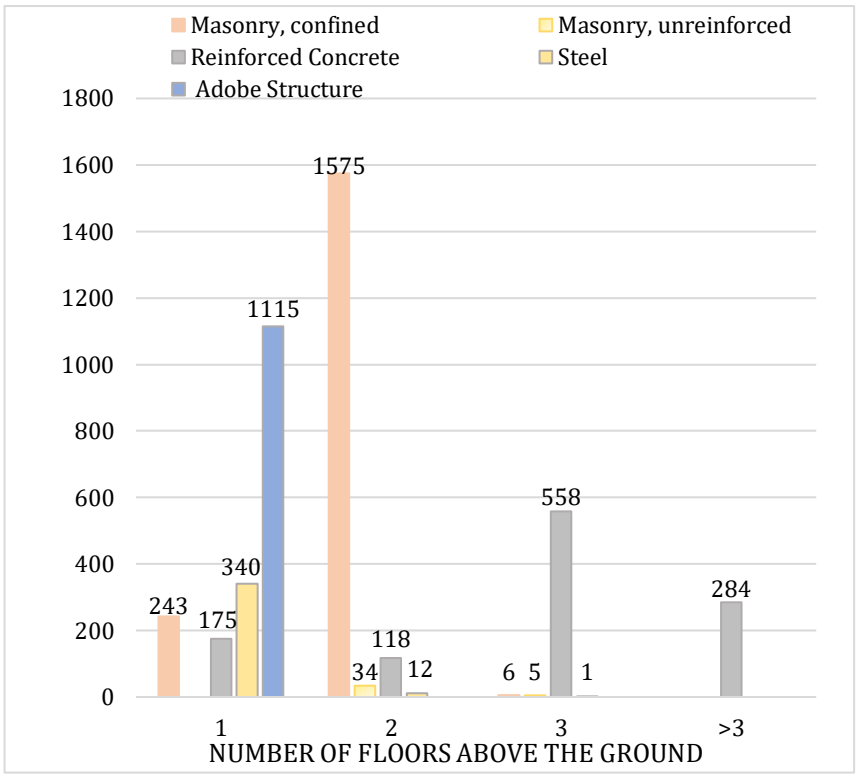

Figure 3. Number of buildings at Strumica city according to: the number of floors above the ground

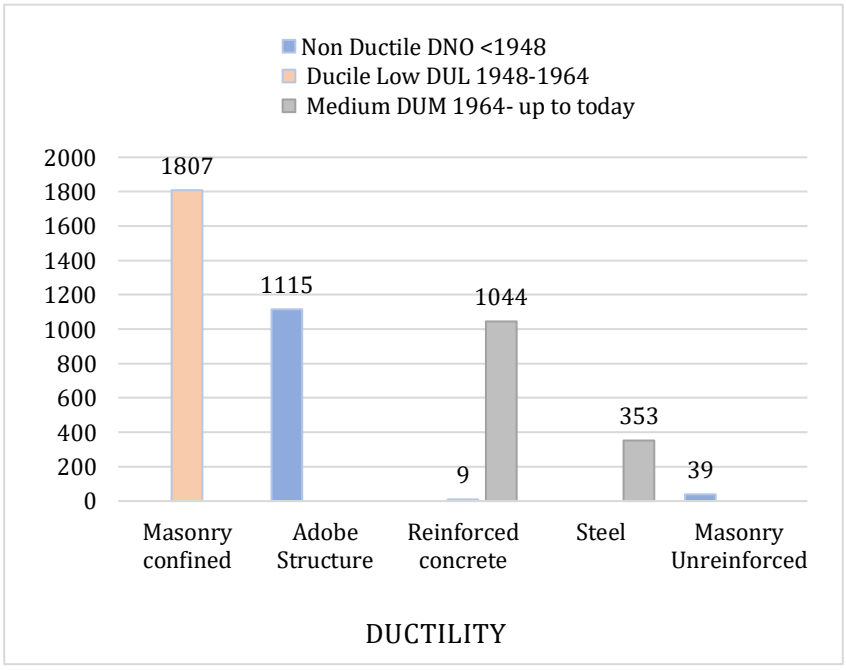

Figure 4. Number of buildings at Strumica city according to: ductility of building structures

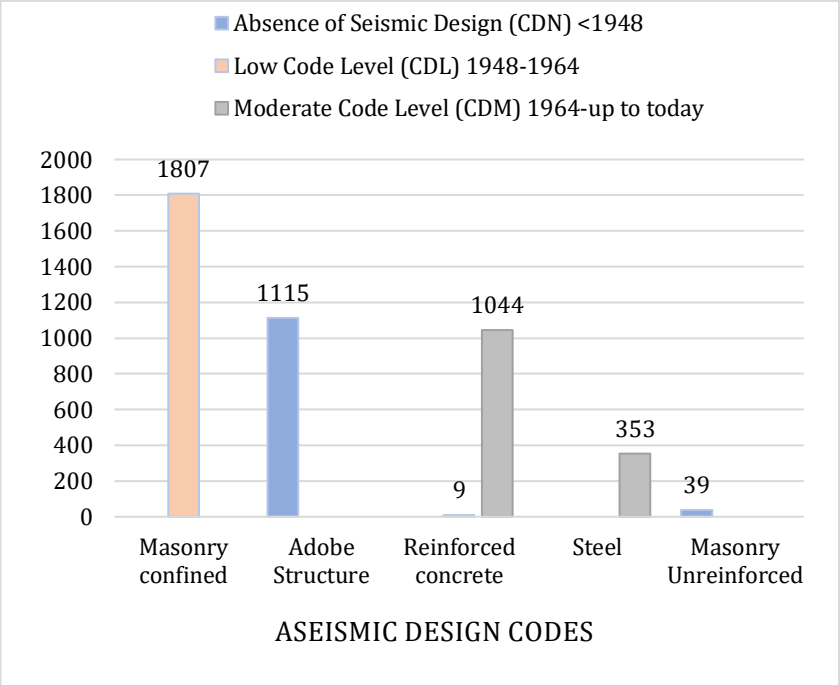

Figure 5. Number of buildings at Strumica city according to aseismic design codes

Although the detailed description of building attributes is of great importance when creating the most relevant exposure model, nowadays researchers tend to simplify building taxonomies when creating a city's exposure model to completely exclude incomplete and/or unreliable information in connection with the existing building stock. The obtained results for the building stock at a city level (4367 buildings) presented in Fig. 2 show that in terms of construction material, masonry confined buildings (MCF_LWAL) are the most common group of buildings represented with a total number of 1807 buildings. The second most common group of buildings in the city such as: garages, utility areas, and sheds known as adobe and earthen structures (MUR-ADO) are represented with a total of 1115 buildings.

Regarding the height of the buildings, the largest number of buildings at the city level:1575 buildings are two-floor masonry confined buildings (G+1) (Fig. 3).

Regarding the ductility of the buildings, most of the analyzed building structures at the city level:1807 buildings are low ductility structures (built in the period 1948-1964) (Fig. 4).

Regarding the period of construction of the buildings and the implementation of the codes for seismic design [17], [18] the largest number of buildings, or a total of 1807 buildings, were built in the period 1948-1964 (low code level) following the evolution of seismic design codes and construction practices in RNM, based on [17] (Fig. 5).

After defining the dominant building classes of the analyzed buildings at a city level, according to the building taxonomy scheme developed by GEM [16] (tab.1), The authors visually inspected buildings in the field. In tab. 2 photos/examples of typical buildings for the respective typology are shown.

Table 2. Building classes in Strumica City (current state)

		
MUR-ADO_LWAL-DNO_H1	**MUR-STDRE_LWAL-DNO_H2**	**MCF_LWAL-DUL_H3**

CR_LFINF-CDM_H2

CR_LDUAL-DUM_H8

CR_LFM-CDM_H4

CR_LWAL-DUM_H5

S_LFINF-DUM_H1

S_LFM-DUM_H1

3.3 Data processing and visualization from the strumica database

The ultimate goal of developing the exposure model for the city of Strumica is to make the collected data useful for planning and preventing earthquakes and other disasters simple, accessible for wider use, and timely updated. As the focal points in exposure modeling involve adding new data, changing, and harmonizing available existing data and its visualization, a computer open-source system Quantum GIS, a geographic information system (GIS) [21] is chosen as a system that can collect, store, analyze, and display geo-referenced data for the chosen city. The distribution of buildings in the city of Strumica, respecting the material, the load-resisting system of buildings, number of floors above ground are shown in Fig. 6 using QGIS.

4 Conclusion

The development and application of exposure models are of great importance to promptly predict and assess building damage and losses. In this paper, throughout the data collection stages, a large number of building attributes were observed and recorded, however, only simplified taxonomies that discard most of the important information about the existing building stock, are used. To examine the overall earthquake performance of buildings through earthquake risk assessment, this exposure model includes the following attributes: longitude and latitude and a building string that contains construction material, year/period of construction or ductility of building structures, and height of buildings above ground.

A three-step methodology was applied to develop an exposure model for the city of Strumica. In the first step, all the necessary building attributes are identified, collected institutionally or on the field, and finally synthesized into an integrated whole. In the second step, according to the adopted methodology for the classification of building typology developed by GEM [16], the existing building taxonomies at the city level are defined. The final third step is visualizing the obtained results using the geographic information system (QGIS) program [21]. Using this program, verified and reliable data on the built construction stock are graphically displayed and easily readable by the general public.

The purpose of this study is not to provide a detailed analysis of the existing building stock in the city because it is a long process that requires a series of additional research and numerous financial resources. This study represents an attempt to make an expert technical assessment of the building stock at a city level, which would greatly help decision-makers to take timely measures for the prevention and mitigation of the consequences of earthquakes as natural disasters. It should be promptly updated and further developed by the ones interested in risk assessment.

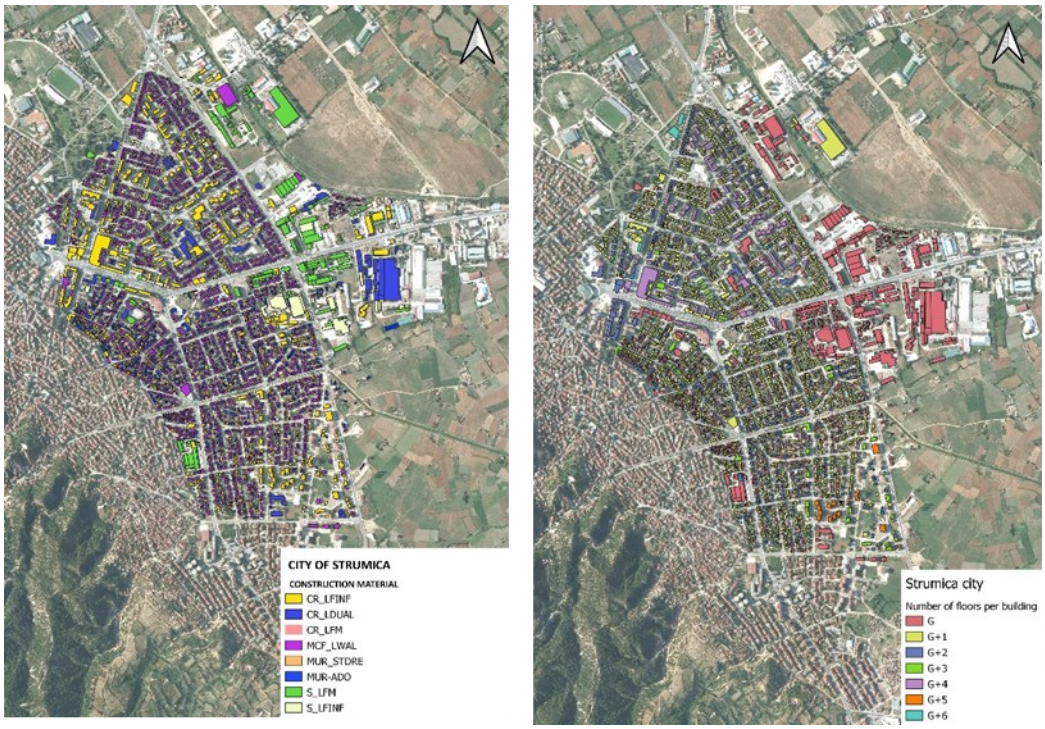

Figure 6. Strumica Database Buildings Using QGIS: a) construction material, b) number of floors above ground

Credit authorship contribution statement

Nadica Angova Kolevska: Data curation, Formal analysis, Investigation; Resources, Software, Visualization, Writing - original draft.

Marija Vitanova: Supervision, Validation, Writing - review & editing.

Nadica Angova Kolevska, Marija Vitanova: Conceptualization, Methodology, Project administration.

Declaration of competing interest

The authors declare that they have no known competing financial interests or personal relationships that could have appeared to influence the work reported in this article

Acknowledgments

I want to express my sincere gratitude and appreciation to my PhD supervisor Prof. Dr. Marija Vitanova for professionally guiding and motivating me through my research, enabling me to finish it successfully. I also want to thank the Municipality of Strumica especially the Department of Urban Planning in the city and the Real Estate Cadastre Agency of Macedonia located in Strumica, who allowed me access and provided all the necessary information and data related to the existing building stock in the city as a case study of this publication.

References

[1] G. Pavic, M. Hadzima-Nyarko, B. Bulajic, Z. Jurkovic. Development of Seismic Vulnerability and Exposure Models - A case study of Croatia. *Sustainability.* 12 (2020) 973. https://doi.org/10.3390/su12030973

[2] Terminology on Disaster Risk Reduction, UN-ISDR. https://www.unisdr.org/we/inform/terminology, 2009 [accessed 16 February 2024].

[3] A. Reisinger, M. Howden, C.Vera et al. The concept of risk in the IPCC Sixth Assessment Report: a summary of cross working Group discussions, Geneva: IPCC Intergovernmental panel on climate change. 2020.

[4] G. Uva, C. A. Sanjust, S. Casolo, M. Mezzina. The ANTAEUS Project for the Regional Vulnerability Assessment of the Current Building Stock in Historical Centres. International Journal of Architectural Heritage, 10 (2016) 20-43. http://dx.doi.org/10.1080/15583058.2014.935983.

[5] M. Jian, R. Anirudh, V. Silva, K. Liu, M. Wang. A township-level exposure model of residential buildings for mainland China. Scholarly Journal, 108 (2021)1:35. https://link.springer.com/article/10.1007/s11069-021-04689-7

[6] Strumica Municipality. https://en.wikipedia.org/wiki/Strumica_Municipality [accessed 20 March 2024].

[7] N. Dumurdjanov, Z. Milutinovic, R. Salic, "Seismotectonic Model Backing the PSHA and Seismic Zoning of Republic of Macedonia for National Annex to MKS EN 1998-1:2012 Eurocode 8. Journal of Seismologs. 24 (2012) 319–341. https://link.springer.com/article/10.1007/s10950-020-09912-9.

[8] Think Hazards (demo instance). https://thinkhazard.org/en/report/2951-fyr-of-macedonia-strumica/EQ," [Online]. [accessed 20 March 2024].

[9] V. Cejkovska, L. Pekevski, K. Drogreska, J. Najdovska. Report per the Project of the Standardization Institute of the Republic of Macedonia entitled National Annexes for Eurocodes, Faculty of Natural Sciences and Mathematics, Seismological Observatory. Ss. Cyril and Methodius University, Skopje. 2016.

[10] Земјотресот Пехчево-Кресна- најсилен на Балканот. Порта 3, Скопје, 2017. (in Macedonian). https://www.porta3.mk/zemjotresot-pehchevo-kresna-najsilen-na-balkanot/. [Online]. [accessed 28 September 2024].

[11] Разурнувачкиот земјотрес во Валандово од 1931 година. Порта 3, Скопје, 2017. (in Macedonian). https://www.porta3.mk/razurnuvachkiot-zemjotres-vo-valandovo-od-1931-godina/. [Online]. [accessed 28 September 2024].
[12] Државен завод за статистика. Република Северна Македонија. (in Macedonian) https://popis2021.stat.gov.mk/. Online]. [accessed 28 September 2024].
[13] Agency for Real Estate Cadastre - Republic of North Macedonia. "https://ossp.katastar.gov.mk/OSSP/ [Online]. [accessed 20 March 2024].
[14] QGIS Web Site https://qgis.org/en/site [accessed 20 March 2024].
[15] A. Dogangun, A. Uran, R. Livaoglu. Seısmıc Performance Of Masonry Buıldıngs Durıng Recent Earthquakes in Turkey. 14th World Conference on Earthquake Engineering (14WCEE), Beijing (2008). https://www.iitk.ac.in/nicee/wcee/article/14_05-04-0079.PDF
[16] S. Brzev, C. Scawthorn, A. Charleson, L. Allen, M. Greene, K. Jaiswal, V. Silva. GEM Building Taxonomy Version 2.0, GEM Technical Report 2013-02 V1.0.0," GEM Foundation, Pavia (2013).
[17] M. Paz. International handbook of earthquake engineering practices, Dordrecht: Springer Science+Bussiness Media, 1994.
[18] Yepes-Estrada, A. Calderon, C. Costa, H. Crowley, J. Dabbeek, M. Hoyos, L. Martins, N. Paul, A. Rao, V. Silva. Global building exposure model for earthquake risk assessment. Earthquake Spectra. 39 (2023) 2212-2235. https://doi.org/10.1177/87552930231194048.
[19] Official Gazette of RM 01 02 2010. https://www.slvesnik.com.mk/besplaten-pristap-do-izdanija.nspx#. [accessed 28 September 2024].
[20] State Statistical Office. Total resident population, households, and dwellings in the Republic of North Macedonia, Census 2021," the Republic of North Macedonia. State Statistical Office. Skopje, 2022.
[21] G. Palino, E. Sparks. QGIS: An Introduction to an Open-Source Geographic Information System. Missisipi State University, Missisipi.

Building Materials and Structures

GUIDE FOR AUTHORS

In the journal *Building Materials and Structures*, the submission and review processes take place electronically. Manuscripts are submitted electronically (online) on the website **https: // www.dimk.rs.** The author should register first, then log in and finally submit the manuscript which should be in the form of editable files (e.g. Word) to enable the typesetting process in journal format. All correspondence, including Editor´s decision regarding required reviews and acceptance of manuscripts, take place via e-mail.

TYPES OF ARTICLES

The following types of articles are published in *Building Materials and Structures:*

Original scientific article. It is the primary source of scientific information, new ideas and insights as a result of original research using appropriate scientific methods. The results are presented briefly, but in a way to enable readers to assess the results of experimental or theoretical/numerical analyses, so that the research can be repeated and yield with the same or results within the limits of tolerable deviations.

Review article. It presents the state of science in particular area as a result of methodically systematized, analyzed and discussed reference data. Only critical review manuscripts will be considered as providing novel perspective and critical evaluation of the topics of interest to broader BMS readership.

Preliminary report. Contains the first short notifications of research results without detailed analysis, i.e. it is shorter than original research paper.

Technical article. Reports on the application of recognized scientific achievements of relevance to the field of building materials and structures. Contain critical analysis and recommendations for adaption of the research results to practical needs.

Projects Notes. Project Notes provide a presentation of a relevant project that has been built or is in the process of construction. The original or novel aspects in design or construction should be clearly indicated.

Discussions. Comment on or discussion of a manuscript previously published in *Building Materials and Structures*. It should be received by the Editor-in-Chief within six months of the online publication of the manuscript under discussion. Discussion Papers will be subject to peer review and should also be submitted online. If Discussion Paper is selected for publication the author of the original paper will be invited to respond, and Discussion Paper will be published alongside any response that the author.

Other contributions

Conference Reports. Reports on major international and national conferences of particular interest to *Building Materials and Structures*. Selected and/or awarded papers from the ASES Conferences are published in Special issues.

Book Reviews. Reviews on new books relevant to the scope of *Building Materials and Structures*.

PREPRINTS

These are the author's own write-up of research results and analysis that has not been peer reviewed, nor had any other value added to it by a publisher (such as formatting, copy-editing, technical enhancements and the like). Authors can share their preprint anywhere at any time. If accepted for publication, we encourage authors to link from the preprint to their formal publication via its Digital Object Identifier (DOI). Preprints should not be added to or enhanced in any way in order to appear more like, or to substitute for, the final versions of articles.

MANUSCRIPT STRUCTURE

The manuscript should be typed one-sided on A4 sheets. Page numbers should be included in the manuscript and the text should be single spaced with **consecutive line numbering** - these are essential peer review requirements. The figures and tables included in the single file should be placed next to the relevant text in the manuscript. The corresponding captions should be placed directly below the figure or table. If the manuscript contains Supplementary material, it should also be submitted at the first submission of the manuscript for review purposes.

There are no strict rules regarding the structure of the manuscript, but the basic elements that it should contain are: Title page with the title of the manuscript, information about the authors, abstract and keywords, Introduction, Materials / Methods, Results and Conclusions.

The front page

The front page contains the title of the manuscript which should be informative and concise; abbreviations and formulas should be avoided.

Information about the authors are below the title; after the author's name, a superscript number is placed indicating his/her affiliation, which is printed below the author's name, and before the abstract. It is obligatory to mark the corresponding author with superscript *) and provide his/her e-mail address. The affiliation should contain the full name of the institution where the author performed the research and its address.

Abstract

Abstract should contain 150-200 words. Motivation and objective of the conducted research should be presented; main results and conclusions should be briefly stated as well. References and abbreviations should be avoided.

Keywords

Keywords (up to 10) should be listed immediately after the abstract; abbreviations should be used only if they are generally accepted and well-known in the field of research.

Division into chapters

The manuscript should be divided into chapters and sub-chapters, which are hierarchically numbered with Arabic numbers. The headings of chapters and sub-chapters should appear on their own separate lines.

At the end of the manuscript, and before the references, it is obligatory to list the following statements:

CRediT authorship contribution statement

For transparency, we require corresponding authors to provide co-author contributions to the manuscript using the relevant CRediT roles. The CRediT taxonomy includes 14 different roles describing each contributor's specific contribution to the research output. The roles are: Conceptualization; Data curation; Formal analysis; Funding acquisition; Investigation; Methodology; Project administration; Resources; Software; Supervision; Validation; Visualization; Roles/Writing - original draft; and Writing - review & editing. Note that not all roles may apply to every manuscript, and authors may have contributed through multiple roles.

Declaration of competing interest

Corresponding authors, on behalf of all the authors of a submission, must disclose any financial and personal relationships with other people or organizations that could inappropriately influence their work. Examples of potential conflicts of interest include employment, consultancies, stock ownership, honoraria, paid expert testimony, patent applications/registrations, and grants or other funding. All authors, including those *without* competing interests to declare, should provide the relevant information to the corresponding author (which, where relevant, may specify they have nothing to declare).

Declaration of generative AI in scientific writing

This guidance only refers to the writing process, and not to the use of AI tools to analyze and draw insights from data as part of the research process. Where authors use generative artificial intelligence (AI) and AI- assisted technologies in the writing process, authors should only use these technologies to improve readability and language. Applying the technology should be done with human oversight and control, and authors should carefully review and edit the result, as AI can generate authoritative-sounding output that can be incorrect, incomplete or biased. AI and AI-assisted technologies should not be listed as an author or co-author, or be cited as an author. Authorship implies responsibilities and tasks that can only be attributed to and performed by humans. Authors should disclose in their manuscript the use of AI and AI- assisted technologies in the writing process by following the instructions below. A statement will appear in the published work. Please note that authors are ultimately responsible and accountable for the contents of the work.

Disclosure instructions

Authors must disclose the use of generative AI and AI-assisted technologies in the writing process by adding a statement at the end of their manuscript in the core manuscript file, before the References list. The statement should be placed in a new section entitled 'Declaration of Generative AI and AI-assisted technologies in the writing process'.

Statement: During the preparation of this work the author(s) used [NAME TOOL / SERVICE] in order to [REASON]. After using this tool/service, the author(s) reviewed and edited the content as needed and take(s) full responsibility for the content of the publication.
This declaration does not apply to the use of basic tools for checking grammar, spelling, references etc. If there is nothing to disclose, there is no need to add a statement.

Acknowledgments

State the institutions and persons who financially or in some other way helped the presented research. If the research was not supported by others, it should also be stated in this part of the manuscript.

Appendices

The manuscript may have appendices. If there is more than one appendix, they are denoted by A, B, etc. Labels of figures, tables and formulas in appendices should contain the label of the appendix, for example Table A.1, Figure A.1, etc.

ABBREVIATIONS

All abbreviations should be defined where they first appear. Consistency of abbreviations used throughout the text should be ensured.

MATH FORMULAE

Formulae should be in the form of editable text (not in the format of figures) and marked with numbers, in the order in which they appear in the text. The formulae and equations should be written carefully takinginto account the indices and exponents. Symbols in formulae should be defined in the order they appear, right below the formulae.

FIGURES

- figures should be made so that they are as uniform in size as possible and of appropriate quality for reproduction;
- the dimensions of the figures should correspond to the format of the journal: figures with a width approximately equal to the width of 1 column (± 80 mm width), width of 2 columns (± 170 mm width) or width of 1.5 columns (± 130 mm width);
- figures should be designed so that their size is not disproportionately large in relation to the content;
- the text on the figures should be minimal and the font used should be the same on all figures (Arial, Times New Roman, Symbol);
- figures should be placed next to the appropriate text in the manuscript and marked with numbers in the order in which they appear in the text;
- each figure should have a caption that is placed below the figure - the caption should not be on the figure itself.

In cases of inadequate quality of reproduction, the author should be required to submit figures as separate files. In this case, the figure should be saved in TIFF (or JPG) format with a minimum resolution of 500 dpi.

TABLES

- tables should be in the form of editable text (not in the format of figures);
- tables should be placed next to the appropriate text in the manuscript and marked with numbers in the order in which they appear in the text;
- each table should have a caption that is placed below the table;
- the tables should not show the results that are already presented elsewhere in the manuscript - duplicating the presentation of results should be avoided;
- tables are without vertical lines as boundaries between cells and shading cells.

REFERENCES

Citation in the text

Each reference cited in the text should be in the reference list (and vice versa). It is not recommended to list unpublished results or personal communications in the reference list, but they can be listed in the text. If they are still listed in the reference list, the journal style references are used, with 'Unpublished results' or 'Personal communication' instead of the date of publication. Citing a reference as ‘in press’ means that it is accepted for publication.

Web references

Web references are minimally listed with the full URL and the date when the site was last accessed. These references can be included in the reference list, but can also be given in a separate list after the reference list.

Reference style

In text: References are given in the text by a number in square brackets in the order in which they appear in the text. Authors may also be referred to directly, but the reference number should always be given.

In reference list: References marked with a number in square brackets are sorted by numbers in the list.

Examples

Reference to a journal publication:

[1] V.W.Y. Tam, M. Soomro, A.C.J. Evangelista, A review of recycled aggregate in concrete applications (2000-2017), Constr. Build. Mater. 172 (2018) 272-292. https://doi.org/10.1016/j.conbuildmat.2018.03.240.

Reference to a book:

[3] A.H. Nilson, D. Darwin, C.W. Dolan, Design of Concrete Structures, thirteenth ed., Mc Graw Hill, New York, 2004.

Reference to a chapter in an edited book:

[4] J.R. Jimenez, Recycled aggregates (RAs) for roads, in: F Pacheco-Torgal, V.W.Y. Tam, J.A. Labrincha, Y. Ding, J. de Brito (Eds.), Handbook of recycled concrete and demolition waste, Woodhead Publishing Limited, Cambridge, UK, 2013, pp. 351–377.

Reference to a website:

[5] WBCSD, The Cement Sustainability Initiative, World. Bus. Counc. Sustain. Dev. http://www.wbcsdcement.org.pdf/CSIRecyclingConcrete-FullReport.pdf, 2017 (accessed 7 July 2016).

SUPPLEMENTARY MATERIAL

Supplementary material such as databases, detailed calculations and the like can be published separately to reduce the workload. This material is published 'as received' (Excel or PowerPoint files will appear as such online) and submitted together with the manuscript. Each supplementary file should be given a short descriptive title.

ETHICS IN PUBLISHING

Authors are expected to respect intellectual and scientific integrity in presentation of their work. The journal publishes manuscripts that have not been previously published and are not in the process of being considered for publication elsewhere. All co-authors as well as the institution in which the research was performed should agree to the publication in the journal.
Authors are expected to submit completely original research; if the research of other researchers is used, it should be adequately cited. Authors who wish to include in their manuscript images, tables or parts of text that have already been published somewhere, should obtain permission from the Copyright owner and provide a proof in the process of submitting the manuscript. All material for which there is no such evidence will be considered the original work of the author. To determine the originality of the manuscript, it can be checked using the Crossref Similarity Check service. For more information, please see our Ethics and Malpractice Statement.

The Journal and Publishers imply that all authors, as well as responsible persons of the institute where the research was performed, agreed with the content of the submitted manuscript before submitting it. The Publishers will not be held legally responsible should there be any claims for compensation.

PEER REVIEW

This journal uses a single blind review process, which means that the authors do not know the names of the reviewers, but the reviewers know who the authors are. In the review process, the Editor-in-Chief first assesses whether the contents of the manuscript comply with the scope of the journal. If this is the case, the paper is sent to at least two independent experts in the field, with the aim of assessing its scientific quality and making recommendation regarding publication. If the manuscript needs to be revised, the authors are provided with the reviewers' remarks. The authors are obliged to correct the manuscript in accordance with the remarks, submit the revised manuscript and a special file with the answers to the reviewers within the given deadline. The final decision, whether the paper will be published in journal or not, is made by the Editor-in-Chief.

AFTER ACCEPTANCE

Once accepted for publication, the manuscript is set in the journal format. Complex manuscript is sent to the authors in the form of proof, for proof reading. Then, authors should check for typesetting errors, and whether the text, images, and tables are complete and accurate. Authors are asked to do this carefully, as subsequent corrections will not be considered. In addition, significant changes to the text and authorship at this stage are not allowed without the consent of the Editor-in-Chief. After online publication, changes are only possible in the form of Erratum which will be hyperlinked to manuscript.

COPYRIGHT

Authors retain copyright of the published papers and grant to the publisher the non-exclusive right to publish the article, to be cited as its original publisher in case of reuse, and to distribute it in all forms and media.

The published articles will be distributed under the Creative Commons Attribution ShareAlike 4.0 International license (CC BY-SA). It is allowed to copy and redistribute the material in any medium or format, and remix, transform, and build upon it for any purpose, even commercially, as long as appropriate credit is given to the original author(s), a link to the license is provided, it is indicated if changes were made and the new work is distributed under the same license as the original.

Users are required to provide full bibliographic description of the original publication (authors, article title, journal title, volume, issue, pages), as well as its DOI code. In electronic publishing, users are also required to link the content with both the original article published in *Building Materials and Structures* and the license used.

Authors are able to enter into separate, additional contractual arrangements for the non-exclusive distribution of the journal's published version of the work (e.g., post it to an institutional repository or publish it in a book), with an acknowledgement of its initial publication in this journal.

OPEN ACCESS POLICY

Journal *Building Materials and Structures* is published under an Open Access license. All its content is available free of charge. Users can read, download, copy, distribute, print, search the full text of articles, as well as to establish HTML links to them, without having to seek the consent of the author or publisher.
The right to use content without consent does not release the users from the obligation to give the credit to the journal and its content in a manner described under *Copyright*.

Archiving digital version

In accordance with law, digital copies of all published volumes are archived in the legal deposit library of the National Library of Serbia in the Repository of SCIndeks - The Serbian Citation Index as the primary full text database.

Cost collection to authors

Journal Building Materials and Structures does not charge authors or any third party for publication. Both manuscript submission and processing services, and article publishing services are free of charge. There are no hidden costs whatsoever.

DISCLAIMER

The views expressed in the published works do not express the views of the Editors and the Editorial Staff. The authors take legal and moral responsibility for the ideas expressed in the articles. Publisher shall have no liability in the event of issuance of any claims for damages. The Publisher will not be held legally responsible should there be any claims for compensation.

Financial support

MINISTRY OF EDUCATION, SCIENCE AND TECHNOLOGICAL DEVELOPMENT OF REPUBLIC OF SERBIA

INSTITUTE FOR TESTING OF MATERIALS-IMS INSTITUTE, BELGRADE

SERBIAN CHAMBER OF ENGINEERS

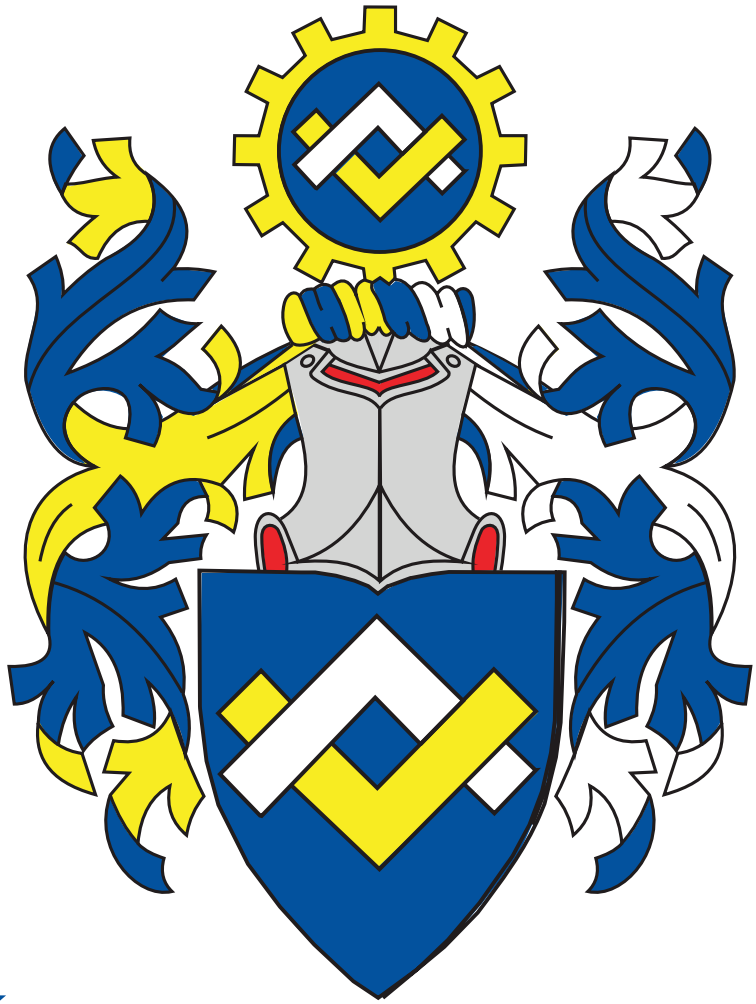

INŽENJERSKA KOMORA SRBIJE

Ringlock

Doka modularni sistem skela.

Bezbedno i efikasno rešenje za skele. Široka oblast primena.

PROVIDING ATPAC COMPLETE SCAFFOLDING SOLUTIONS

Pristupne skele

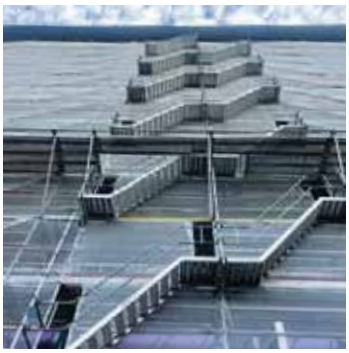

Skele za stambene objekte

Skele za poslovne objekte

Stepenišni toranj

Doka Serb d.o.o. | Svetogorska 4 | 22310 Šimanovci | Srbija | **T** +381 (0)22 400 100 | serb@doka.com | **www.doka.com/rs**

ACO. The future of drainage.

ACO

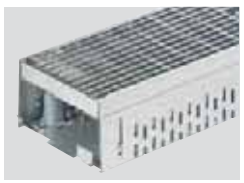

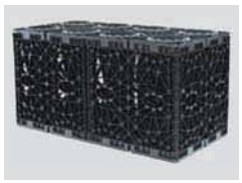

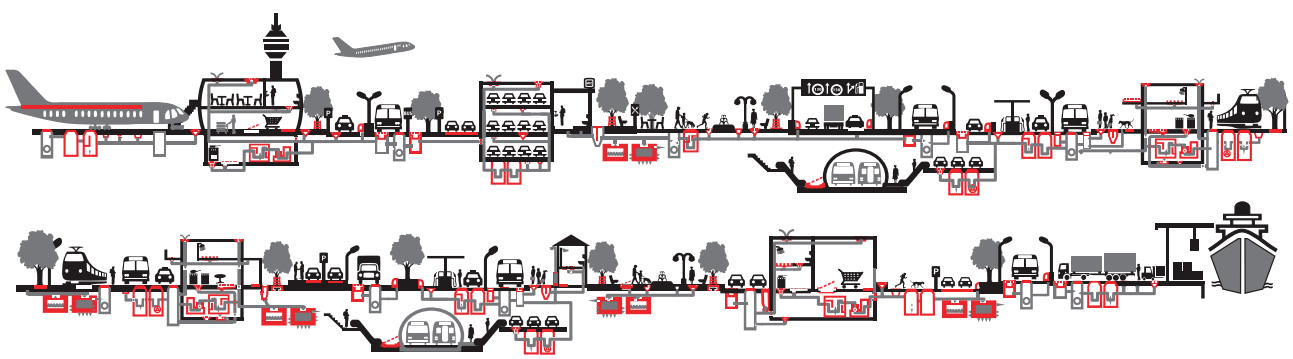

aco.rs

INSTITUT IMS AD
BEOGRAD

CENTAR ZA PUTEVE I GEOTEHNIKU

U okviru centra posluju odeljenja za geotehniku, nadzor i terenska ispitivanja, projektovanje saobraćajnica, laboratorija za puteve i geotehniku. Značajna aktivnost centra usmerena je ka terenskim i laboratorijskim geološko - geotehničkim istraživanjima i ispitivanjima terena za potrebe izrade projekno - tehničke dokumentacije, za različite faze i nivoe projektovanja objekata visokogradnje, niskogradnje, saobraćaja i hidrogradnje, kao i za potrebe prostornog planiranja i zaštite životne sredine. Stručni nadzor, kontrola kvaliteta tokom građenja, rekonstrukcije i sanacije objekata različite namene, izrada studija, ekspertiza, konsultantske usluge, kompletan konsalting u oblasti geotehničkog inženjeringa, neke su od delatnosti centra.

Ispitivanje šipova

- **SLT metoda (Static load test)**
- **DLT metoda (Dynamic load test)**
- **PDA metoda (Pile driving analysis)**
- **PIT (SIT) metoda (Pile (Sonic) integrity testing)**
- **CSL - Crosshole Sonic Logging**

- **Ispitivanje šipova**
  - **Geotehnička istraživanja i ispitivanja – in situ**
    - **Laboratorija za puteve i geotehniku**
      - **Projektovanje puteva i sanacija klizišta**
        - **Nadzor**

Tondach

Krovni sistemi

Najlepši krov u komšiluku

Continental Plus Natura je premium crep u natur segmentu! Dobro poznatog oblika, trajan i veoma otporan, a povrh svega pristupačan, naprosto oduzima dah svima. Čak i vašim komšijama!

Continental Plus Natura crep potražite kod ovlašćenih Tondach partnera.

Wienerberger

PUT INŽENJERING

Put inženjering d.o.o punih 25 godina radi kao specijalizovano preduzeće za izgradnju infrastrukture u niskogradnji i visokogradnji, kao i proizvodnjom kamenog agregata i betona. Preduzeće se bavi i transportom, uslugama građevinske mehanizacije i specijalne opreme.

Za spravljanje betona koristimo drobljeni krečnjački agregat sa našeg kamenoloma, deklarisanih frakcija, kontrolisane vlažnosti. Kompletan proces proizvodnje i kontrole kvaliteta vršimo prema važećim standardima.

Kao generalni izvođač radova, vršimo koordinaciju svih učesnika na projektu, planiranje, praćenje i nabavku materijala, kontrolu kvaliteta izvedenih radova, poštujući zadate vremenske rokove i finansijski okvir investitora.

Obradu armature vršimo brzo, stručno i kvalitetno, sa kompjuterskom preciznošću i dimenzijama po projektu.

Osnovi princip našeg poslovanja zasniva se na individualnom pristupu svakom klijentu i pronalaženje najoptimalnijeg rešenja za njegove transportne i logističke potrebe.

Koristeći inovativne tehnike i kvalitetan građevinski materijal iz sopstvenih resursa, spremni smo da odgovorimo na mnoge zahteve naših klijenata iz oblasti niskogradnje.

Naša kompanija u oblasti visokogradnje primenjuje sistem prefabrikovnih betonskih elemenata koji u odnosu na klasičnu gradnju ima brojne prednosti.

Usluge građevinskom mehanizacijom vršimo tehnički ispravnim mašinama, sa potrebnim sertifikatima kako za rukovaoce građevinskim mašinama tako i za same mašine.

Osnovna prednost prefabrikovane konstrukcije jeste brzina kojom konstrukcija može biti projektovana, proizvedena, transportovana i namontirana.

Prednapregnute šuplje ploče su konstruktivni elementi visokog kvaliteta, proizvedeni u fabrički kontrolisanim uslovima.

Raspolažemo opremom i mašinama za sve zemljane radove, kipere i dampere za rad u teškim terenskim uslovima, automiksere i pumpe za beton, autodizalice, podizne platforme.

Izvodimo hidrograđevinske radove u izgradnji kanalizacionih mreža za odvođenje atmosferskih, otpadnih i upotrebljenih voda, izvođenjem hidrograđevinskih radova u okviru regulacije rečnih tokova, kao i izvođenjem hidrotehničkih objekata.

Izrađujemo betonske "New Jersey profile" koji se u svetu koriste za preusmeravanje saobraćaja i zaštitu pešaka u toku izgradnje puta, kao i Betonblock sistem betonskih blokova.

Sakupljanje i privremeno skladištenje otpada vršimo našim specijalizovanim vozilima i deponujemo na našu lokaciju sa odgovarajućom dozvolom. Kapacitet mašine je 250 t/h građevinskog neopasnog otpada.

Površinski kop udaljen je 35 km od Niša. Savremene drobilice, postrojenje za separaciju i sejalica efikasno usitnjavaju i razdvajaju kamene agregate po veličinama. Tehnički kapacitet trenutne primarne drobilice je 300 t/h.

Uslugu transporta vršimo automikserima, kapaciteta bubnja od 7 m³ do 10 m³ betonske mase. Za ugradnju betona posedujemo auto-pumpu za beton, radnog učinka 150 m³/h, sa dužinom strele od 36 m.

NIŠ
Knjaževačka bb, 18000 Niš - Srbija
+381 18 215 355
office@putinzenjering.com

BEOGRAD
Jugoslovenska 2a, 11250 Beograd – Železnik
+381 11 25 81 111
beograd@putinzenjering.com

MOBECO

www.putinzenjering.com

Mapei proizvodi i rešenja su izbor onih koji znaju da prepoznaju kvalitet, posvećenost svakom detalju i višedecenijsko iskustvo u građevinskoj industriji.

Zato birajte pažljivo. Birajte kvalitet.

Mapei, svetski lider u proizvodnji građevinskih lepkova, hidroizolacija i masa za fugovanje.

Saznaj više na **www.mapei.rs**

MAPEI®

ŽIVI KVALITETNO

MATEST
YOUR PARTNER IN TESTING

iT TECH

INELAS ERECO d.o.o

MATEST "iT TECH" KONTROLNA JEDINICA

JEDNA TEHNOLOGIJA MNOGO REŠENJA

IT Touch Techlogy je Matestov najnoviji koncept koji ima za cilj da ponudi inovativna i user-friendly tehnologiju za kontrolu i upravljanje najmodernijom opremom u domenu testiranja građevinskih materijala

Ova tehnologija je srž Matestove kontrolne jedinice, software baziran na Windows platformi i touch screen sistem koji je modularan, fleksibilan i obavlja mnoge opcije

iT TECH pokriva
- INOVATIVNOST
- INTERNET KONEKCIJA
- INTERFEJS SA IKONICAMA
- INDUSTRIJALNA TEHNOLOGIJA

SISTEM JEDNOG RAZMIŠLJANJA JEDNOM SHVATIŠ - SVE TESTIRAŠ

NAPREDNA TEHNOLOGIJA ISPITIVANJA ASFALTA

- GYROTRONIC - Gyratory Compactor
- ARC - Electromechanical Asphalt Roller Compactor
- ASC - Asphalt Shear Box Compactor
- SMARTRACKER[tm] - Multiwheels Hamburg Wheel Tracker, DRY + WET test environment
- SOFTMATIC - Automatic Digital Ring & Ball Apparatus
- Ductilometers with data acquisition system

MULTIFUNKCIONALNI RAMOVI ZA TESTIRANJE

- CBR/Marshall digital machines
- Universal multispeed load frames
- UNITRONIC 50kN or 200kN Universal multipurpose compression/flexural and tensile frames

OPREMA ZA GEOMEHANIČKO ISPITIVANJE

- EDOTRONIC - Automatic Consolidation Apparatus
- SHEARLAB - AUTOSHEARLAB - SHEARTRONIC Direct / Residual shear testing systems
- Triaxial Load Frame 50kN

MIXMATIC - Automatic Programmable Mortar Mixer

INELAS ERECO D.O.O
Tošin bunar 274a, 11070 , Novi Beograd tel. +381 11 2284 574 email. info@inelasereco.rs

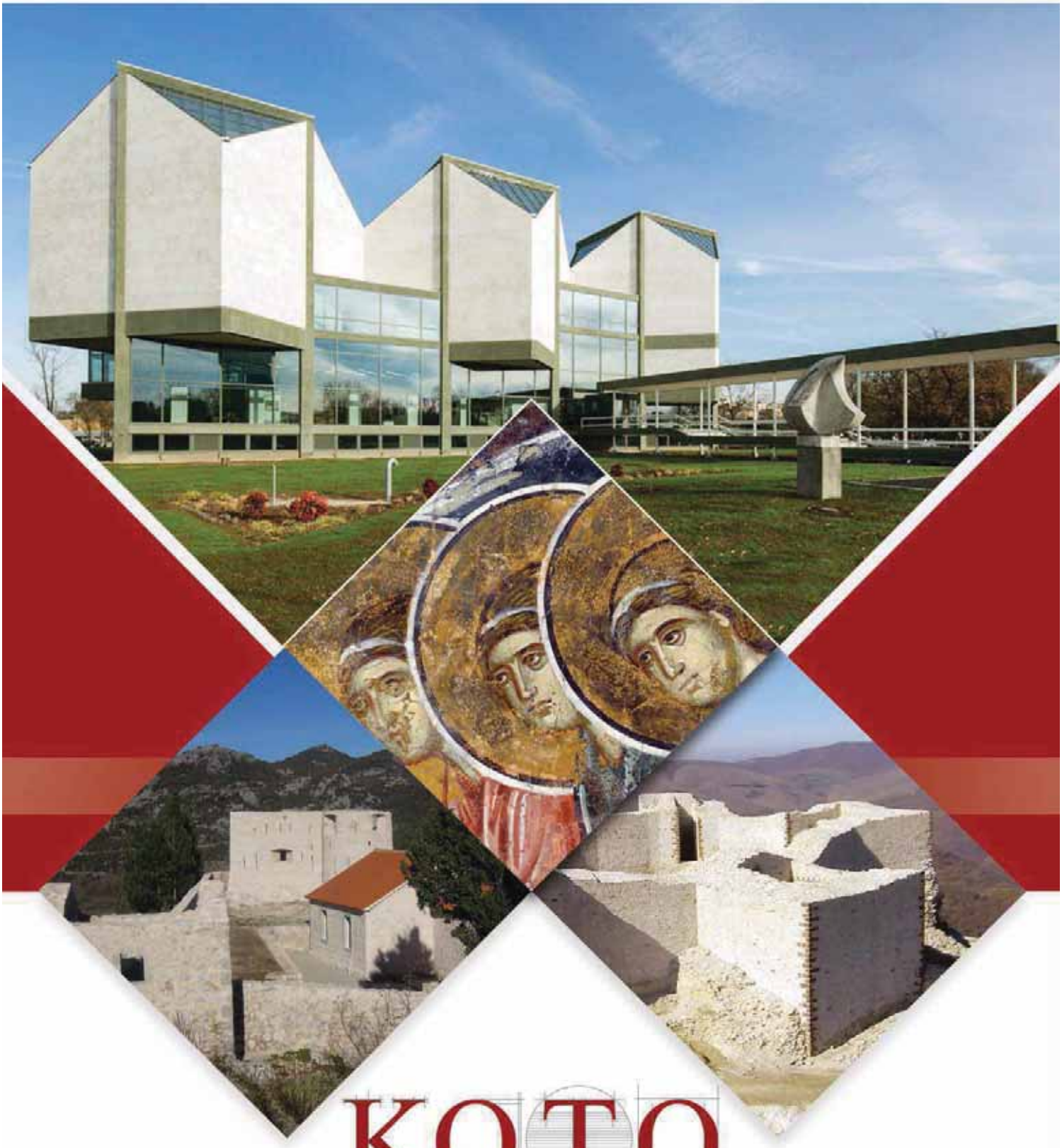

KOTO

www.koto.rs | office@koto.rs | 011 309 7410 | Vojvode Stepe br. 466, Beograd

INNOVATIVE CONSTRUCTION TECHNOLOGIES

NOVKOL

Samarska 6
(bivši Surčinski put 1k),
11077, Novi Beograd, Srbija

+381117129180
+381117129194
+381117129324
+381112607979
+381112607981

Fax:
+381117129183

office@novkol.co.rs
priprema@novkol.co.rs